Unlocking the Potential of Renewable Energy for E-kerosene Production in Brazil

Zur Erlangung des akademischen Grades eines

Doktors der Ingenieurwissenschaften (Dr.-Ing.)

von der KIT-Fakultät für
Wirtschaftswissenschaften
des Karlsruher Instituts für Technologie (KIT)

genehmigte

DISSERTATION

von

M.Sc. Ying Deng
geb. in Sichuan, China

Tag der mündlichen Prüfung: 09. August 2023
Hauptreferent: PD Dr. Patrick Jochem
Korreferent: Prof. Dr. Frank Schultmann

— *To my family* / 致我的家人

Kurzfassung

Diese Dissertation beschäftigt sich mit der Fragestellung wie ein Land zukünftig zu einem geeigneten Produzenten und Exporteur von nachhaltigem Kerosin im zukünftigen globalen Markt hierfür werden und gleichzeitig Ziele zur Schaffung einer CO_2-neutralen Stromversorgung erreichen kann. Ein idealtypischer Kandidat für eine solche Untersuchung ist das Land Brasilien. Es verfügt über beträchtliche erneuerbare Energieressourcen, große Flächepotenziale und eine etablierte Rolle als Exporteuer von Biokraftstoffen. Allerdings existieren für Brasilien bisher noch keine Strategien zur Produktion von E-Kerosin, die auf einer CO_2-neutralen Energieversorgung basieren.

Frühere Studien in diesem Bereich haben sich in erster Linie auf techno-ökonomische Untersuchungen zur optimalen Auslegung von Einzelkomponenten innerhalb der E-Kerosin-Produktionskette beschränkt. Diese Dissertation erweitert diesen Fokus hin zu modellbasierten Szenario-Analysen der nationalen Energieversorgung, um sektorübergreifende Auswirkungen zu berücksichtigen. Der Neuheitswert gegenüber existierenden nationalen Szenariostudien ist neben der Integration von Produktionsketten für E-Kerosin die räumliche Modellauflösung, welche Untersuchungen auf Ebene der Bundesstaaten und somit Standortaussagen für die zukünftig benötigte Energieinfrastruktur erlaubt. Die derzeit für Brasilien verwendeten Energiesystemmodelle weisen Einschränkungen auf - sie sind entweder nicht quelloffen, haben keine ausreichende Auflösung oder vernachlässigen die Energiebilanzierung von Flugtreibstoffen. Für diesen Zweck wurde im Rahmen dieser Dissertation das Energiesystem-Optimierungsmodell PyPSA-Brazil entwickelt. Es handelt sich um ein vollständig quelloffenes, auf öffentlichen Datensätzen basierendes Modell. Damit stellt es für Untersuchung

von Szenarien der nationalen Energieversorgung selbst im Vergleich zu Modellen vieler Industrieländer einen bedeutenden Fortschritt hin zu transparenten Planungsprozessen in Brasilien dar.

Der erste Teil dieser Dissertation befasst sich mit der Zusammenstellung eines umfassenden, offenen Datensatzes für die Szenarioanalyse. Dieser Datensatz umfasst Zeitreihendaten von variablen, erneuerbaren Stromerzeugungspotenzialen, Stromlastprofilen, Zuflüssen für die Wasserkraftwerke, grenzüberschreitendem Stromaustausch, Geodaten zur administrativen Aufteilung der brasilianischen Bundesstaaten sowie Kraftwerksdaten, Netzwerktopologie, Biomasse-Wärmekraftwerkspotenziale und Szenarien der Energienachfrage. Im zweiten Teil wird ein quelloffenes Energiesystem-Optimierungsmodell auf der Grundlage des kuratierten Datensatz erstellt, um die Synergien eines vollständig dekarbonisierten Stromsystems bei gleichzeitiger Produktion von E-Kerosin in Brasilien zu untersuchen. Die Kompromisse zwischen der Versorgung mit E-Kerosin und konkurrierenden Optionen, wie Biokerosin und konventionellem Kerosin, werden ebenfalls untersucht.

Die Ergebnisse legen nahe, dass ein dekarbonisiertes Energiesystem in Brasilien im Jahr 2050 zu Stromgestehungskosten von 50,3 €/MWh verursachen würde, wobei die Hälfte der Elektrizität aus Wind- und Sonnenenergie erzeugt wird. Die Integration der E-Kerosin-Produktion verringert die Abregelung der erneuerbaren Erzeugung und die Abhängigkeit von der Wasserkraft. Der Anteil von E-Kerosin an der Deckung des Kerosinbedarfs schwankt zwischen 2,7% und 51,1%, und die nivellierten Produktionskosten liegen zwischen 113,3 €/MWh und 227,3 €/MWh. Diese Schwankungen werden durch die Produktionskosten von Biokerosin, die Kohlenstoffpreise und die Exportabsichten beeinflusst.

Diese Feststellungen sind von Bedeutung für politische Entscheidungsträger und Interessengruppen im brasilianischen Energiesektor, insbesondere für diejenigen, die sich mit nachhaltiger Energie und luftfahrtbezogenen Umweltfragen beschäftigen. Die hier entwickelte Methodik könnte als Grundstein für andere Länder dienen, die darauf abzielen, Produzenten und Exporteure von CO_2-neutralem E-Kerosin zu werden.

Abstract

This dissertation deals with how a country transitions into a suitable producer and prospective exporter of sustainable aviation fuels in the upcoming global market while progressing towards a carbon-neutral national power system. One candidate for this endeavour is Brazil. It has substantial renewable resources, extensive acreage, and considerable expertise in bioenergy production. However, Brazil has not yet developed strategies for producing e-kerosene that is underpinned by a carbon-neutral energy supply.

While much of the existing literature primarily explores the economic performance and optimal configuration of components in the e-kerosene production chain, this research broadens this focus to model-based scenario analysis of national energy supplies to include cross-sectoral impacts. The novelty of this approach is that besides integrating e-kerosene production chains, the granular spatial resolution of the model allows investigations at the level of the federal states, thus aiding future location decisions for necessary energy infrastructure. The current energy system models used for Brazil exhibit limitations: they are either closed-source, lack sufficient resolution, or disregard the energy balancing of aviation fuels. In response, the energy system optimisation model, PyPSA-Brazil, was developed as part of this dissertation. The PyPSA-Brazil model is completely open-source and relies on publicly available data sets. Therefore, it represents a significant step towards transparent planning processes in Brazil for exploring national energy supply scenarios, even compared to models of many industrialised countries.

The first phase compiles a comprehensive open data set for scenario analysis. This data set includes various elements: (i) time series data of variable renewable potentials, electricity load profiles, inflows for the hydropower plants, and cross-border electricity exchanges; (ii) geospatial data on the administrative division of the Brazilian federal states; and (iii) tabular data with power plant information, aggregated grid network topology, biomass thermal plant potential, and scenarios of energy demand. In the second phase, an open-source energy system optimisation model is established based on the curated dataset to investigate the potential synergies of a fully decarbonised power system with simultaneous e-kerosene production in Brazil. It further discusses the trade-offs between e-kerosene supply and competing options such as biokerosene and conventional kerosene.

The results indicate that attaining a carbon-neutral power system in Brazil in 2050 would result in an average electricity cost of 50.3 €/MWh, wherein wind and solar sources contribute to half of the energy generation. Integrating e-kerosene production reduces the renewable curtailment and the reliance on hydropower. The e-kerosene share in meeting kerosene demand varies between 2.7% and 51.1%, and its levelised cost for production ranges from 113.3 €/MWh to 227.3 €/MWh. These variations are influenced by biokerosene production costs, carbon pricing, and export intentions.

These findings are significant for policymakers and stakeholders in Brazil's energy sector, especially those concerned with sustainable energy and aviation-related environmental issues. The methodology developed herein could serve as a cornerstone for other countries aspiring to become producers and exporters of carbon-neutral e-kerosene.

Preface

This dissertation presents a collection of publications contributing to a broader research theme on the design of carbon-neutral energy systems. The publications are organised both chronologically and thematically and include the following:

Y. Deng, K.-K. Cao, W. Hu, R. Stegen, K. von Krbek, R. Soria, P. R. R. Rochedo, and P. Jochem. **Harmonized and Open Energy Dataset for Modeling a Highly Renewable Brazilian Power System.** *Scientific Data*, 10(1), p.103, 2023. ISSN 2052-4463. DOI 10.1038/s41597-023-01992-9.

I am the lead contributor responsible for assembling and analysing raw data, coding and documenting data sets, and writing. This paper is open access and includes a ready-to-use data set and an openly accessible code repository.

Y. Deng, K.-K. Cao, M. Wetzel, W. Hu, and P. Jochem. **E-kerosene Production and Export in Carbon-neutral Power Systems – A Solution for Sustainable Aviation?**. 2023. *Submitted to Journal of Scientific Reports*.

I am primarily responsible for initiating the research, implementing simulations, evaluating outcomes, and writing the manuscript. The newly developed model will be made publicly accessible.

Additional contributions of mine extend to several peer-reviewed articles, some of which have been submitted for review, while others are currently in progress. However, these works do not form a part of the present dissertation:

Y. Deng, K.-K. Cao, and B. Wanke. **Designing a Brazilian energy system model for studying energy planning at high spatial and temporal resolution**. 2021.

DOI `10.46855/energy-proceedings-9781`. *13th International Conference on Applied Energy*.

W. Hu, Y. Scholz, M. Yeligeti, L. von Bremen, and Y. Deng. **Downscaling ERA5 Wind Speed Data: A Machine Learning approach considering Topographic Influences.** Environmental Research Letters 18: 094007, 2023. DOI 10.1088/1748-9326/aceb0a.

Y. Deng, C. Jardim Reis Souza, K.-K. Cao, T. Pregger, and P. Jochem. **Biokerosene Production in Brazil: A Spatio-temporal Techno-economic Assessment.** 2023. *Manuscript in progress*.

W. Hu, Y. Scholz, M. Yeligeti, and Y. Deng. **Projecting future electricity demand in the context of climate change: a temperature-dependent dynamic regression model.** 2023. *Manuscript in progress*.

The impact of this dissertation has been disseminated through presentations delivered at high-level academic conferences, publications in leading peer-reviewed journals, and engagements such as talks and workshops with policymakers and prestigious Brazilian universities. The following conference, workshop, and technical visit have featured this work.

- The 13th International Conference on Applied Energy, held virtually from November 29 to December 02, 2021.
- Pre-launch of teaching material on Sustainable Aviation Fuel (SAF) at ProQR Workshop, held virtually on December 01, 2021.
- Launch of teaching material on SAF in teacher training in Rio de Janeiro, Brazil, from May 2-6, 2022
- Technical visits to relevant sectoral institutions such as the National Agency for Oil, Gas and Biofuels (ANP) and the National Energy Research Office (EPE), Federal University of Rio de Janeiro (UFRJ) in Rio de Janeiro and Brasília, Brazil, from May 8-12, 2022.

Acknowledgements

Throughout my enriching four-year PhD journey, I have been incredibly fortunate to receive outstanding support and encouragement from many who have made this work possible.

First and foremost, my heartfelt gratitude goes to my dear supervisors, PD Dr Patrick Jochem and Dr Karl-Kiên Cao. Your invaluable guidance, unwavering support, and constructive feedback have shaped my research trajectory. Patrick, your exceptional insights and expertise have challenged me to cultivate resilience and intellectual independence as early as possible, propelling me to steadfastly surmount the challenges inherent in my research. Kiên, your mentorship and constructive critique have contributed significantly to my growth as a researcher. Whatever the challenge, you have been a safe boat for me on the journey. I am also grateful for the engaging small talks we have shared in the pantry and on the way back, as they have enriched my perspectives and fostered continuous growth.

I sincerely thank my colleague, Manuel, for his invaluable contributions through thoughtful discussions, explanations, and insightful comments on this work whenever I needed them. Your input has been pivotal in refining my ideas. To Wenxuan, Mengzhu, Carina, and Ben, I am profoundly grateful for our spirited discussions and stimulating exchanges, which have broadened my understanding and sparked new avenues of exploration. Each of you has played a significant role in shaping the intellectual fabric of my research. I also express my gratitude to Thomas for his prompt response, invaluable assistance, and extraordinary suggestions, all of which have greatly enhanced the quality of my work.

The generous support of the Klimaneutrale Alternative Kraftstoffe (ProQR) project grant from the Deutsche Gesellschaft für Internationale Zusammenarbeit (GIZ) is gratefully acknowledged for funding my PhD within the framework established by the German Federal Ministry for the Environment, Nature Conservation, and Nuclear Safety (BMU). This funding has been instrumental in realising my research endeavour, and I sincerely appreciate the opportunity it has provided.

I want to extend my great appreciation to Professor Rafael Soria from Universidad San Francisco de Quito for introducing me to many excellent energy data sources and providing valuable insights and comments during our bi-weekly meetings. Your expertise and guidance have significantly elevated my research quality, and I am sincerely grateful for your consent to this work.

Amidst this transformative journey, my family has been a firm source of unconditional love and support. To my mum, I am incredibly grateful for your dedication to nurturing our dreams. Without your enduring presence and support, I would not have reached the milestones I achieved today. Chao, my sister, your constant presence, heart-warm companionship, and uplifting encouragement through the ups and downs of this journey has been invaluable. I would also like to express my gratitude to Tao, who has become integral to my family. Our shared moments, whether through engaging conversations, culinary adventures, invigorating hikes, or simple togetherness, have brought immeasurable joy and profound encouragement. Finally, I thank my friends, who have shared unique memories with me at various stages of the past four years.

I could not have embarked on this journey alone, and I have succeeded because of all of you. From the bottom of my heart, thank you!

Contents

Acronyms

Acronyms

AC Alternating Current

AEL Alkaline Electrolysis

ANA National Water Agency (Portuguese: Agência Nacional de Águas e Saneamento Básico)

ANAC National Civil Aviation Agency (Portuguese: Agência Nacional de Aviação Civil)

ANEEL National Electric Energy Agency (Portuguese: Agência Nacional de Energia Elétrica)

ANP National Agency for Petroleum, Natural Gas and Biofuels (Portuguese: Agência Nacional do Petróleo, Gás Natural e Biocombustíveis)

ASC Average System Cost

ASTM American Society for Testing and Materials

ATAG Air Transport Action Group

ATJ Alcohol-to-jet

BECCS Bioenergy with Carbon Capture and Storage

BP the British Petroleum Company

CF Capacity Factor

CCEE	Electric Energy Commercialization Chamber (Portuguese: Câmara de Comercialização de Energia Elétrica)
CCS	Carbon Capture and Storage
CCU	Carbon Capture and Utilisation
COPPE	the Research Institute Energy Planning Program, Graduate School of Engineering of Federal University of Rio de Janeiro
CORSIA	Carbon Offsetting and Reduction Scheme for International Aviation
CRS	Coordinate Reference System
DAC	Direct Air Capture
DEA	Danish Energy Agency and Energinet
DNI	Direct Normal Irradiance
DSHC	Direct Fermentation of Sugars to Hydrocarbons
EnDAT	Energy Data Analysis Tool
EAR	Stored Energy (Portuguese: Energia Armazenada)
ENA	Affluent Natural Energy (Portuguese: Energia Natural Afluente)
ENTSO-E	European Network of Transmission System Operators for Electricity
EPA	Environmental Protection Agency
EPE	National Energy Research Office (Portuguese: Empresa de Pesquisa Energética)
ERF	Emissions Reduction Factor
EU	European Union
E2P	Energy to Power
FOM	Fixed Operation and Maintenance

FT Fischer–Tropsch

GDP Gross Domestic Product

GHG Greenhouse Gas

GHI Global Horizontal Irradiance

HDCJ Hydrotreated Depolymerized Cellulosic Jet

HEFA Hydro-processed Esters and Fatty Acids

HVDC High Voltage Direct Current

IATA International Air Transport Association

IBGE the Brazilian Institute of Geography and Statistics (Portuguese: Instituto Brasileiro de Geografia e Estatística)

ICAO International Civil Aviation Organization

IEA International Energy Agency

iNDC Intended Nationally Determined Contributions

IPCC Intergovernmental Panel on Climate Change

IRENA International Renewable Energy Agency

ISO International Organization for Standardization

KKT Karush-Kuhn-Tucker

LCOE Levelised Cost of Electricity

LCOF Levelised Cost of Fuel

LMP Local Marginal Price

LP Linear Programming

MILP Mixed-integer Linear Programming

MME Ministry of Mines and Energy (Portuguese: Ministério de Minas e Energia)

NDC	Nationally Determined Contribution
NTC	Net Transfer Capacity
OECD	Organisation for Economic Cooperation and Development
ONS	National Electricity System Operator (Portuguese: Operador Nacional do Sistema Elétrico)
PDA	Open Data Portal (Portuguese: Portal de Dados Abertos)
PEM	Proton Exchange Membrane Electrolysis
PNE	National Energy Plan (Portuguese: O Plano Nacional de Energia)
PtG	Power-to-gas
PtL	Power-to-liquid
PV	Photovoltaic
PyPSA	Python for Power System Analysis
RQ	Research Question
RTK	Revenue Tonne Kilometer
rWGS	Reverse Water-gas Shift
UNFCCC	United Nations Framework Convention on Climate Change
US	United States
vRES	Variable Renewable Energy Source
VOM	Variable Operation and Maintenance
SAF	Sustainable Aviation Fuel
SDG	Sustainable Development Goal
SIN	National Interconnected Network (Portuguese: Sistema Interligado Nacional)
SOEL	High Temperature Solid Oxide Electrolysis

TEA Techno-economic Assessment

Symbols

H_2	Hydrogen
CO_2	Carbon Dioxide
CO	Carbon Monoxide
CO_2e	Carbon Dioxide Equivalent
H_2O	Water

1 Introduction

Attaining net-zero carbon dioxide (CO_2) emissions by the middle of the century and net-zero Greenhouse Gas (GHG) emissions by the end of century is both urgent and challenging (IPCC 2022b). The challenges arise from the Paris Agreement of limiting global warming well below 1.5 °C, which mandates rapid and substantial solutions to climate change that might impose short-term burdens on society (IPCC 2022a). Among the various sectors contributing to GHG emissions, the aviation has seen a continuous rise and faces difficulties in reversing this trend (Lee et al. 2009).

The persistent dependence of the aviation sector on conventional jet fuel amplifies this obstacle. This fuel is an energy-dense liquid fuel that lacks commercially competitive substitutes (Masiol and Harrison 2014). From 2000 to 2017, aviation contributed, on average, 2.4% of global carbon emissions due to fuel consumption (IEA 2019, p II.19). Aircraft engine exhaust consists of 72% CO_2, 28.6% water (H_2O), and a meagre 0.1% comprising trace compounds, including nitrogen oxides and sulphur. About 90% of these emissions take place at cruising altitudes between 9 km and 12 km (Masiol and Harrison 2014). Non-CO_2 emissions have warming effects comparable to CO_2, and when considered, the aviation sector's contribution to climate change is nearly double (Lee et al. 2009). A recent calculation for 2000-2018 demonstrates that the combined climate warming effect from both non-CO_2 and CO_2 emissions triples when compared to CO_2 emissions alone (Lee et al. 2021). Moreover, beyond climate change, the emissions adversely degrade air quality and heighten noise pollution. For instance, the uptick in nitrogen oxides (NOx) emissions corresponds to a staggering 16,000 premature global deaths each year (Yim et al. 2015).

The efforts to mitigate aviation's climate impact have historical roots. Initial global concerns about the impact of aviation surfaced in the early 1970s (Wilson and Matthews 1971), and the Intergovernmental Panel on Climate Change (IPCC) highlighted these concerns in 1999 (Penner et al. 1999). However, it was not until the beginning of the 21st century that governments and industry began to facilitate sustainable development in aviation. The journey started with the European Commission Directive 2003/87/EC (EU 2003) and saw significant momentum with the International Air Transport Association (IATA)'s proposal in 2013 for carbon-neutral growth from 2020. This proposal targets halving CO_2 emissions by 2050 relative to 2005 levels (Harvey 2013, Schäfer et al. 2016). As of October 2021, the aviation industry commits to achieving a carbon-neutral future from 2050 (IATA 2021).

1.1 Options for decarbonising the aviation industry

On how to decarbonise the aviation industry, there are a range of mitigation strategies: (i) technological advancements for fuel consumption efficiency, reduced aircraft weight, and next-generation aircraft designs such as electric or hydrogen-powered flights; (ii) better traffic management to avoid unnecessary fuel consumption and flying distances, and optimal operational strategies for higher passenger numbers; (iii) establishing market-based emissions reduction measures like emissions trading, taxes and offsets, known as the Carbon Offsetting and Reduction Scheme for International Aviation (CORSIA); and (iv) using Sustainable Aviation Fuels (SAFs) (Schäfer et al. 2016).

The aviation sector has already made significant progress in efficiency. Between 1970 and 1980, CO_2 intensity experienced a significant 5% annual drop, primarily due to improved engine efficiency. More recently, operational efficiency has increased by 54% compared to 1990 (ATAG 2021). Using narrow-body aircraft in the United States (US), for instance, is expected to reduce life-cycle CO_2 emissions by approximately 2% per year up to 2050 (Schäfer et al. 2016).

Additionally, the International Civil Aviation Organization (ICAO) projects that continued advancements in engine efficiency, aerodynamics, and capacity utilisation will curtail jet fuel demand and emissions by roughly 1-1.3% per year until 2037 (ICAO 2019a).

Although all-electric or hydrogen aircraft have the potential to eliminate direct combustion emissions, which reduce air pollutants and non-CO_2 warming impacts (Schäfer et al. 2018), they face challenges. The energy sources used in aviation primarily consist of liquid hydrocarbon fuels, which have high volumetric and gravimetric density (ASTM 2022). This trend is likely to continue until 2050, especially for long-haul air transport (ICAO 2018b). A shift to alternative energy sources, such as hydrogen or electricity, would necessitate considerable modifications to the aircraft or early retirement of existing fleets, especially in long-haul air transport (ICAO 2022b). Furthermore, Altman (2020) explains that without breakthroughs in battery chemistry, electrification is not feasible for main propulsion due to the low energy density of batteries. Specifically, jet fuel possesses an energy density of about 43 $\mathrm{MJ/kg}$, while the most efficient lithium-ion batteries in today's electric vehicles have only 0.72 $\mathrm{MJ/kg}$ (Holladay et al. 2020). In addition, the large-scale rollout of electric aircraft is further constrained by uneconomical charging and utilisation times, harsh operating conditions and limitations related to charging infrastructure, charging door slots, and range capacity (Wheeler and Bozhko 2014). When it comes to the commercial use of hydrogen in aviation, a radical redesign of the engine, airframe, and fuel supply chain would be necessary, making their use in commercial aviation unlikely (Bauen et al. 2020).

The adoption and expansion of SAFs, as shown in Figure 1.1, emerge as one of the most significant sustainable solution as it can be effectively used throughout an entire fleet. This is crucial considering the long service lives of aircraft fleets, often measured in decades (ICAO 2022b).

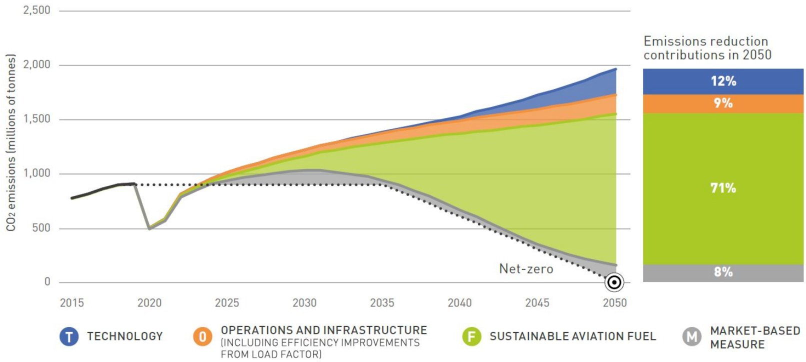

Figure 1.1: Aviation decarbonisation trajectory to 2050 aligned with 1.5 °C goal ("aggressive sustainable fuel deployment" scenario from ATAG (2021, p. 25)).

1.2 Sustainable aviation fuels

SAFs comply with the CORSIA Sustainability Criteria (ICAO 2018a, p. I-1-1). SAFs, being renewable or waste-derived, should safeguard ecologically sensitive territories, promote local socio-economic development, and avoid competing with food and water resources from 2024 (ICAO 2021b, p. 2). SAFs need to adhere to fundamental chemical and physical characteristics specified in ASTM[1] D7566 and D1655 standards (ASTM 2018, 2022) . These standards ensure their compatibility with conventional jet fuel in modern aircraft engines without any degradation in performance or operability.

SAFs fall under two categories: biokerosene and e-kerosene. Biokerosene is derived from biomass, the only renewable carbon-containing energy source (Kaltschmitt and Neuling 2018). Despite long-standing research interest in biokerosene, concerns persist about its scalability for mass utilisation, land-use impacts and environmental sustainability (Wang et al. 2019, Altman 2020, Connelly et al. 2015). For biokerosene to be sustainable, it should come from waste or rotational crops, aligning with ICAO's sustainability requirements (ICAO 2018a).

[1] ASTM stands for American Society for Testing and Materials (ASTM).

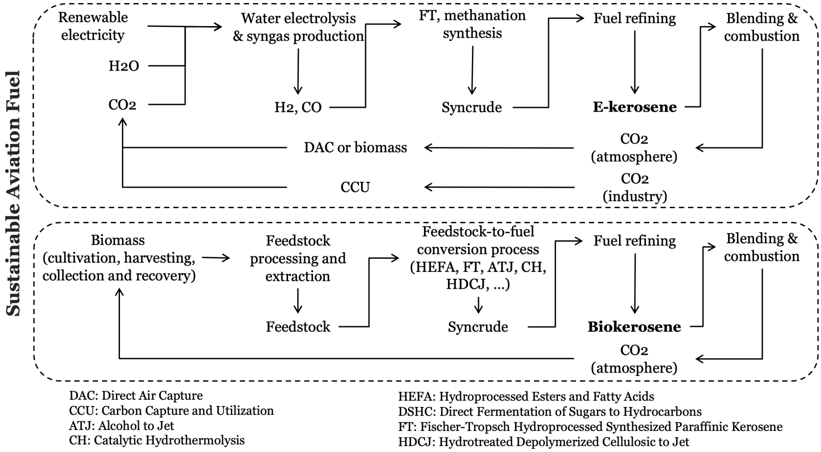

Figure 1.2: Value chain of SAF: a comparison of biokerosene and e-kerosene (original figure based on Cervi et al. (2021), Carvalho et al. (2019), ICAO (2022b), Schmidt et al. (2018), Becattini et al. (2021), Drünert et al. (2020), ICAO (2022a)).

The available biomass holds promise for future jet fuel markets in the US (Holladay et al. 2020). However, the feasibility of large-scale sustainable biokerosene production remains a question, as does the innovation needed for its commercialisation (Altman 2020).

GHG emissions from SAFs mirror those from petroleum-based jet fuel during combustion. In terms of life-cycle GHG emissions, SAFs outperform, with mandates requiring them to stay below 80.1 $g\,CO_2e/MJ$. This amounts to at least a 10% reduction from the average life-cycle GHG intensity baseline of 89 $g\,CO_2e/MJ$ (ICAO 2022a). SAFs can be made from diverse feedstocks such as biomass, residues, and waste, through different technologies like Hydro-processed Esters and Fatty Acids (HEFA), Alcohol-to-jet (ATJ), and Fischer–Tropsch (FT). The effectiveness of SAFs in reducing environmental impacts highly depends on the production pathways (Prussi et al. 2021). Figure 1.3 illustrates the life-cycle GHG emission values of biokerosene-type SAFs, varying between 5.2-73.4 $g\,CO_2e/MJ$, which depend on the production pathways. Biogenic biokerosene-type SAFs have a net-zero CO_2 cycle – the CO_2 emissions during combustion are balanced out by the CO_2 absorbed during photosynthesis. E-kerosene type SAFs might cut GHG emissions to 0.9-4.0 $g\,CO_2e/MJ$. Yet, accounting for non-CO_2 effects, these values could rise to 8.8-12.0 $g\,CO_2e/MJ$ (Micheli et al. 2022). Specific SAFs, such as those based on FT or ATJ pathways, are purely paraffinic hydrocarbons, free of aromatic compounds or sulphur (ASTM 2018). They provide higher specific energy, lower energy density, and altered emission properties (Masiol and Harrison 2014, Lobo et al. 2011). These environmental advantages make SAFs a vital element in advancing a GHG-constrained future (IATA 2018, Prussi et al. 2021).

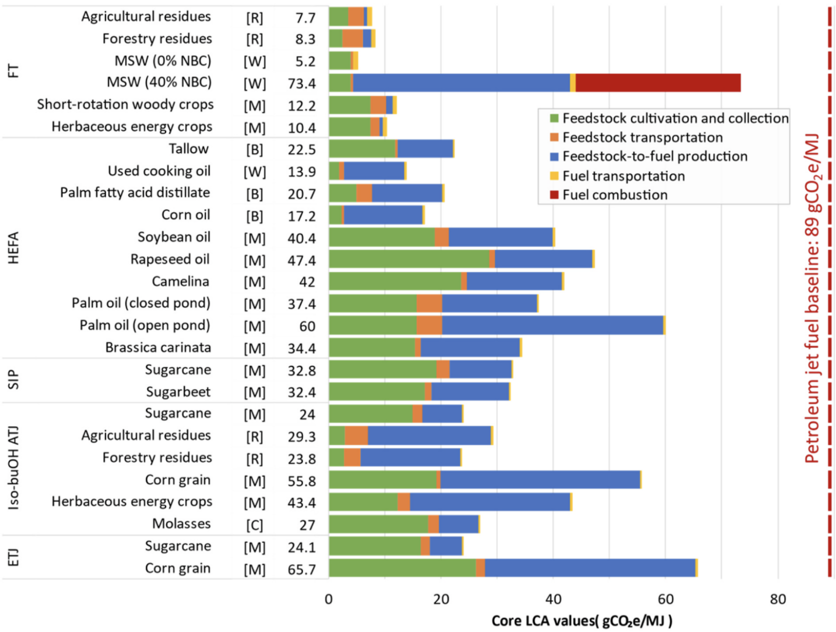

Figure 1.3: CORSIA default life-cycle emissions value for SAF (Prussi et al. 2021).

1.3 E-kerosene

E-kerosene is a synthetic liquid hydrocarbon fuel that is an e-fuel (others include products such as hydrogen (H_2), synthetic methane and methanol) (Ueckerdt et al. 2021). The synthesis of e-kerosene involves the combination of CO_2 and H_2, where H_2 is derived through the electrolysis of water using renewable electricity (Schmidt et al. 2018).

The production process requires three primary feedstocks: electricity, CO_2, and water (H_2O) (Ueckerdt et al. 2021). When the electricity used in the process comes from renewable sources, the resulting e-kerosene can be considered carbon neutral. CO_2 sources vary; they may be fossil carbon captured from industrial exhausts using Carbon Capture and Utilisation (CCU) or be extracted directly from the atmosphere through Direct Air Capture (DAC). Nonetheless, it is crucial to underscore that using fossil CO_2 does not contribute to long-term climate neutrality, as it yields a net release of fossil CO_2 into the atmosphere (Ueckerdt et al. 2021).

The H_2 required in the synthesis is generated through the electrolysis of water, which splits H_2O into H_2 and oxygen (O_2). Several technologies, such as Alkaline Electrolysis (AEL), Proton Exchange Membrane Electrolysis (PEM), High Temperature Solid Oxide Electrolysis (SOEL), and a high-temperature co-electrolysis (Co-SOEL) facilitate this process (Buttler and Spliethoff 2018).

Synthesising e-kerosene predominantly occurs through two pathways: FT synthesis and methanol synthesis (Schmidt et al. 2018). The FT process is a well-established route and is the only pathway presently recognised under the aviation fuel specification ASTM D7566 (ASTM 2018). The FT synthesis yields a mixture of water and hydrocarbons of assorted carbon chain lengths, commonly known as FT crude, also called syncrude. To convert syncrude into kerosene, it undergoes fuel conditioning, which involves distillation to separate the hydrocarbons within the desired carbon chain range, and hydrocracking to facilitate the final product conversion (König et al. 2015). The produced synthetic kerosene allows a blend of up to 50% with conventional petroleum-derived jet fuel (ICAO 2022b).

1.4 Opportunities for using e-kerosene

The synthesis of e-kerosene from renewable energy sources, such as solar and wind, presents not only an avenue for harnessing renewable energy but also offers a means of providing grid ancillary services to counterbalance the intermittent nature of renewable power generation (Decker et al. 2019, Schmidt et al. 2018). This development is particularly advantageous for regions with abundant solar and wind resources and supports the broader goal of aviation decarbonisation while promoting the integration of renewable energy sources into the energy infrastructure (Davis et al. 2018).

E-kerosene's compatibility with existing aviation infrastructure distinguishes it from alternative fuels like hydrogen or electricity, which require substantial modifications to existing infrastructure (ICAO 2022b, Batteiger et al. 2022). Additionally, when compared with biokerosene production through HEFA or ATJ, e-kerosene production exhibits minimal water and land requirements (Schmidt and Weindorf 2016).

E-kerosene could significantly reduce the carbon footprint of aviation due to its potential for net-zero life-cycle CO_2 emissions (Becattini et al. 2021), with limited GHG emissions of 0.9-12.0 $\mathrm{g\,CO_2e/MJ}$ (Micheli et al. 2022). E-kerosene produced from the FT pathway has a low-to-zero levels of aromatics and sulphur content, leading to reduced particle emissions and improved environmental outcomes (Moore et al. 2017, Batteiger et al. 2022).

However, the economic viability and scalability of e-kerosene production pose a significant hurdle, with process efficiencies ranging 0.34 to 0.48 (Batteiger et al. 2022). Making e-kerosene competitive with conventional kerosene and biokerosene would require significant innovation in technologies like electrolysis, carbon absorption and extraction, and the production of large amounts of cheap renewable electricity (Federal Republic of Germany 2021). In this regard, countries with abundant renewable energy resources could play a role in advancing the production and adoption of e-kerosene (Batteiger et al. 2022).

1.5 The Brazilian energy system

The development of green energy carriers, like e-kerosene, may redefine the dynamics of global importers and exporters in energy markets. Key drivers of this transformation include generation cost, area-specific resource potential, political stability, energy policy framework and trade (Perner and Bothe 2018). Regions harnessing renewable energy efficiently, due to favourable conditions and technical expertise, are well-positioned to meet the global demand for liquid energy carriers (Perner and Bothe 2018). In this context, Brazil, rich in renewable resources, is a notable contender for e-kerosene production and supply (Breyer et al. 2022).

Geographically, Brazil spans an expansive continental territory of 8,547,404 km^2 and has an extensive coastline of about 8,700 km. Additionally, its exclusive economic zone (EEZ) in the Atlantic stretches over 4,500 km^2 (IBGE 2018a, EPE 2020c).

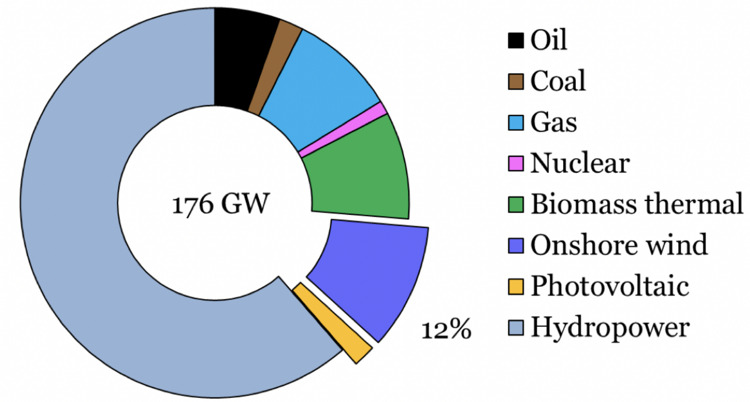

Figure 1.4: Installed capacity of power plants in 2021 (Own illustration based on Section 3.2.3).

By 2021, renewables made up 46.2% of Brazil's primary energy use, significantly ahead of global average (13.5%) and the rate in Organisation for Economic Co-operation and Development (OECD) countries (15.1%) (BP 2022). While the

Brazilian energy system predominantly relies on hydroelectricity, it also uses biofuels such as biodiesel and ethanol, limits petroleum consumption, and gradually incorporates solar and wind energy (Lima et al. 2020). However, even with substantial wind and solar radiation assets, their adoption remains nascent (ESMAP 2020, EPE 2022b). They represent only 12% of total installed capacity in 2021 (cf. Figure 1.4).

Brazil possesses one of the world's largest hydrographic basins, contributing to nearly 12% of global surface freshwater. With over 4 million hectares dedicated to dams and reservoirs, Brazil's hydro resources are substantial (Andrade et al. 2020, Nogueira et al. 2014). However, an over-reliance on hydroelectricity exposes Brazil to energy insecurities due to potential extreme hydrological variations (Bogdanov et al. 2019). Moreover, most untapped hydropower potential lies in the sensitive Amazon region, where constructing new facilities brings complex social and environmental challenges (Soito and Freitas 2011, Nogueira et al. 2014).

In the recent Nationally Determined Contribution (NDC), Brazil pledges to climate neutrality by 2050 (UNFCCC 2022). The country aims to diversify its energy sources, favouring non-hydro renewables in the future (Herreras Martínez et al. 2015). A unified direction on what infrastructure must be built and where, including solar and wind plants, storage systems, and transmission lines, is yet to be established (EPE 2022b).

Given these factors, it is crucial to understand the Brazilian energy system in detail and explore its potential contribution to the global energy transition.

1.6 Thesis outline

This dissertation employs an innovative energy system optimisation model to conduct a model-based scenario analysis, seeking to inform policy decisions on promoting e-kerosene production for Brazilian aviation sector. The analysis investigates the feasibility of Brazil to produce and export e-kerosene, whilst concurrently decarbonising its power system. The dissertation is structured as follows:

Chapter 2 offers a thorough literature review, including political strategies related to SAFs, economic assessments of e-kerosene, and the existing energy system models and data used in the context of Brazil. Through a funnel-like approach, this chapter identifies knowledge gaps and sheds light on the Research Questions (RQs) and the corresponding novelty and contribution of this dissertation.

Chapter 3 responds to the scarcity of proper energy data by presenting an open and comprehensive energy data set used for modelling the Brazilian energy system. The data set consists of time series, geospatial, and tabular data.

Chapter 4 introduces a novel open-source energy system model, tailored to assess the e-kerosene production without compromising the carbon neutrality of the Brazilian power system. This model makes up for the lack of suitable models and stands aligned with modern trends in energy system modelling. This chapter further elaborates on the rationale behind using Python for Power System Analysis (PyPSA) modelling framework, describes the model boundary through its objectives and constraints, and outlines the scenario definition.

Chapter 5 assesses 34 scenarios to evaluate challenges and prospects associated with the scaling up of e-kerosene production and its potential contribution to Brazil's energy system. The chapter investigates the synergies of supplying additional electricity for e-kerosene production within a fully decarbonised power system. The analysis also considers cost comparisons between biokerosene, conventional kerosene, and e-kerosene, taking into account different biokerosene production costs and carbon prices. In addition, this chapter includes an analysis of export costs and e-kerosene volumes across diverse export targets. Ultimately, it highlights Brazil's potential as an e-kerosene exporter by comparing its production costs internationally.

Chapter 6 reflects upon the limitations and recommendations for future research in this dissertation, while Chapter 7 gives a concise summary of the core conclusions and their implications. The findings imply that producing e-kerosene in

Brazil is feasible and cost-effective compared to biokerosene and conventional jet fuels. Becoming an exporter of SAFs strengthens the advantages of developing e-kerosene. Despite some inevitable limitations due to the data availability and model assumptions, the insights derived from this research stand to empower policymakers to discern the benefits of investing in e-kerosene and astutely guide policy-making in assessing e-kerosene production prospects in Brazil.

2 State of the Art

Contents of this chapter are based on

Y. Deng, K.-K. Cao, W. Hu, R. Stegen, K. von Krbek, R. Soria, P. R. R. Rochedo, and P. Jochem. **Harmonized and Open Energy Dataset for Modeling a Highly Renewable Brazilian Power System.** *Scientific Data*, 10(1), p.103, 2023. ISSN 2052-4463. DOI 10.1038/s41597-023-01992-9.

Y. Deng, K.-K. Cao, M. Wetzel, W. Hu, and P. Jochem. **E-kerosene Production and Export in Carbon-neutral Power Systems – A Solution for Sustainable Aviation?**. 2023. *Submitted to Journal of Scientific Reports*.

2.1 Political strategies for advancing sustainable aviation fuels in global and Brazilian contexts

Using SAFs in aviation is one of the most critical steps towards a carbon-constrained future, a goal that is advocated by both governments and the aviation industry.

The Air Transport Action Group (ATAG), in its Waypoint 2050 report, claims that SAFs are likely to contribute 71% of carbon reductions by mid-century, with e-kerosene accounting for half of all such fuels (ATAG 2021, p. 79). The European

Union (EU) exhibits a proactive stance in this domain and establishes policies and regulations to promote the production and application of SAFs in aviation. The European Commission proposes that SAFs should constitute 5% of aviation fuel by 2030, with a secondary objective of 0.7% for e-kerosene. By 2050, SAF's proportion is expected to climb to 63% and e-kerosene's share to remain a minimum of 28% (European Commission 2021). Germany demonstrates its echo of this commitment through an ambitious roadmap. Both the federal and state governments in Germany, in collaboration with industry stakeholders, plan to boost e-kerosene production to set sights on a 0.5% share ($\sim$ 50,000 tons) by 2026, growing to 2% ($\sim$ 200,000 tons) by 2030 (Federal Republic of Germany 2021).

Shifting the focus to South America, Brazil is in the process of formulating a national strategy for leveraging SAFs (Ministry of Infrastructure 2019). This builds on Brazil's rich history of regulatory initiatives to promote the use of biokerosene. Key milestones include: (i) the establishment of National Agency for Petroleum, Natural Gas and Biofuels (Portuguese: Agência Nacional do Petróleo, Gás Natural e Biocombustíveis) (ANP) through Brazilian Law No.9478 of 1997 (Federal Government of Brazil 1997), (ii) ANP Resolution No. 17 of 2006 to regulate the distribution of aviation fuels (ANP 2006), (iii) ANP Resolution No.37 of 2009 to specify the blending of fossil jet fuel (Jet A1) with biokerosene (ANP 2009), (iv) Brazilian Law No.12490 of 2011 (Biofuel Law) (Federal Government of Brazil 2011), (v) Brazilian Bill No.506 of 2013 to create National Biokerosene Program (ANP 2013), (vi) ANP Resolution No.63 of 2014 to define the specification for biokerosene (ANP 2014), and (vii) Brazilian Law No.13576 of 2017, which presents the national Biofuel Policy, RenovaBio (Federal Government of Brazil 2017).

2.2 Research on sustainable aviation fuels

2.2.1 Potential for carbon-neutral kerosene exports

Attention is increasingly directed towards the supply and export of green energy carriers, such as hydrogen, methane, ammonia, methanol and other synthetic fuels, which indirectly utilise carbon-neutral renewable electricity (cf. Lebrouhi et al. (2022), Egerer et al. (2023), Roos (2021), Wang et al. (2023)). These carriers can displace fossil carriers and become global energy commodities, offering solutions to energy-scarce countries and hard-to-abate sectors (Perner and Bothe 2018). Among nations poised to make a mark in the export of green energy carriers, Brazil is distinguished as a competitive force (Ikonnikova et al. 2023).

Despite growing interest, kerosene with high Emissions Reduction Factor (ERF)[1] – sustainable biokerosene and e-kerosene – is often under-discussed in publications as a globally traded energy carrier. As an alternative to conventional jet fuel, SAFs have the potential to become a critical enabler facilitating the sustainable evolution of the capital-intensive aviation industry (ATAG 2021). However, most studies aim to improve the availability and affordability of SAFs (ICAO 2022b), while scenarios frequently present SAFs making up only a limited fraction of the end consumption of a country (Drünert et al. 2020).

2.2.2 Potential for e-kerosene production in Brazil

Research on SAFs has been on biokerosene and its production through different pathways (cf. Wang et al. (2019), Mawhood et al. (2016), Bauen and Nattrass (2018)). Many studies have evaluated the techno-economic potential of biokerosene in Brazil (cf. Cervi et al. (2020), Cortez et al. (2016), Carvalho et al. (2019), Klein et al. (2018), Cervi et al. (2021)), building upon the long experience

[1] The Emissions Reduction Factor (ERF) quantifies the net life-cycle CO_2 benefits of SAFs by accounting for the CO_2 savings from feedstock production or growth, and incorporating the emissions incurred during fuel production (ATAG 2021, p. 103).

in biofuel production and favourable agroecological conditions. Two noteworthy studies, Cervi et al. (2020, 2021), analyse biokerosene's production chain and costs over space and time. Their findings highlight that producing biokerosene from biomass crops and their residues could be a cost-effective option for meeting Brazil's future kerosene consumption demands, especially when compared to conventional jet fuel. In contrast to the surge in biokerosene research and political actions, the potential for producing e-kerosene in Brazil seems inconclusive.

2.3 Economic feasibility assessment of e-kerosene

The versatility of e-kerosene is offset by high costs and uncertain availability (Ueckerdt et al. 2021). Estimating its potential relates to understanding the economic performance of e-kerosene production.

Two main approaches dominate this examination. The first, Techno-economic Assessment (TEA) zooms into the economic performance and optimal configuration of a specific technology or site. This method assesses metrics such as capital costs, operating costs, and revenues in terms of technical and financial input parameters (Hansen 2019). On the other hand, the model-based energy scenario analysis approach takes a whole-system perspective. Using mathematical formulations, it reflects the qualitative and quantitative interconnections between the components of a real-world energy system, offering evidence for strategic energy decisions in an uncertain future (Cao et al. 2016).

Publications that concentrate on the economic performance of e-kerosene production more frequently adopt the TEA approach and analyse the value chain based on efficiency and plant capital costs, life-cycle GHG emissions, feedstock, and energy supply, among others, to determine the optimal configuration of the segment of its production chain (Brynolf et al. 2018). TEA results yield a wide range of e-fuel production costs, from $200\,€/\mathrm{MWh}$ to $280\,€/\mathrm{MWh}$ today and $160\,€/\mathrm{MWh}$ to $210\,€/\mathrm{MWh}$ for 2030 (Brynolf et al. 2018). TEA provides a cost-benefit analysis for plant viability, but its results can vary significantly due to the differences in applied methodology, level of detail, system boundaries, and assumptions about techno-economic factors and market prices, making them less comparable across studies (Holladay et al. 2020).

TEA studies, as envisioned in Ueckerdt et al. (2021), Decker et al. (2019), König et al. (2015), Drünert et al. (2020), often assume that the power feed-in is set exogenously. This assumption may overlook the cost of balancing supply and demand, market dynamics, environmental implications (e.g., CO_2 emissions, climate costs), as well as economic and technical factors. Each of these factors can in turn affect production costs and decisions regarding technology installation. Furthermore, with the development of green energy carriers like e-kerosene, the investigation of their exchange, storage and final demand effects across sectors is becoming increasingly important (Hansen 2019). Accounting balance-of-system cost in fuel costing, as advocated in Ridjan et al. (2014), leads to better accuracy. An optimisation-based TEA approach bridges the gap in system dynamics by including components related to electricity supply, such as electric resistance heating, storage of electricity, hydrogen, and heat grid interconnection (Sherwin 2021). However, this study by Sherwin (2021) only examines a few sites in the US and does not consider the local economic viability of e-kerosene production throughout the country. In studies that assess the nationwide potential of renewable power generation, the focus is often not on e-kerosene specifically. For instance, some studies explore the production of hydrogen from hybrid Photovoltaic (PV)-wind power plants with battery storage (Fasihi and Breyer 2020), or the production of a variety of energy carriers including hydrogen, methane, methanol, FT-based fuels, ammonia, as demonstrated by Global PtX Atlas (Pfennig et al. 2022).

2.4 Model-based scenario approach for analysing e-kerosene

The formulation of an efficacious energy strategy requires considerations beyond merely deploying SAF (ATAG 2021). When looking at the feasibility of investing in e-kerosene production facilities for the aviation sector, a holistic approach to energy system analysis can offer insights into the national energy system, particularly the supply of renewable electricity, and provide sufficient details to bridge the gap in production chain analysis (Hansen 2019).

In contrast to the deterministic renewable energy costs in TEA, the model-based scenario analysis approach endogenously calculates the cost of electricity production while analysing the supply and demand balance of the energy system.

From an energy system analysis perspective, a joint consideration of the energy sector and e-kerosene production is necessary if one aims to assure net-zero emissions at the system level (Davis et al. 2018). Most model-based energy scenario analysis contemplates minimal (Child et al. 2019) or no use of e-fuels while assuming deep or full direct electrification of one or all end-use sectors (Schlachtberger et al. 2017). For those envisioning the use of e-fuels in energy system models, the form of e-fuels does not centre on e-kerosene but rather (i) the use of biological resources and production of biofuels (Bramstoft et al. 2020), (ii) methanol and methane (Ridjan et al. 2014), or (iii) hydrogen and methane (Lux et al. 2021). Often, the model-based energy scenarios either completely ignore the aviation sector, do not mention it, or consider it only as part of the overall transportation sector (Brown et al. 2018b). Some research, such as Lester et al. (2020), involves a system perspective and calculates the electricity price endogenously, but they do not root the prospect in a local context across the country. As a result, little is currently known about the possibility of simultaneously scaling up e-kerosene and renewable electricity production in a nationwide Brazilian energy system.

In modelling the export of green energy carriers, most studies assume optimal locations for renewable energy stations overseas. However, few studies account for the carbon neutrality of exporting countries regarding their electricity supply and internal demand for the exported energy carriers. For instance, research by Ueckerdt et al. (2021) infer optimal locations within the exporting countries based on electricity prices, highlighting methane and gasoline shipments from Northern Africa and Australia to EU ports. In a related context, Watanabe et al. (2010) and Heuser et al. (2019) spotlight Argentina's Patagonia for its renewable advantages, recommending hydrogen production to cater to the Japanese market. Additionally, Song et al. (2021) offer insights into supply chain costs, exploiting offshore potentials in China for Japan's hydrogen demand. In the Maghreb region and Morocco, Fasihi et al. (2017) and Hank et al. (2017) examine the production of methane, FT-based diesel, and other energy carriers, harnessing the best PV and wind sources for EU consumption. Lastly, Hampp et al. (2023) recommend exporting e-fuels (i.e., hydrogen, methane, ammonia, methanol, and FT-based fuels) from countries like Spain, Denmark, Morocco, Egypt, Saudi Arabia, Argentina, and Australia to Germany. However, these authors often neglect the exporting countries' internal energy demand, which is crucial considering their commitments to carbon neutrality in end-use sectors.

In summary, it is important to consider the carbon-neutrality target and the balance of the green energy carriers from the viewpoint of the exporter country. Doing so might result in a different selection of export candidates, highlighting an area that warrants further research.

2.5 Advancements in energy system modelling for Brazil

The success of a model-based approach in formulating consistent energy scenarios is tied to adequate and comprehensive energy system modelling. As Chang et al. (2021) outline in their work, forthcoming modelling frameworks are likely to feature (i) the deployment of open energy data and open-source modelling frameworks, (ii) the inclusion of more temporal details, and (iii) a reinforcement of cross-sectoral synergies.

2.5.1 Open energy data for Brazil

2.5.1.1 Benefits of being open source

Open science endorses the use of open models in assisting the transition to carbon-neutral energy systems. Such models, typically filled with data sets specific to the power system, offer numerous benefits. They can promote swarm intelligence, encourage collaboration and innovation, reduce duplicative efforts, enhance credibility and legitimacy, ensure transparency to policy discussions, and make high-quality data and planning tools accessible to researchers and government agencies that lack the financial resources for commercial options (Pfenninger et al. 2018).

2.5.1.2 Openness issues on availability of energy data

Despite these advantages, obstacles remain related to the diverse sources of energy data and their respective accessibility and licensing conditions, which affect the degree of openness of the modelling workflows (Pfenninger et al. 2018). Another hurdle in making data openly accessible is balancing the desire to grant access to as much data as possible with the need to protect commercial and personal information from potential misuse (Pfenninger et al. 2017). Governmental entities may be apprehensive about sharing their data and models due to concerns about the potential ramifications on societal and economic stability. As a result, the pursuit of transparency in political and social discourse may be offset by the need for stability, leading some governments to withhold information (Pfenninger et al. 2017). Moreover, the raw data that underlies an energy system model necessitates processing before it can be effectively utilised, which presents its own set of challenges (Pfenninger et al. 2017). For this reason, open data can bolster efforts to enhance transparency (Pfenninger et al. 2017).

2.5.1.3 Energy data availability

Publicly available data sets for energy system modelling are more comprehensive in developed countries, particularly in the EU, where they cover specific parts of the energy system such as the transmission grid (Matke et al. 2016, ENTSO-E 2023), generation capacity (ENTSO-E 2023), and renewable energy feed-in (Pfenninger and Staffell 2016, Staffell and Pfenninger 2016), as well as complete and readily available options such as the RE-Europe data set (Jensen and Pinson 2017). Other than the openly available data sets, there are several platforms, for instance, the Open Energy Platform [2] and Open Power System Data platform (Wiese et al. 2019), that coordinate various open data sets such as climate, demand profiles, transmission grids, and scenarios for modelling the European power system.

In contrast, energy system models for developing countries use opaque and, in most cases, barely accessible data sets. Language barriers may further hinder researchers who belong to a different language region from utilising available energy data.

Focusing on Brazil, an important data set for modelling the Brazilian energy system is published in the context of Brazil's National Ten-Year Expansion Plan (EPE 2020c). This data set contains the input data for the corresponding investment model (EPE 2020b). However, modellers who would like to use this data set, must have Portuguese language skills and modelling experience. The latter is necessary (e.g., to understand the context behind certain abbreviations or numerical values), which may be either based on empirical data or generically made up to fill data gaps. In particular, the data set is provided for four electric zones plus ten nodes, which limits analyses at higher spatial resolutions, for instance, on the state level.

Therefore, enhancing the utility of Brazil's existing energy data, by addressing the lack of spatial detail, harmonisation, and English translation, is crucial for effective application in popular energy system modelling frameworks like PyPSA.

[2] `https://openenergy-platform.org/`

By bridging this gap, researchers gain the tools necessary to replicate the Brazilian energy system or improve the integration into global energy models starting from a common basis.

2.5.2 High-resolution and open models

Typically, energy system optimisation models are resolved in time, space and on a technological level. Temporal resolutions can be characterised as low (1-12 time slices, e.g., 4 seasons and 3 days/nights), medium (36-288 time slices, e.g., representative days), and high (8,760 time slices, every hour of the year) (Chang et al. 2021). The spatial resolution can be characterised by low spatial resolution – single node modelling – and high spatial resolution for many nodes. The relevant level of techno-economic detail in the model is measured by (i) whether the plant is modelled as fully flexible with fixed efficiency (low level) or as having efficiency delays and time-varying ramp constraints and start-up costs (high level), (ii) whether storage is modelled without (low level) or with self-discharge (high level), and (iii) the lack of generators, storage, and energy demand variability (low level) or presence (high level) (Prina et al. 2020).

Models with coarse spatial and temporal resolutions are easier to solve and require fewer data (Ringkjøb et al. 2018). Nonetheless, applying such models on a national or broader level may engender inaccuracies, especially as wind and solar energy penetration increases (Poncelet et al. 2016). These inaccuracies stem from the dependence of the economic potential and costs of generating wind, solar and derived energy carriers (such as e-kerosene) on their specific locations and the ability to accommodate fluctuating renewable sources in meeting energy demand (Pfenninger et al. 2014).

Prior Brazilian energy planning studies have employed a few energy system models. MESSAGE-Brazil (Nogueira et al. 2014), BLUES[3] (Rochedo et al. 2018), and REMix-CEM (Fichter et al. 2017), for instance, are designed for capacity expansion with typical time slices. Noteworthy investigations such as those by Dranka and Ferreira (2018), Gils et al. (2017), Barbosa et al. (2016) have prioritised time resolution at an hourly scale. These studies, however, limit their scope to predefined transmission among four electric regions, thereby neglecting the benefits and bottlenecks associated with interstate cooperation. Therefore, Brazil still lacks an energy model that merges both high temporal and federal state-level resolutions.

Furthermore, models like EnergyPLAN (Dranka and Ferreira 2018), REMix (Gils et al. 2017), and LUT Energy System Transition model (Barbosa et al. 2016), which optimise system cost per hour, are closed source (according to Ringkjøb et al. (2018)). This restriction thus challenges more effective and broader collaboration and social debates (Kriechbaum et al. 2018). In particular, the lack of open-source models for Brazil complicates understanding the various assumptions made or the interrelationships represented in the mathematical models. As a result, existing model-based scenario analysis may not be fully comprehensible to scientists, stakeholders, and other interested individuals or groups (Pfenninger et al. 2018).

2.5.3 Cross-sectoral integration

Future modelling frameworks indicate more cross-sectoral synergy, which helps with the understanding of how various end-use sectors will impact the energy transition (Chang et al. 2021).

[3] Brazilian Land Use and Energy System (BLUES) is an Integrated Assessment Model (IAM) that simulates the evolution of the Brazilian energy, industrial and waste sectors, along with their associate emissions, in accordance with climate targets for 2050 (See `https://www.iamcdocumentation.eu/index.php/Reference_card_-_BLUES` for document).

Several energy studies for Brazil have explored the applications of e-fuels across multiple sectors, such as heating, road and rail transport (Gils et al. 2017), seasonal storage for the power sector (Barbosa et al. 2016), and marine shipping (Müller-Casseres et al. 2021). Yet, a conspicuous shortfall persists in the sector coupling to aviation. Thus, models employed in previous studies must adapt to evolving trends in energy system modelling and the emergence of the aviation sector.

2.5.4 Conclusions

The investigation into sustainable e-kerosene supply in Brazil underscores the crucial role of tailored energy system models. The existing models are insufficient for the scope of this research. Thus, it is imperative to conceive a novel energy system model that takes into account the interplay between national power supply and kerosene production. This model should be computationally at a high resolution, enhance system accuracy under high wind and solar shares, and ensure open accessibility for comprehensive analysis. Further efforts in model development are needed in this regard.

2.6 Objectives and contributions

Chapter 2 of this dissertation reviews the current understanding of SAF production in the literature and identifies several gaps. These gaps include (i) the lack of research on e-kerosene production as part of SAF, (ii) insufficient consideration of e-kerosene production from a potential exporter's perspective, (iii) the need for a model-based scenario analysis approach to achieve a holistic systems perspective, and (iv) the need for a new open source model populated by open data. This dissertation aims to bridge these research gaps, which is summarised in Table 2.1.

Table 2.1: Literature gaps and dissertation contribution.

Research on sustainable aviation fuel

Study	Fuel type	Approach	Kerosene trade-offs	Time scope	Regional scope
Wang et al. (2019)	biokerosene	review, TEA	No	—	—
Mawhood et al. (2016)	biokerosene	review, TEA	No	next 5-10 years	—
Bauen and Nattrass (2018)	biokerosene	review, TEA	No	2020, 2030	global
Cortez et al. (2016)	biokerosene	review, TEA[a]	No	—	Brazil
Carvalho et al. (2019)	biokerosene	TEA	No[b]	—	Brazil
Klein et al. (2018)	biokerosene	TEA	No	—	Brazil
Cervi et al. (2020)	biokerosene	TEA	No	2015, 2030	Brazil
Cervi et al. (2021)	biokerosene	TEA	No[b]	2015, 2030	Brazil
This dissertation	e-kerosene, biokerosene, fossil kerosene	model-based scenario	Yes	2050	Brazil

Export of green energy carrier

Study	Carriers	Exporter	Renewable	Buyer	Approach	Open data and model	Fuel balance
Ueckerdt et al. (2021)	methane, gasoline	Morocco, Australia	—	EU	TEA	partially	No
Lebrouhi et al. (2022)	hydrogen	—	—	—	review, TEA	—	—
Egerer et al. (2023)	ammonia	Australia	wind	Germany	model-based scenario	No	No
Roos (2021)	ammonia, hydrogen	South Africa	solar, wind	Germany	TEA	No	No
Wang et al. (2023)	hydrogen, methane, ammonia, methanol	Australia	solar, onshore wind	Germany, Japan	TEA	No	No

Watanabe et al. (2010)	hydrogen	Argentina	wind	Japan	TEA	—	No
Song et al. (2021)	hydrogen	China	offshore wind	Japan	TEA	partially	No
Fasihi et al. (2017)	methane, FT-based diesel	Maghreb region	solar, wind	EU	TEA	No	No
Hank et al. (2017)	hydrogen, methane, methanol, ammonia	Morocco	solar, wind	EU	TEA	No	No
Hampp et al. (2023)	hydrogen, methane, ammonia, methanol, FT-based fuels	Argentina, Australia, Denmark, Spain, Morocco, Egypt, Saudi Arabia	—	Germany	TEA	Yes	No
This dissertation	carbon-neutral kerosene	Brazil	solar, wind, biomass, hydropower	—	model-based scenario	Yes	Yes
Economic feasibility study: approach and power feed-in							
Study	**Carriers**		**Approach**		**Open data and model**	**Power feed-in**	
Ueckerdt et al. (2021)	methane, gasoline		TEA		partially	exogenous	
Decker et al. (2019)	methane		TEA		partially	exogenous[c]	
König et al. (2015)	FT-fuel		TEA		No	exogenous	
Drünert et al. (2020)	e-kerosene[d]		TEA		partially	exogenous	
Sherwin (2021)	e-kerosene[d]		TEA		partially	exogenous	
Fasihi and Breyer (2020)	hydrogen		TEA		partially	endogenous	
Pfennig et al. (2022)	hydrogen, methane, methanol, FT-based fuels, ammonia		TEA		No	endogenous[e]	
This dissertation	sustainable e-kerosene		model-based scenario		Yes	endogenous	

Incorporating fuel in model-based scenario approach				
Study	**Integrate fuel usage**	**Consider aviation sector**	**Scope**	
Brown et al. (2018b)	hydrogen and methane	No	EU	
Child et al. (2019)	PtG fuel	No	EU	
Schlachtberger et al. (2017)	No	No	EU	
Bramstoft et al. (2020)	biofuel and biokerosene	No	Denmark	
Lux et al. (2021)	methanol and methane	No	MENA region	
Lester et al. (2020)	biofuel, e-fuel, e-biofuel[f]	No	country level (Nordic + German)	
This dissertation	e-kerosene	Yes	local level of Brazil	
Brazilian energy system model				
Study	**Model name**	**Temporal resolution**	**Spatial resolution**	**Open source**
Nogueira et al. (2014)	MESSAGE-Brazil	typical time slices	3 subsystems	No
Rochedo et al. (2018)	BLUES	typical time slices	5 regions	No
Fichter et al. (2017)	REMix-CEM	typical time slices	4 regions	No
Dranka and Ferreira (2018)	EnergyPLAN	hourly	4 regions	No
Gils et al. (2017)	REMix	hourly	13 nodes[g]	No
Barbosa et al. (2016)	LUT Energy System Transition model	hourly	5 regions	No
This dissertation	PyPSA-Brazil	hourly	27 federal states	Yes

[a] The selection of promising feedstocks and pathways primarily guides this investigation.

[b] The study limits to comparing itself with the constant market price of conventional jet fuel.

[c] The study uses surplus power as power feed-in.

[d] The study explores various system setups for e-kerosene production and acknowledges that the sustainability of e-kerosene depends upon the carbon source.

[e] The study ignores the electricity, fuel balance, and grid topology.

[f] The e-biofuel refers to the production of biomass and green hydrogen.

[g] The system comprises 13 nodes: 7 with supply-demand balance, 3 for generation only, and 3 as connectors.

Consequently, the overarching RQ of this dissertation is: What would be the implications if Brazil were to emerge as a leading exporter of carbon-neutral kerosene by 2050 while achieving carbon neutrality in its power system? To address this question comprehensively, the following sub-questions arise:

RQ1. How can the scale-up of sustainable e-kerosene production be modelled without jeopardising the 100% renewable target for Brazilian electricity generation?

RQ2. How would a carbon-neutral Brazilian power system appear at high temporal and spatial resolution?

RQ3. What could be the local impacts of e-kerosene production in Brazil, and what constraints and opportunities might arise from its expansion in the energy system?

- RQ3.1. Could renewable energy be sufficient for electricity generation when e-kerosene completely meets Brazil's kerosene demand in 2050?
- RQ3.2. What could a future carbon-neutral power system look like with and without e-kerosene production?
- RQ3.3. In light of uncertain biokerosene production costs and carbon prices, what might be the share of e-kerosene in Brazil?
- RQ3.4. What could be the export cost if Brazil becomes an exporter of carbon-neutral kerosene?

This dissertation provides several unique contributions in the field:

- A pioneering investigation delves into the feasibility of producing e-kerosene as a net exporter. It offers valuable insight for positioning Brazil as a potential global leader in exporting carbon-neutral kerosene - an avenue not explored previously from a national energy system perspective.

- For the first time, this dissertation conducts a comprehensive analysis of the cost competitiveness among e-kerosene, biokerosene, and conventional kerosene in Brazil. It endogenously calculates the cost of electricity by evaluating the supply and demand dynamics of electricity and kerosene in the energy system. Doing so reveals the economic implications of each kerosene type in a way that previous studies have not.
- Extending beyond previous research that focused solely on optimising the production chain of e-kerosene or biokerosene, this dissertation provides a holistic view of the energy system at the federal-state level in Brazil. This broad approach facilitates informed decision-making regarding the placement of necessary energy infrastructure.
- This dissertation establishes a first-ever open-source Brazilian energy system model populated by well-documented and publicly available energy data. The openness of this model facilitates continuous research on SAFs in Brazil and their impact globally. Such a resource is invaluable to the research in this field, as no similar models exist.
- This dissertation is the first to make structured, open-access, English-language energy data available for energy system modelling research in Brazil. This overcomes the language barrier previously faced by researchers, providing a significant contribution to the field.
- Employing the state-of-the-art PyPSA framework to build PyPSA-Brazil – a high-resolution, large-scale energy system model – is another novel aspect of this dissertation. This marks the first application of the PyPSA framework in a Brazilian context.

3 Harmonised and Open Energy Data Set for Modelling a Highly Renewable Brazilian Power System

Contents of this chapter are based on

Y. Deng, K.-K. Cao, W. Hu, R. Stegen, K. von Krbek, R. Soria, P. R. R. Rochedo, and P. Jochem. **Harmonized and Open Energy Dataset for Modeling a Highly Renewable Brazilian Power System.** *Scientific Data*, 10(1), p.103, 2023. ISSN 2052-4463. DOI 10.1038/s41597-023-01992-9.

3.1 Introduction

The generation profile and production costs of Variable Renewable Energy Source (vRES) vary with the weather. Factors influencing this variation include the spatial location and the availability of wind resources and solar radiation. This correlation indicates that the decision problems in the operation and planning of reliable, stable, and carbon-neutral power systems rely on large-scale models and data sets.

In this context, the emphasis of this chapter lies on enhancing the applicability of Brazil's existing energy data for energy systems modelling. The unveiling of the first accessible, spatially explicit, harmonised, and English-translated version of Brazil's energy data presents an opportunity. This data enables replication of the Brazilian energy system and fosters its integration into worldwide energy models, thus setting a shared foundation.

The assembled data set comprises the following subcategories as detailed in the Section 3.2: (i) geospatial data for Brazil, (ii) aggregated grid network topology, (iii) vRES potentials – profile and installable generation capacity, (iv) geographically installable capacity of biomass thermal plants, (v) hydropower plants inflow, (vi) existing and planned power generators with their capacity, (vii) electricity load profile, (viii) scenarios of sectoral energy demand, and (ix) cross-border electricity exchanges. This data set is geographically resolved by Brazilian federal states, and its time series data is resolved hourly, spanning 2012-2020.

This way, the presented data set provides the essential information and foundation for the operational and expansion planning studies necessary to explore Brazil's highly decarbonised energy future. For example, the data set is applied in the PyPSA-Brazil model (cf. Deng et al. (2021)) to assess the impact of transmission grid expansion in the Brazilian power system. The data set published here has been updated and includes more years of data than the version used by Deng et al. (2021).

3.2 Methods

This dissertation aims to create a consolidated set of energy data for Brazil, drawing from openly accessible original data sets.

Table 3.1 summarises the sources and licensing of the raw data applied to each data set subcategory within this dissertation. Subsequent subsections delve into the understanding of energy data within the Brazilian context, detail the extraction process from data sources, and discuss assumptions underpinning the creation and processing of these data sets.

Table 3.1: Summary of original open accessible data sets used and their license.

Subsection	**Raw data set**	**Data license**
Geospatial data for Brazil	IBGE – Municipal Mesh Data (IBGE 2021)	ODbL[a]
Grid network topology	EPE Webmap (EPE 2020d)	ODbL
Renewable potentials (wind and solar)	Buchhorn et al. (2020), Lehner and Döll (2004), Dudley (2013), Land and Water Development Division, FAO (2020), Silva et al. (2007), Hersbach et al. (2020)[b]	citations[c]
Installable capacity for biomass thermal plant	Portugal-Pereira et al. (2015)	citations
Inflow for the hydropower plants	ONS – Historical Natural Energy Inflow for Each Region (ONS 2021c)	ODbL
Power plants	ANEEL-SIGA (ANEEL 2021b)	ODbL
Electricity load profiles	ONS – Historical Regional Load Curve (ONS 2021d), National Energy Research Office (Portuguese: Empresa de Pesquisa Energética) (EPE) – Statistical Yearbook of Electricity (EPE 2021)	ODbL
Scenarios of electricity demand	IEA (2021a), EPE and MME (2020), Baptista et al. (2022), van Soest et al. (2021), Riahi et al. (2021)	citations
Cross-border electricity exchanges	ONS – Historical Energy Exchanges (ONS 2021e)	ODbL

[a] The abbreviation ODbL refers to Open Data Commons Open Database License (`https://opendatacommons.org/licenses/odbl/1-0/`). The Open Data Policy, established by Law NO.8777 (Federal Government of Brazil 2016), guides the federal executive branch in releasing open government data in Brazil. The policy formulates the Open Data Portal (Portuguese: Portal de Dados Abertos) (PDA) for each federal agency, along with a platform – the Brazilian Open Data Portal. These data sets have an ODbL.

- The law explicitly grants unrestricted permission to reuse databases published in an open format, as stated in Federal Government of Brazil (2016, CAPÍTULO I, Art.3º-IV).
- The law emphasises that both the data provided by the federal executive branch and the information regarding active transparency can be freely used by the public authorities and society, as indicated in (Federal Government of Brazil 2019, Art. 4º)

[b] These data sets are input data used by the Energy Data Analysis Tool (EnDAT) (Scholz 2012, Stetter 2014). EnDAT is in the process of being open source. The renewable potential data published here is the first Brazilian data set produced by EnDAT.

[c] Permission has been granted for the republication of the data used in this dissertation after necessary modifications. However, it is imperative to note that this permission does not grant public access to the original data.

3.2.1 Geospatial data for Brazil

Brazil has five macroeconomic regions, four electric regions, 27 federative units (26 states and one federal district — Brasília), and 5,572 municipalities.

The provided data set exhibits a spatial resolution of ISO 3166-2 level (ISO 2022) and comprises a representation of 27 regions, illustrated in Figure 3.1.

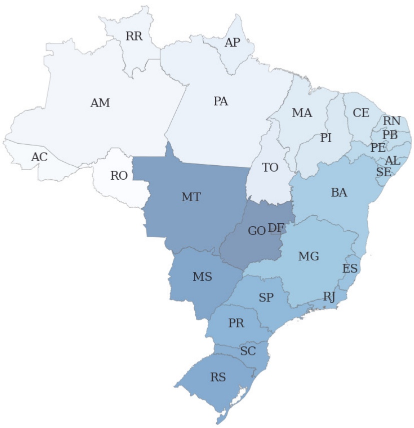

Code	Name	Code	Name
AC	Acre	PB	Paraíba
AL	Alagoas	PR	Paraná
AP	Amapá	PE	Pernambuco
AM	Amazonas	PI	Piauí
BA	Bahia	RJ	Rio de Janeiro
CE	Ceará	RN	Rio Grande do Norte
DF	Distrito Federal	RS	Rio Grande do Sul
ES	Espírito Santo	RO	Rondônia
GO	Goiás	RR	Roraima
MA	Maranhão	SC	Santa Catarina
MT	Mato Grosso	SP	São Paulo
MS	Mato Grosso do Sul	SE	Sergipe
MG	Minas Gerais	TO	Tocantins
PA	Pará		

Figure 3.1: 27 regions defined according to ISO 3166-2 – Brazilian federal states.

3.2.1.1 Data collection

Even though there are several map sources, the original data set used is from the Brazilian Institute of Geography and Statistics (Portuguese: Instituto Brasileiro de Geografia e Estatística) (IBGE) (IBGE 2021). This choice is not only motivated by the licensing but also because IBGE is Brazil's official map source and is considered the most credible source for the country's borders and topography. The shapefile's Coordinate Reference System (CRS) is SIRGAS 2000 (commonly known as EPSG:4674).

3.2.1.2 Data processing

In the original data set (IBGE 2021), these attributes are converted to English, and the CRS is re-projected to EPSG:4087. Only the federation state and the geometric information of the polygon are retained. In addition, representative coordinates (x, y) of the federal states are added and are considered as the centroid of the state polygon.

Table 3.2: Electrical regions defined in the National Interconnected Network (Portuguese: Sistema Interligado Nacional) (SIN) and the federal states covered.

Electric regions in SIN	Federal states
North (N)	Pará, Tocantins, Maranhão, Amapá, Amazonas, Roraima
Northeast (NE)	Piauí, Ceará, Rio Grande do Norte, Paraíba, Pernambuco, Alagoas, Sergipe, Bahia
Southeast/Midwest (SE)	Espírito Santo, Rio de Janeiro, Minas Gerais, São Paulo, Goiás, Distrito Federal, Mato Grosso, Mato Grosso do Sul, Acre, Rondônia
South (S)	Rio Grande do Sul, Santa Catarina, Paraná

3.2.2 Aggregated grid network topology

The power grid connects all power generators and loads. In Brazil, the electricity grid, known as the SIN, is managed by the National Electricity System Operator (Portuguese: Operador Nacional do Sistema Elétrico) (ONS). ONS divides Brazil into four electric regions, including several federal states, as shown in Table 3.2. SIN has a total length of 167,000 km and connects almost the entire country (96.6% of the national territory), except for some isolated places in the northern region. Over the next few decades, 434 lines with a total length of 32,000 km are planned to be built (EPE 2020d).

3.2.2.1 Data collection

EPE is a state-owned organisation in Brazil that conducts studies and research to provide technical support for outlining medium- and long-term energy planning in Brazil for the design and implementation of national energy policy. EPE identifies potential energy sources for national development and contributes to research for auctions in the energy sector.

The complete grid topology of Brazil is taken from the data set published by the EPE, called EPE Webmap (EPE 2020d). The original data sets are in shapefiles, with transmission line data as the line layer and substation and generator data as the point layer. All lines, substations, and power plants have individual shapefiles, classified by their operational status – existing or planned – and, for power plants in particular, by their plant type. The CRS of the shapefile is SIRGAS 2000. The attributes are specified in Portuguese and include name, plant operator, voltage level, year of operation, and line length, among others. Substations, transmission lines, and different types of power plants shapefiles are used to derive the network topology. Table 3.3 lists the number of records in the original data sets used.

Table 3.3: Number of the lines, substations, and power plant units in the original data set.[a]

	Existing	**Planing**	**Total**
Number of lines	1,589[b]	453	2,042
Number of substations	735	165	900
Number of power plants	2,904[c]	274	3,178

[a] The author downloaded these statistics in April 2021, and there may be slight discrepancies compared to the current version owing to continuous updates.
[b] The data set comprises predominantly lines operating at 230 kV and 500 kV, with the lowest voltage level recorded at 69 kV. Of these, three lines are rated at 800 kV. There are 115 lines with a length of less than 1 km, while seven lines extend beyond 2,000 km.
[c] It includes hydropower plants, wind onshore, PV, fossil-thermal, biomass-thermal, and nuclear power plants.

3.2.2.2 Data processing

The dissertation includes the presentation of two aggregated networks: one that encompasses solely the existing network and another that incorporates both the existing and planned networks.

Each federal state is modelled as a node located in its geometric centre, connected by transmission lines in operation and in the National Ten-Year Plan (EPE 2020c). An assumption is made that the existing and planned transmission lines are operational, regardless of the scenario year, thus allowing for the aggregation of transmission capacity without considering the reference year. The original data does not provide information on the connection of the lines to substations or power plants; however, this is necessary to construct the grid topology. To overcome this limitation, a heuristic method is employed to connect the starting and ending points of transmission lines to nearby substations or power plants. The analysis has three parts: pre-processing, mapping, and a combined step of aggregating and representing, as displayed in Figure 3.2. Geospatial analysis is conducted using the Geopandas package in Python.

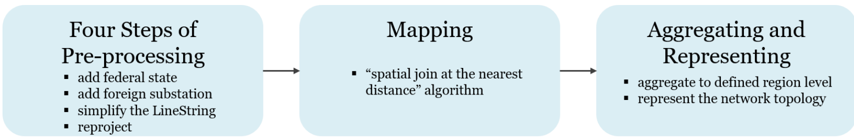

Figure 3.2: Overview of processing grid network data.

Before the mapping action, there are four pre-processing steps to make the "spatial join at the closest distance" algorithm effective.

1. `add federal state`: The federal states to which the substations and power plants belong are added to the attribute table according to their geographical locations.
2. `add foreign substation`: Information on existing foreign substations connected to the SIN is added manually based on EPE and MME (2020).

This is because the transmission lines indicated in the original line layer contain international connections, while information about substations outside Brazil is not specified. Added attributes include the name of the substation, the operator, the voltage, and the geometry. In addition, a new attribute, namely state, is added to identify the country to which it belongs using the ISO 3166-1 alpha-3 code. The state of the substation abroad is three characters, whereas in Brazil it is two characters. The geometry added manually is the longitude and latitude where the substation is located. An exception is the SE Macagua substation, located in Venezuela. Its actual location is (8.304, -62.668). However, it is designated as (4.530, -61.138). This is because, in the original data, the transmission line to the Boa Vista substation ends here. Additionally, the heuristic algorithm is based on the nearest distance criterion.

3. `simplify the LineString`: The transmission line layer needs further processing – converting MultiLineString to LineString and changing closed LineString to open LineString.

4. `reproject`: The shapefiles are reprojected to EPSG:4087 so that the distance-based calculations are robust.

After pre-processing, the mapping of the start and end points of the line layer to the substation and power plant geometry is achieved using the “sjoin_nearest” function from the Geopandas package in Python. The maximum distance to query the nearest geometry starts from an initial distance of 1 km and increases by 1 km in each subsequent query. Table 3.4 reveals the statistics of the mapping results, where sub_0 represents the start point, and sub_1 represents the endpoint. More than 90% of the mappings (96.1% of the starting points and 94.4% of the ending points) are within 1 km. The line with the most significant mapping deviation is LT 230 kV Itapaci – Mineradora Maracá (as named in the original data), with a length of 85 km. The deviation is particularly pronounced at its endpoint, where the nearest point is the Itapaci substation.

The final step is to aggregate these lines to represent the network topology between each federal state. Depending on the federal state information, only trans-state

Table 3.4: Statistical summary of the mapping – distance to sub_0 and to sub_1. Note: sub_0 is the starting substation, while sub_1 is the end substation in the mapping.

	to sub_0 (km)	**to sub_1 (km)**
count[a]	2402	2402
mean	1.3	1.4
std	2	3
min	1	1
50%	1	1
90%	1	1
95%	1	2
max	4.8	8.2

[a] The unit km does not apply to this row.

transmission is selected. This selection assumes that potential grid bottlenecks are not considered inside the federal states, i.e., copper-plates assumption (Cao et al. 2018). The original data set does not have information on whether the lines are Alternating Current (AC) or HVDC lines. There are several duplicate entities for HVDC lines, such as Porto Velho - Araraquara and Xingu - Estreito; these records are removed. The transfer capacity of the HVDC lines is supplemented manually with information from various sources, as specified in Table 3.5.

The number of circuits in each transmission line is added to calculate the transfer capacity of AC lines. “C1” and “C2” in the line names represent the first circuit and the second circuit, marking each line of the parallel circuit, while “CD” indicates a double circuit (EPE 2020a). Therefore, each line defaults to a single circuit, while lines with a “CD” tag in the line name are set to a double circuit. However, the original data set had no information on the physical characteristics of the lines, such as the conductor resistance, inductance, and capacitance of each transmission line. The assumption here is that each line consists of four bundles of conductors. The remaining transmission lines of different voltage levels are unified as parallel lines of 380 kV, thus forming an equivalent transmission network. This enables adding transmission capacities that start in one federal state and end in

Table 3.5: Transfer capacity of High Voltage Direct Current (HVDC) lines added manually.

Line name	Transfer capacity (MW)	Source
LT 600 kV Foz do Iguaçu – Ibiúna C1	3150	Rodrigues et al. (2019)
LT 600 kV Foz do Iguaçu – Ibiúna C2	3150	Rodrigues et al. (2019)
LT 600 kV Coletora Porto Velho – Araraquara, C1/C2	3150	Graham et al. (2012)
LT 600 kV Coletora Porto Velho – Araraquara, C3/C4	3150	Graham et al. (2012)
LT 230 kV Coletora Porto Velho – Porto Velho, C1	400	Graham et al. (2012)
LT 230 kV Coletora Porto Velho – Porto Velho, C2	400	Graham et al. (2012)
LT 800 kV CC Xingu – Estreito	4000	Esmeraldo (2020)
LT 800 kV CC Xingu – Terminal Rio	4000	Esmeraldo (2020)
LT 800 kV CC Graça Aranha – Silvânia	4000	Esmeraldo (2020)
LT 500 kV Rincón de Santa Maria – Garabi I C1	1100	Graham et al. (2002)
LT 500 kV Rincón de Santa Maria – Garabi II C1	1100	Graham et al. (2002)
LT 230 kV Livramento 2 – Rivera C1	70	EPE (2020c)
LT 500 kV Candiota – Melo C1	500	EPE (2020c)

another identical federal state. The lines in the equivalent transmission system are assumed to be three-phase overhead lines and of type 490-AL1/64-ST1A (Oeding and Oswald 2011).

The transfer capacity (apparent power) is calculated by:

$$S = \sqrt{3}UI. \tag{3.1}$$

The transfer efficiency results from:

$$f = 1 - \frac{3\mathrm{R}_L^{'} I^2 n}{S} \tag{3.2}$$

where

S : apparent power, MW
U : voltage level, kV
I : nominal current of the wire, kA
$R_L^{'}$: conductor's DC resistance at operating temperature for the wire, Ω/km
n : number of bundle conductor, n=4
f : transfer efficiency (1 minus the effective loss per line).

In aggregation, transmission capacity is accumulated, and efficiency and line length are averaged out. Figure 3.3 illustrates the results.

The primary focus of this dissertation is on gathering data derived from the original transmission network data set. While recognising the potential value in analysing distribution network data at the regional level, it is important to note the limited availability of appropriate public data sources for such analysis, as far as the current understanding extends.

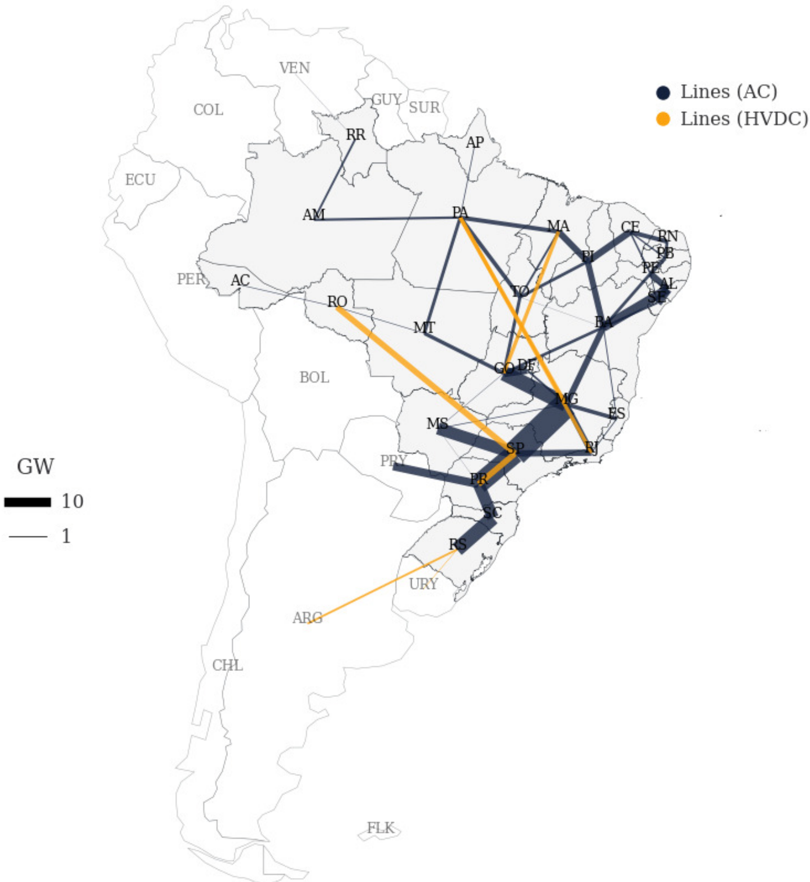

Figure 3.3: Transfer capacity between the defined regions, GW.

3.2.3 Power plants

Generators are an integral part of the energy industry, responsible for producing electricity and injecting it into the grid to reach consumers.

3.2.3.1 Data collection

There are several official generator databases in Brazil, for example, ANEEL-SIGA (ANEEL 2021b) published by National Electric Energy Agency (Portuguese: Agência Nacional de Energia Elétrica) (ANEEL), EPE Webmap (EPE 2020d), ONS Historical Database (ONS 2022a). ANEEL-SIGA is the Generation Information System and contains information on power plants from the granting phase to the decommissioning phase. EPE Webmap refers to the Geographic Information System of the Brazilian Energy Planning Studies. It is a geo-referenced database containing official information for Brazil's medium and long-term energy planning. The power plants in the ONS Historical Database mainly refer to those which are operated by ONS and are part of its SIN. Generally, when a power plant is in operation, it implies it is connected to the SIN. Some exceptions exist, such as isolated systems supplied by local generations and not connected to the SIN.

Power plants delegated by ANEEL have a single generation unit code – CEG (company identification code). Table 3.6 explains its format. All three data sets have CEG, renamed "plant_id" for clarity. The types of plants considered in the three data sets are different, as shown in Table 3.7. ONS defines the coarsest power plant types. ONS distinguishes hydroelectric power generation from hydropower and pump types, whereas ANEEL-SIGA and EPE Webmap do not provide information on pump types. To compare data sets by plant type, installed capacities for generation are aggregated to the plant types defined in `Harmonised` in Table 3.7. In addition, both ANEEL-SIGA and EPE Webmap provide geographic coordinates, while the ONS Historical Database reveals only the electric regions and federal states in which the plant units are located. ANEEL-SIGA and EPE Webmap include both operational and planned power units, while ONS includes only the operational power plants.

Table 3.6: CEG nomenclature.

<table>
<tr><th colspan="2">GGG.FF.UF.999999-D</th></tr>
<tr><th>Part</th><th>Explanation</th></tr>
<tr><td>GGG</td><td>generation type (cf. Table 3.10)</td></tr>
<tr><td>FF</td><td>the fuel type abbreviation</td></tr>
<tr><td>UF</td><td>federal state abbreviation</td></tr>
<tr><td>999999-D</td><td>unique number with identification digit</td></tr>
</table>

Table 3.7: The types of power plants used in the three data sets.

<table>
<tr><th>Harmonised</th><th>ONS Historical Database</th><th>EPE Webmap</th><th>ANEEL-SIGA</th></tr>
<tr><td>solar_pv</td><td>solar_pv</td><td>solar_pv</td><td>solar_pv</td></tr>
<tr><td>on_wind</td><td>on_wind</td><td>on_wind</td><td>on_wind</td></tr>
<tr><td>nuclear</td><td>nuclear</td><td>nuclear</td><td>nuclear</td></tr>
<tr><td rowspan="2">thermal</td><td rowspan="2">thermal</td><td>biomass_thermal</td><td rowspan="2">thermal</td></tr>
<tr><td>fossil_thermal</td></tr>
<tr><td rowspan="4">hydro</td><td rowspan="2">hydro</td><td>small_hydro</td><td>small_hydro</td></tr>
<tr><td>mini_hydro</td><td>mini_hydro</td></tr>
<tr><td rowspan="2">hydro_pump</td><td>hydro</td><td>hydro</td></tr>
<tr><td></td><td>wave</td></tr>
</table>

Ideally, combining all three data sets would yield a comprehensive and cohesive data set, but merging the three data sets into one is challenging due to their different granularities and lack of complementarity. Since they are all official data sets, it is also challenging to determine which data set is more reliable. Table 3.8 gives the statistics of the three data sets regarding the number of data entities, attributes, unique plant IDs and names, while Table 3.9 describes the total installed capacity for each plant type. Table 3.8 highlights the varying number of data entities, with ANEEL-SIGA covering the most entities and attributes. In addition, only the ANEEL-SIGA data set has a unique and complete identification of the plant IDs. Hence, the data entities of EPE Webmap and ONS Historical Database can be grouped compared to ANEEL-SIGA. Despite having an equal number of attributes, the ONS Historical Database includes specific details not present in ANEEL-SIGA. These details, such as names and IDs of power plant units used only by ONS, are less relevant for energy system analysis. In contrast to ANEEL-SIGA, the ONS Historical Database lacks information on planned power plant units and geography. ANEEL-SIGA covers almost all attributes provided by ONS Historical Database and EPE Webmap. Table 3.9 indicates that the total installed capacity of each type of plant in the EPE Webmap and ONS Historical Database is similar but contains the less installed capacity of wind, PV and thermal plant types compared to ANEEL-SIGA. The difference between the three data sets may result from the following reasons:

1. EPE Webmap covers mainly centralised generation, whose operating mechanisms are self-generation and public utilities. In addition to the plants in the EPE Webmap, the ANEEL-SIGA database includes distributed generation under the net metering scheme and small-scale backup generators. ONS Historical Database contains the plants dispatched in SIN.

2. The data set updates between ONS Historical Database, EPE Webmap, and the ANEEL-SIGA database are not synchronised. ONS publishes information on operating power plants on an annual basis – the latest data until December 2022 are used. The latest update of the EPE Webmap was in September 2020. On the contrary, the ANEEL-SIGA database is constantly updated with the granting of power plants. However, the historical versions of ANEEL-SIGA are not accessible.

3. Plant units are defined differently. ANEEL documents each data entity of plant unit based on when they received their grant, while ONS defines projects based on their operating units.

Table 3.8: Statistical comparison of data entities between data sets – ANEEL-SIGA, EPE Webmap, and ONS Historical Database.

Number of	ANEEL-SIGA	EPE Webmap	ONS Historical Database
data entities	10541	3178	4191
attributes	15	11	15
unique plants IDs	10541	3160	1389
unique plants names	10283	2984	1388

Table 3.9: Comparison of installed capacity per plant type between data sets – ANEEL-SIGA, EPE Webmap, and ONS Historical Database. Note: the installed capacity is the sum of units operating in 2018, and the plant type is defined by `Harmonised` in Table 3.7.

Type	ANEEL-SIGA (GW)	EPE Webmap (GW)	ONS Historical Database (GW)
hydro	111.37	110.41	110.43
nuclear	3.34	3.40	1.99
on_wind	31.00	20.95	22.35
solar_pv	24.07	4.76	6.43
thermal	52.45	44.86	34.81

As a result of the above discussion, using ANEEL-SIGA as the original input is deemed appropriate for several reasons: (i) available geographic coordinates, (ii) it covers all relevant attributes for the energy system analysis of the other two data sets, (iii) more data entities with a higher total installed capacity than the other two data sets, which include operating and planned plant units, (iv) unique and complete identifier of the data entities – plant ID, and (v) continuously updated.

There are 10,541 power plant units with 21 attributes in ANEEL-SIGA. From the database, these attributes include the name of the power plant, the plant ID, operational status (“operation”, “construction”, and “construction not started”), federal state in which it is located[1], the city it belongs to, plant type, primary energy source, fuel type, installed capacity, geographic coordinates of each generator, production capacity, primary fuel type, time in operation, and phase-out time. The CRS used for the ANEEL-SIGA data set is SIRGAS 2000, with coordinates expressed in degrees minutes seconds (DMS).

The power plants are matched based on the plant IDs to provide insight into the consistency of ANEEL-SIGA compared to EPE Webmap and ONS Historical Database. Prior to the matching process, capacity, federal state, plant name, plant type and operation status are grouped based on plant ID (cf. Deng (2023a)). ANEEL-SIGA and EPE Webmap have 3,035 data entities with identical plant IDs, while EPE Webmap contains 130 data entities not present in ANEEL-SIGA, and conversely, 7,512 entities found in ANEEL-SIGA are absent from EPE Webmap. Even when plant IDs match, discrepancies might be observed in installed capacity for 300 entities, federal state information for 77 entities, and the plant unit name for 277 entities. ANEEL-SIGA and ONS Historical Database have 1,330 data entities with matching plant IDs. ONS Historical Database has 71 data entities with unique plant IDs, while ANEEL-SIGA boasts 9,216 unique entities. Similar to the EPE Webmap comparison, even with matching plant IDs between ANEEL-SIGA and ONS, discrepancies can arise in installed capacity (292 entities), federal state details (36 entities), and plant unit names (132 entities).

3.2.3.2 Data processing

Although the ANEEL-SIGA data is displayed online through PowerBI, the platform only provides a download link. There are slight inconsistencies between the downloaded files, for instance, plant coordinates and plant names. Therefore, the data set provided here is based on the version downloaded by the authors on June 9, 2021.

[1] Each entity can be a single power plant or a power plant unit consisting of multiple power plants, for example, a wind farm operating multiple wind turbines. The location of the power plant units determines the federal state.

The ANEEL-SIGA data is constantly updated. The coordinates of the power plants need to be added to ensure completeness, and they should fall within the Brazilian range. Since all city names are provided, missing coordinates for plants are assigned based on the respective city's location. An individual power plant unit associated with more than one city can have multiple values in the "city" property. For those plant units, only the first value of the city name is considered. There are 847 entities with missing coordinates or coordinates outside Brazil. Once the coordinates have all been replenished, information on the federal states is updated with the coordinates.

The installed capacity of each power plant unit determines its physical size. In the original data set, the capacity is given in kilowatts and provided separately for granting, regulation and inspection purposes. The granted capacity is the capacity considered in the act of granting, whereas the regulated capacity corresponds to the capacity considered from the commercial operation of the first generating unit. The actual guaranteed power, on the other hand, represents the average actual production. Given that information on the regulation capacity may not be available for all power plant units, the granted capacity is deemed a suitable representation of the installed capacity. In addition, the units of installed capacity are converted to megawatts.

The information on the types of power plants in the original data set is divided into eight types: large hydropower plant, small hydropower plant, mini-hydropower plant, wave power plant, thermoelectric plant, thermonuclear plant, wind power plant, and PV power plant. These types are summarised in Table 3.10. In this work, the wave power plant "Porto do Pecém" in the state of Ceará, which has a power of 0.05 MW, is classified as a small hydropower type. Depending on the properties of the fuel source, thermal power plants are subdivided into oil-fired, natural gas-fired, coal-fired, and biomass-fired. In total, therefore, there are ten generic types of plants. Figure 3.4 illustrates the results of power plant distribution.

Most entities have incomplete dates for commissioning and decommissioning. According to ONS (2022b), the missing date information indicates that the plants

Table 3.10: Power plants description and their abbreviations[a]

Short name[b]	Full name	Abbreviation[c]	Explanation
hydro	Large hydropower plant	UHE	The hydropower plant has a capacity greater than 5 MW but less than 50 MW, excluding those identified as small hydro.
small_hydro	Small hydropower plant	PCH	The hydropower plant has a capacity greater than 5 MW and up to 30 MW with reservoir area of up to 13 km^2.
mini_hydro	Mini hydropower plant	CGH	The hydropower plant has a capacity of 5 MW or less.
wave	Wave power plant	CGU	It harnesses kinetic energy from ocean waves to generate electricity, derived from the dynamic water movement of the sea. Porto do Pecém in Ceará, Brazil, stands as the only facility of this kind in Brazil with a capacity of 0.05 MW.
biomass_thermal, fossil_thermal	Thermoelectric plant	UTE	Electricity generating involves harnessing the energy released from various heat-generating sources such as bagasse from various plants, wood chips, fuel oil, diesel, natural gas, enriched uranium, and natural coal.
nuclear	Thermonuclear plant	UTN	Thermoelectric power plant relies on the energy released through nuclear fission of uranium as a primary energy source.
on_wind	Wind power plant	EOL	The conversion of wind's kinetic energy into electrical energy is accomplished through onshore wind power plants. It is important to note that offshore wind farms, referred to as off_wind, are not currently operational and lack an official abbreviation.
solar_pv	PV power plant	UFV	It converts the sun's energy into electricity through the photovoltaic effect, where materials exposed to light produce a voltage or corresponding current.

[a] The information is sourced from EPE and MME (2020), ANEEL (2021b).
[b] The terms are the short name used in the model (Deng 2023a) and in Section 3.2.3.
[c] The abbreviations are based on the full names of the types of power plants in Portuguese. These abbreviations are commonly used in Brazilian publications and institutions and have been deliberately retained here for convenience and understanding.

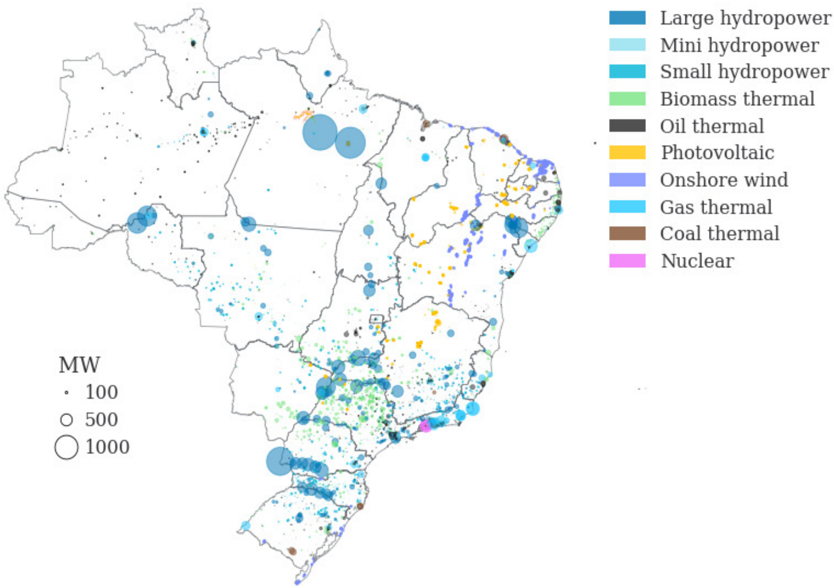

Figure 3.4: Existing and planned power plant capacity.

are active. For entities where the commissioning and decommissioning dates are both missing, it is presumed that these plants are still operational. Finally, the reference year is added.

In the post-processing, the installed capacity of the power plants is aggregated by the federal state for each reference year according to the type and operational status of the power plant. This aggregation encompasses capacities derived from public service, self-generating, or independent production. The installed capacity of the reference year is determined under the assumption that the operational status of the plants is operational and that the commission time precedes the base year or is not specified. Records in the original data set pertaining to power plants with an operational status of either "construction" or "not started construction" are reclassified as "planning". Finally, the values are accumulated according to the federal state, plant type, and operational status. The installed capacity differs based on the specified reference year, while the planned capacity is the same across all reference years. This is because 68.8% of the entities lack a decommissioning date, and as such, the decommissioning information is disregarded. As a result, the installed and planned capacity (GW) for each reference year is available under the dedicated project folder (Deng 2023a).

The exclusion of economic parameters of the generating units is intended. Cost assumptions for each power plant, based on fuel type, are provided by Jensen and Pinson (2017). However, there is a lingering scepticism regarding the applicability of these cost assumptions in the scenario study. Harmonising cost assumptions for generators is a complex task due to the wide range of cost estimates across different sources for each generator technology. In addition, the base year, scenario year, and technology horizon significantly impact the cost assumptions in the scenario analysis. For example, EPE (2020b) gives the cost assumptions for the scenario year 2029, which is used for the Brazilian National Ten-Year Energy Research Study.

Furthermore, when comparing the data set presented in this dissertation with the European data set of power plants provided by Powerplantmatching (Gotzens et al. 2019), several gaps in information become apparent. These gaps involve the dates of installation, retrofitting and decommissioning, as well as the type of each hydroelectric plant and the relevant technical parameters such as volume, dam height and storage capacity.

3.2.4 Installable capacity for biomass thermal plants

Biomass can be burnt directly for heating or power generation or converted into oil or natural gas substitutes. In the last 15 years, the generation of electricity from biomass thermal plants in Brazil has been increasing, from 6 GW to 14 GW, accounting for 13% of the capacity matrix of electricity for 2020. Sugarcane bagasse is the primary source of biomass (ANEEL 2021b).

3.2.4.1 Data collection

To the knowledge of the authors, there are no studies that have specifically investigated the energy production potential of biomass thermal plants in Brazil. However, Portugal-Pereira et al. (2015) address the geographically installable capacity. Estimations suggest the potential for installable capacity from agricultural and agro-industrial residues where it is technically, environmentally sustainable and economically feasible. The theoretical capacity defines the maximum available bioenergy, subject to biophysical and agroecological conditions that hold down the growth of crops and residues, such as temperature, solar radiation, rainfall, and soil properties. Environmental constraints limit this potential, as agricultural residues are critical biome regulators. As for the environmentally sustainable potential, the authors apply a theoretical constraint for removing residues to ensure environmental sustainability, such as preventing soil erosion and maintaining nutrient recycling. On the other hand, techno-economic viability refers to the fraction of the environmentally sustainable potential available under technological possibilities and logistic restrictions. It considers the competition of other non-energy uses of residues. As a result, only biomass residues spread within a 50 km radius from the power substations are economically feasible to be used in centralised power plants based on direct combustion of biomass in a Rankine power plant with an average efficiency of 18%. According to their assessment, the total economic potential in Brazil is 39 $\mathrm{TW\,h/yr}$. With permission, the results of the research on economic potential $\mathrm{MW\,h/yr}$, spatially resolved at the municipal level, have been shared.

3.2.4.2 Data processing

The primary energy source used in today’s biomass thermal plants is sugarcane bagasse, which is the dry pulpy substance remaining after grinding sugarcane to extract their juice. The contribution of residues is relatively small and thus negligible. Therefore, only the economic potential of biomass from residues is considered as additional installable capacity beyond the already existing and planned installations.

As a first step, the potential production is converted into the additional installable capacity by assuming an annual availability factor of biomass at 0.6 (Soria et al. 2016). Then the values are aggregated at the federal-state level.

The biomass thermal plants referenced in Soria et al. (2016) come from centralised plants previously published by ANEEL, which is no longer accessible. It is assumed that the geographic distribution of the biomass thermal plants considered in Soria et al. (2016) is similar to that covered in the Section 3.2.3. To facilitate calculations, a constant number of 8,760 hours per year is used, regardless of whether it is a leap year. This simplification allows us to calculate the geographically installable capacity for each state as follows:

$$C_i = \sum_i \left(\frac{PR}{f \cdot 8760} + CI_i + CP_i\right) \tag{3.3}$$

where

C	: geographically installable capacity, MW
i	: the federal state
PR	: the residual potentials at municipality level, MWh
f	: annual availability factor
CI	: installed capacity of biomass thermal plants, MW
CP	: planning capacity of biomass thermal plants, MW.

Since the installed capacity differs for each reference year, the geographically available installed capacity varies accordingly. Therefore, data is presented for each reference year to illustrate the changes.

3.2.5 Electricity load profiles

Future energy systems are likely to shift to renewable electricity as the primary energy source. As a result, the design of these systems must increasingly consider both the temporal and spatial distribution of energy consumption. This is particularly relevant due to the mounting prominence of vRES (highly fluctuating in time and asynchronous across regions) and the dynamic changes in consumption patterns, such as the rising adoption of more efficient electric vehicles supplanting their fossil fuel counterparts, as well as the amplified cooling demand resulting from climate impact and the ongoing evolution of digitisation (Brown et al. 2018b, Davis et al. 2018).

3.2.5.1 Data collection

EPE analyses and projects electricity consumption and load in the Brazilian electric sector by sourcing historical data and projections from distribution agents, self-producers, and free consumers (EPE 2022a). The ONS, on the other hand, oversaw the reported the load and the generation of power plants of national power system it supervised until 02/03/2021. Since then, ONS began reporting on a global load, which includes the generation of plants outside its direct oversight (ONS 2022e).

ONS publishes hourly load profiles for its four electric regions in SIN (ONS 2021d), while EPE provides annual sectoral electricity consumption or consumers for each federal state (EPE 2021). Table 3.2 indicates each electric region and the federal states it contains. ONS's hourly profile covers the period of 1999-2020, while the EPE data set ranges from 2012 to 2020 (retrieved in April 2021). However, the value of total power consumption provided by ONS is greater than that of EPE (cf. Table 3.11).

The disparity between the data sets provided by ONS and EPE chiefly originates from the physical losses in transmission and distribution, along with their physical representation in the SIN (ONS et al. 2016). An illustration of this difference, focusing on the regional variations, is given in Table 3.11. It should be noted that the time series data, as released by ONS, adheres to the UTC-3 – Brasília Time.

Table 3.11: Comparison of annual electricity consumption differences by electric region between ONS and EPE data sets.

Year	N	NE	S	SE
2012	-4%	17%	11%	14%
2013	7%	16%	10%	9%
2014	17%	14%	9%	12%
2015	20%	16%	10%	13%
2016	21%	17%	12%	14%
2017	22%	18%	12%	14%
2018	24%	19%	11%	13%
2019	25%	18%	11%	14%
2020	22%	19%	11%	13%

3.2.5.2 Data processing

The ONS data set includes an hourly time series for each of its four electric regions in the SIN. However, the ONS data set contains one missing value per year per region, except for 2019 and 2020. Among the missing values, the highest count is observed in 2014, with a total of 25 missing values, specifically for the 1st of February 2014. To address this, values from the preceding week replace the missing ones. In addition, six negative values in the time series for the northern region are trimmed to zero as they are a gross error.

Meanwhile, the EPE data set assists in decomposing the ONS load profiles at the Brazilian federal-state level. The decomposition relies on two allocation factors – annual consumption and number of consumers. This assumption made means that the seasonal, intraweekly, and intraday variations in load profiles remain consistent among states within the same electric region, while the magnitude may differ. The load profiles for each federal state contain the transmission and distribution losses endogenously. It is postulated that states belonging to the same electrical region have the same pattern and different magnitude loss curves. This assumption, though potentially conservative, is based on the inclusion of losses for transmissions between federal states in the Section 3.2.2, which aims to accurately reflect these losses within the provided data set.

As the EPE allocation factors only apply for 2012-2020, the time horizon for electricity consumption in the federal states provided in this study is limited to this period. Figure 3.5 illustrates the results of the electricity load in the federal state, which is the sum of electricity consumption and the physical losses in the SIN.

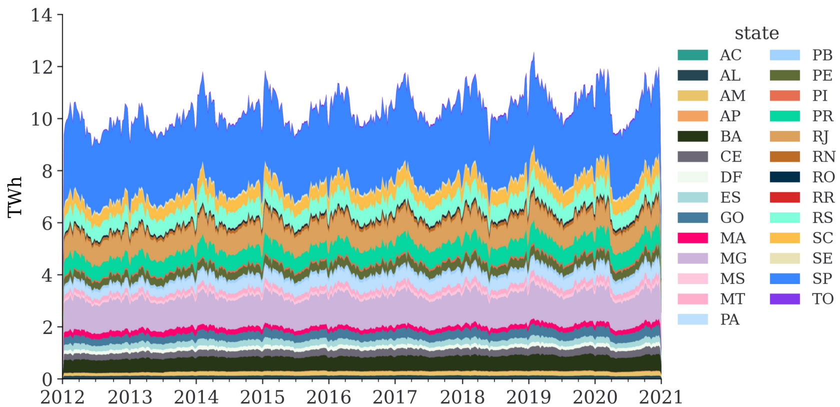

Figure 3.5: Electricity load at federal states (weekly) distributed by annual consumption. The data set to be published is resolved hourly.

3.2.6 Scenarios of energy demand

Energy demand scenarios facilitate a strategic assessment of possible pathways for long-term planning and their respective internal consistency and associated uncertainties. Sector-specific modelling allows variations in demand from different resources and sectors to be estimated nationally. However, diverse models, methods, and assumptions lead to different scenarios and represent research positions.

In energy system studies, future electricity demand can come from other studies or be calculated endogenously in the energy system model. Those energy studies that treat future electricity demand as exogenous need to clarify whether the electricity demand adopted from other sources considers mitigation measures consistent with Brazil's first National Development Plan (2022 update), the Paris Agreement, or other mitigation targets. Otherwise, these studies cannot conclude the contribution of a given scenario to the mitigation targets (e.g., Dranka and Ferreira (2018)). This makes it difficult to interpret their results, especially whether they are consistent with the Paris Agreement.

The updated first Brazilian NDC confirms the commitment to reduce its GHG emissions by 37% in 2025, compared to 2005. Additionally, Brazil pledges to reduce its emissions by 50% in 2030, compared to 2005 and aims to achieve climate neutrality by 2050 as its long-term objective (UNFCCC 2022). Brazil's updated NDC is broad in scope with economy-wide absolute targets. It considers the means of implementing, undertaking mitigation, and adaptation actions across all economic sectors (UNFCCC 2022). These targets would be translated into sectoral policies and measures to be detailed and implemented by the Brazilian federal government. These sectoral initiatives must be exogenously modelled to calculate the sectoral electricity consumption in each region. Only then can energy system models use sectoral electricity consumption as input in energy system studies, allowing for a better understanding of their impact on power system operation and expansion.

A comprehensive understanding of sectoral energy demand published in reputable studies enables researchers in energy system modelling to accurately emulate demand-related parameterisation and manage uncertainties.

3.2.6.1 Data collection

There are numerous scenarios for the future energy demand of Brazil. Three often used ones are: (i) World Energy Outlook (WEO), (ii) EPE's long-term National Energy Plan (Portuguese: O Plano Nacional de Energia) (PNE), and (iii) exogenous energy demand studies by COPPE researchers.

The WEO scenario by the International Energy Agency (IEA) is considered the most authoritative source of insights into the world's energy demand. It updates its sector demand scenarios annually, region by region. The latest WEO study for 2021 (IEA 2021a), "WEO2021" in the following, provides reference data of historical demand for 2010, 2015, 2019, and 2020, as well as the sectoral energy demand scenarios for Brazil to 2050, with a five-year span.

EPE's PNE is a fundamental instrument for Brazil to outline the government's strategy regarding the expansion of the energy sector in the coming decades. The latest plan, 2050 PNE (EPE and MME 2020), was released in December 2020 and extends the horizon to 2050. 2050 PNE provides projections of sectoral demand every ten years (i.e., 2030, 2040, and 2050) depending on the economic and sector assumptions. This comparison relies on the 2050 PNE study (hereafter "PNE2050"), in the following. However, the PNE2050 does not provide numerical data, instead presenting it as a table or charts for each end-use sector. These values, therefore, need to be extracted manually and a CSV file created accordingly.

COPPE is the most prestigious research institute in Brazil that studies energy planning in Brazil and the world. Their scenario studies are referred to as "COPPE". Among the extensive collection of 133 scenarios offered by COPPE, the three latest scenarios are selected due to their distinct transition paths. COPPE scenarios have five-year time steps, although the available data only contain the years 2030, 2040, and 2050. Sectoral demand for 2010 or 2015 is the starting point for the scenario assumptions. In the following, the three COPPE scenarios are shortly described.

To enhance the transparency of energy scenarios (Cao et al. 2016), this work creates a matrix of energy demand scenarios. This matrix (shown in Tables 3.12

to 3.14) provides a summary of the main criteria used by previous studies to model final energy consumption scenarios for Brazil until 2050, following the comparisons described in Junne et al. (2019). Trend scenarios are considered, which maintain a level of effort in climate action similar to current policies and NDCs, and ambitious mitigation scenarios aligned with the global goals until the end of the century on the stabilisation of the average temperature increase of the planet relative to pre-industrial times by 2 °C and 1.5 °C. These scenarios highlight the role that electrification may play in the different sectors to achieve climate goals. However, the electrification of the transport sector in Brazil may not be achievable as in other regions due to the already high share of biofuels and weak distribution of electricity grids (EPE and MME 2020). This is especially evident in the "lowBECCS" scenario, which signifies a low role for bioenergy with carbon capture and storage.

Table 3.12: Comparative analysis of the energy demand scenarios in Brazil – WEO21 study.

Study	**IEA WEO2021**			
Scope	(i) global and regional outlooks, (ii) environmental impacts of energy use on emissions and pollutants, (iii) impact of policy actions and technological change, iv) investment requirements for the fuel supply chain to meet projected energy demand, (v) prospects of modern energy access.			
Scenario	Net Zero Emissions by 2050 Scenario (NZE)[a]	Announced Pledges Scenario (APS)[b]	Stated Policies Scenario (STEPS)[b]	Sustainable Development Scenario (SDS)
	The scenario envisions a "well below 1.5 °C" pathway,[c] leading the global energy sector to achieve net CO_2 emissions by 2050 and meet key energy-related Sustainable Development Goals (SDGs). This scenario considers only the emissions reductions within the energy sector.	It assumes full and timely fulfilment of all climate commitments made by governments, including NDCs and longer-term net-zero goals, objectives, and intentions.	It assesses sector-by-sector to extrapolate current or developing policies and governmental measures around the world.	This outlines an integrated scenario striving to limit temperature rise to "well below 2 °C"[c] and accomplishing the central SDGs, with a target of achieving net zero global emissions by 2070. The associated SDGs include (i) universal access to affordable, reliable, sustainable, and modern energy services by 2030 (SDG 7), (ii) significant reduction in air pollution (SDG 3.9), and (iii) effective action to mitigate climate change (SDG 13).
Narrative	Regarding Brazil, variations exist in the macroeconomic and demographic assumptions across scenarios. Energy demand forecasts are based on the average retail price of fuel used in the end-use, generation, and other conversion sectors. End-use prices are derived from the projected international prices of fossil fuels and subsidy/tax levels. The price of CO_2 differ according to each scenario. However, presenting a comprehensive narrative for each end-use sector within Brazil poses a challenge.			

Model	The analysis employs a hybrid model that combines the data-intensive IEA's World Energy Model (WEM) of the global energy system with the Energy Technology Perspectives (ETP) model, which evaluates technical and economic parameters of energy technologies. The total final energy demand equates to the sum of energy consumption across all end-use sectors modelled. The assessment of the energy consumption considers significant sectoral and end-use detail, derived from historical data on the inventories of existing energy infrastructure and relevant socioeconomic variables. This includes, for example, the number of vehicles in the transportation sector, the production capacity of the industrial sector, and the floor space of buildings. Each sector has a tailored model for energy services demand. For instance, in the residential sector, the demand is divided into space heating, water heating, cooking, lighting, appliances, and space cooling.	
Key drivers	Population • Growth rate (2010-50): 0.3%/year • 2050 Population: 229 million • 2050 Urbanisation (% of population): 92% GDP: • Growth rate (2020-50): 2.6%/year Remaining fossil fuel sources • Oil • Nature gas • Coal Fossil fuel prices • Nature gas • Steam coal	End-use prices • Fuel end-use prices • Electricity end-use prices • Wholesale electricity price Other factors • Carbon price • Derivation of a simplified merit order for thermal power plants • Calculation of average marginal cost in each merit order segment • Estimate of wholesale price based on average marginal cost • Subsidies to fossil fuels
Source	IEA (2021a,b)	

[a] The scope of this analysis is global and does not extend to regional studies.

[b] The research does not aim to achieve a specific result.

[c] The "well below 1.5 °C" and "well below 2 °C" are goals announced in Paris Agreement, limiting the average global temperature increase by 2100 to 2 °C above pre-industrial levels without temperature overshoot (50% probability).

Table 3.13: Comparative analysis of the energy demand scenarios in Brazil – PNE2050 study.

Study	**EPE PNE2050**	
Scope	The 2050 PNE, published by EPE, outlines the government's strategic long-term vision.	
Scenario	Expansion Challenge scenarios (ECS)	Stagnation scenarios (SS)
	The scenario anticipates strong growth in total energy demand, aligned with a national average annual Gross Domestic Product (GDP) growth rate of 3.0%. It projects a 2.2% increase per annum in total final energy consumption from 2015 to 2050, with accelerated growth (2.5%) for the first 15 years, which is more than twice the 2015 consumption.	The scenario reflects that per capita energy consumption remains at 2015 level, with an average annual GDP growth rate of 1.6%. Total energy consumption could grow by an average of 1.4% per year (over 10% in total) from 2015 to 2050.
Narrative	The scenarios consider a stable economic, political, institutional, and social environment that allows for the completion of important structural reforms. These reforms are poised to significantly influence the business environment, investment, and productivity, which, in return, contribute to GDP growth. Therefore, the total final energy demand experiences an increase with a diminishing share of petroleum products and an increasing share of electricity, largely driven by the residential sector.	
Model	The forecast methodology for energy demand consists of three modules: economics study, demand projection, and demand integration. The assumptions are derived from discussions of the main moderators and key uncertainties across sectors (industry, agriculture and livestock, buildings, services, and transport). Long-term economic scenarios serve as the main informational inputs. By elaborating detailed sectoral scenarios, the model estimates national-level changes in demand by source and by sector.	
Key drivers	Population: • Growth rate: 0.3%/year • 2050 Population: 226 million • 2015 Urbanisation: 86% • 2050 Urbanisation: 89% GDP: • GDP growth rate (2016-50): 3.0%/year • GDP per capita: 2.8%	Number of households: • Inhabitants/household (2015): 3.2 • Inhabitants/household (2050): 2.3 • Households (2015): 33 million • Households (2050): 98 million
Source	EPE and MME (2020)	

Table 3.14: Comparative analysis of the energy demand scenarios in Brazil – COPPE study

Study	**COPPE**		
Scope	The integrated long-term scenarios present the demand for Brazil for each five-year period from 2010 to 2050 or 2100, using representative time slices. This analysis explores the competition between technologies and energy sources to meet energy services demand in a cost-efficient way, adhering to policy and emissions targets. The modelled end-use sectors include the industrial, energy, transportation, residential and commercial, and agricultural sectors.		
Scenario	Business as usual (BAU)	2Deg2030	lowBECCS
	The BAU scenario uses the most probable socioeconomic assumptions, extrapolated from the second marker baseline scenario from the Shared Socioeconomic Pathways (SSP2). It does not account for any additional climate policies post-2010.	This mitigation scenario, 2Deg2030, is consistent with increasing global warming up to 2 °C without overshooting above pre-industrial levels by 2100. It builds upon the submitted NDCs actions up to 2030. After 2030, it transitions cost-effectively towards a 2 °C pathway, constrained by a national carbon budget. A national (2011-2050 accumulated) budget of 22 Gt of CO_2[a] is used for simulating the scenario. The carbon budget is derived from a global budget of 1000 Gt of CO_2 in the period from 2011 to 2100[b]. The same socioeconomic assumptions as in the BAU scenario are used in this scenario.	The lowBECCS scenario, another mitigation scenario, aligns with an increase in global warming up to 1.5 °C above pre-industrial levels in 2100. In this scenario, described as an "end-of-century budget" scenario, immediate action in the near term (2020-2030) is built on implemented national policies (NPi) as of 2020. Over the long-term, the CO_2 pathway is constrained by cumulative CO_2 emissions over the entire century, allowing high-temperature overshoot and global net-negative CO_2 emissions (NNCE) in the second half of the century. It utilises a global CO_2 budget of 400 Gt from 2018-2100. This scenario is conservative regarding the role of Bioenergy with Carbon Capture and Storage (BECCS) on a global scale. To only consider the sustainable global BECCS potential, this technology is capped at around 8 Gt CO_2/year in 2100. The middle-of-the-road socioeconomic conditions based on SSP2 are incorporated in this scenario.

Narrative	The presented scenarios serve scientific purposes and can inform decision-making at both the Brazilian government level and globally. The scenarios exogenously determine the useful energy demands for each consumption sector, the food demands, and the reforestation and deforestation. For the short-term modelling, official public data is considered, while international scenarios are used as a reference for the long-term. All three scenarios presented share the same population growth and socioeconomic development trajectory, specifically SSP2, but exhibit different levels of ambition towards achieving global climate goals.		
Model	It is calculated during the COMMIT project using the BLUES model.[c]		This scenario is calculated by the COFFEE v1.1 global model during ENGAGE project.[d]
Key drivers	Population • Growth rate (2015-50): 0.31%/year • 2050 Population: 226.3 million GDP • Growth rate (2015-50): 2.87% • GDP in 2050 (billion US$): 5370.1	Population • Growth rate (2015-50): 0.31%/year • 2050 Population: 226.3 million GDP • GDP growth rate (2015-50): 2.75%/year • 2050 GDP (billion US$): 5257.9	Population • Growth rate (2015-50): 0.40%/year • 2050 Population: 231.9 million GDP • Growth rate (2015-50): 4.01%/year • 2050 GDP(billion US$): 7042.9
Source	Baptista et al. (2022), van Soest et al. (2021)		Riahi et al. (2021)

[a] In this context, emissions refer specifically to the CO_2e of GHG emissions.

[b] The global carbon budget discussed here is linked with a high probability (over 0.66) of maintaining global warming levels below 2 °C by the year 2100, as reported by Allan et al. (2021).

[c] BLUES employs Mixed-integer Linear Programming (MILP) to minimise the total cost of expanding the energy-land system to meet the expected demand for energy services and food. It combines technical, economic, and environmental variables from over 8,000 technologies, with imposed constraints such as reforestation and deforestation scenarios, to yield an optimal solution for the energy and Agriculture, Forest, and Other Land Use (AFOLU) sectors. Additional information can be found at the provided link: `https://www.iamcdocumentation.eu/index.php/Reference_card_-_BLUES`.

[d] The Computable Framework for Energy and the Environment (COFFEE) is a global multi-sectoral partial equilibrium model. It includes 18 regions (including Brazil), and uses the energy system in 2010 as a basis, with a projected horizon of 2100 in five-year time steps. The model aims to assess the potential synergies and trade-offs between energy systems, environmental concerns and climate policy. All energy and land-use systems are included, with a hard link between the two. The macroeconomic inputs into the model come from either exogenous macroeconomic drivers indicating demand growth over time or from the TEA model, which pulls from the SSP database.

3.2.6.2 Data processing

The initial step involves normalising the units of demand values for the three studies to PJ because they are different in the raw data, i.e., PJ for the WEO2021, Mtoe (million tonnes of oil equivalent) for PNE2050 and EJ for COPPE. After that, aliases are assigned in a format of `XXXX_YYYY` to represent the studies and the corresponding scenarios. For example, the alias `COPPE_BAU` represents the Business as Usual (BAU) scenario for the publication of the COPPE studies.

The end-use sectors and energy carriers in PNE2050 and COPPE are aligned with WEO2021 based on IEA (2021a), EPE and MME (2020), Baptista et al. (2022), van Soest et al. (2021), Riahi et al. (2021), as the different definitions prevent comparisons between them. Table 3.15 describes the correspondence. WEO2021 does not provide a value for the end-use sector named "Other". The value for the end-use sector "Other" is considered to be the difference between total final consumption (TFC) and sectoral demand:

$$\mathrm{Other}_i = \mathrm{TFC}_s - D_{s,i}, \tag{3.4}$$

where

Other_i	: energy demand for energy carrier i, in the end-use sector of "Other"
TFC_s	: total final consumption for end-use sector s
s	: end-use sector, $s \in \{\mathrm{Transport, Industry, Buildings}\}$
i	: energy carrier, $i \in \{\mathrm{Total\ liquids, Total\ gases, Total\ solid\ fuels, Total}\}$
$D_{s,i}$	: energy demand for the end-use sector s and the energy carrier i.

PNE2050 data provides the most granular energy carriers, followed by WEO2021, while the COPPE scenarios divide the energy carriers into "electricity", "liquid", "gas", "solid", and "hydrogen". Table 3.15 lists all energy carriers for PNE2050. The WEO2021 scenario data set includes TFC, the total value of energy carriers by physical state, i.e., "total liquids", "total gases", "total solid fuels", as well as some of the more subdivided energy carriers. For instance, "total liquids" consists of “oil products”, “liquid biofuels”, and “hydrogen-based liquid fuels” (IEA 2021a). However, the WEO2021 does not provide data for “liquid biofuels”. Although an energy carrier, “hydrogen”, is provided in the COPPE scenarios, all scenarios have zero values. Therefore, the “hydrogen” is omitted. Even when hydrogen as final energy is zero, there is a critical hydrogen production as an intermediate energy carrier, which is input to produce other final energy forms. This intermediate product is not reported.

Table 3.15: Correspondence between different studies.

WEO2021[a]	PNE2050	COPPE
	end-use sector	
Industry	Industry	Industry
Transport	Transport	Transportation
Buildings	Residential, Service	Residential, Commercial
Other	Agriculture, Non-energy use	Other Sector
	energy carrier	
Total	Total	Total
Electricity	Electricity	Electricity
Total liquids	Oil products, Diesel fuel, Other oil products, Fuel oil, Gasoline C, Hydrated ethanol, Kerosene/aviation gasoline	Liquids[b]
Total gases	Natural gas, Liquefied petroleum gas (LPG)	Gases[c]
Total solid fuels	Coal, Wood, Wood and charcoal, Sugarcane, Other	Solids

[a] The aggregation process employs the definitions for the end-use sectors and energy carriers as outlined by the WEO21 (IEA 2021a).
[b] It includes ethanol, biodiesel, and advanced fuels.
[c] It includes natural gas and LPG.

At the top of Figure 3.6, the total final energy consumption by the combined sector for “Transportation”, “Industry”, “Buildings”, and “Others” is presented. The COPPE and EPE scenarios do not report the consumption of “Others”,

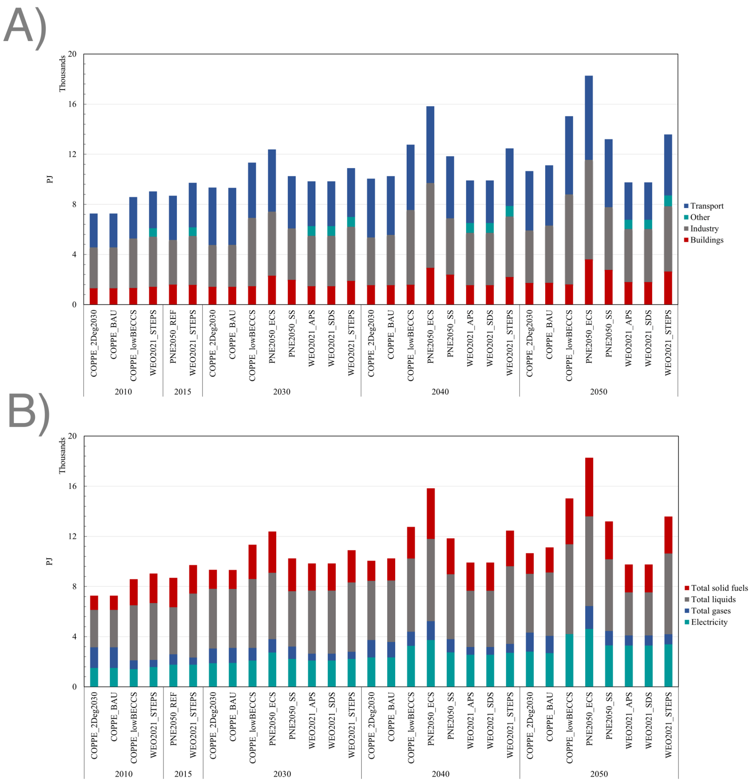

Figure 3.6: Comparison between demand scenarios by different studies – A) by sector and B) by energy carrier.

with EPE's PNE2050 indicating that the three reported sectors account for more than 80% of final energy consumption. "Others" basically considers energy consumption associated with agriculture and livestock. The average final energy consumption in 2015 for the three most important sectors was 7.9 PJ, increasing to 10 PJ in 2030 and reaching 12.4 PJ in 2050. In the long term, there are important variations depending on the scenario, as detailed in Tables 3.12 to 3.14.

The bottom of Figure 3.6 shows the total final energy consumption by energy carrier for each scenario considered. In the long term, electrification is increasingly critical in the three sectors with the highest consumption. Electricity consumption represented 19% in 2010, and the average between the scenarios indicates that it could reach 21% in 2030 and 28% in 2050. There are essential differences in the role that electrification could play between scenarios, especially in the transport sector, where electrification may decline depending on the advancement that BECCS technologies may have in the long term. With a significant development of BECCS, total electricity consumption would be approximately 1.8 PJ in 2050, while with a conservative development of BECCS, total electricity would be approximately 4.4 PJ.

3.2.7 Inflow of hydropower plants

Hydropower is an essential sustainable energy source, particularly in developing countries such as Ecuador, China, and Brazil (IEA 2021a). Hydroelectricity constitutes the largest share of renewable energy sources in the total power generation matrix. With the increasing penetration of vRES, properly representing hydropower in the power system analysis becomes crucial. This is because run-of-river (mostly low-head) hydropower plants usually provide a constant base load (in contrast to vRES). Additionally, other hydropower plants with reservoirs or pump-storage units can compensate for the volatile load introduced by vRES (Sterl et al. 2021). The theoretical output of electric power from hydropower plants is determined by the combination of available water flow and available head height at each location (Killingtveit 2019). The power output is usually limited to the plant's nameplate capacity at the turbine's maximum flow rate.

ONS regulates the capacity of the reservoir system and dispatches 163 plant units of different types, including ten reservoirs, 92 run-of-river units, 60 hydropower plant units with reservoirs, and one pumped storage (ANA 2022). The term "unit", in this context, refers to a cluster of hydropower plants dispatched by ONS. The hydraulic operation of the reservoir systems in Brazil can provide about 210 TWh storage energy (expressed as MWmês in the original data set, where 1 MWmês = 720 $\mathrm{MW\,h/month}$), of which about 69% is located in southeast/central of the SIN, followed by the northeast region at about 18%. The southern and northern regions of the SIN account for 7% and 6% respectively (ONS 2022d).

3.2.7.1 Data collection

Energy system optimisation models often account for known inflows and outflows when modelling hydropower (Stoll et al. 2017). The hydropower representation is typically based on historical operating patterns (time series), which indicate the constraints inherent to the year referenced (Dennis et al. 2011).

ONS publishes time-series data on reservoir inflows, including both Stored Energy (Portuguese: Energia Armazenada) (EAR) and Affluent Natural Energy (Portuguese: Energia Natural Afluente) (ENA) (ONS 2021c). These data sets, updated regularly, offer a range of temporal resolutions from daily to monthly and are aggregated from individual reservoirs to broader categories like basins or equivalent energy reservoirs (Portuguese: Reservatório Equivalente de Energia, REE). EAR reflects the energy potential of the reservoirs based on their water levels, whereas ENA denotes the energy flowing into the hydropower system at aggregated levels. Although these data sets have been utilised in past research (Diuana et al. 2019, Fichter et al. 2017), the absence of metadata obscures the specific attributes they refer to.

Specifically, EAR highlights the energy potential from stored water in reservoirs, which can be used for power generation at both the original and downstream plants, which presents complexities. When the reservoir is at its fullest, this storage capacity of the system is the maximum EAR. The ENA data set has two attributes: gross ENA and storable ENA. The former measures the electricity generation at 65% of the useful operating level of the hydropower plants, corresponding to the natural water flow into the reservoir. The latter equals the difference between the natural water inflow and the flow into the reservoir. Given this, this dissertation employs the ENA attribute to depict the inflow to the hydropower system.

However, using the ENA data set for federal-state level analysis requires an understanding of the cascade of hydropower stations. Even though ONS reveals the basins where the power stations are situated, it limits details to plant names. The challenge arises when attempting to align hydropower stations from ONS (2021c) with the data set mentioned in Section 3.2.3 due to inconsistent nomenclature. To navigate this issue, this dissertation adopts the ENA, spatially resolved by electric region, to represent the hourly feed-in to the hydropower plants and further disaggregates it at the federal-state level.

3.2.7.2 Data processing

The ENA data used is daily resolved and is given in a unit $\mathrm{MW\_month}$ (Portuguese: $\mathrm{MWmês}$). This data is converted to MWh as it is equivalent to the 720 $\mathrm{MW\,h/month}$ (Diuana et al. 2019).

For a representation of hydropower plant inflows in the federal states, a correlation is drawn to the installed capacity for the reference year. This capacity, sourced from the Section 3.2.3, encompasses hydropower plants of different sizes. As a result, the aggregated level of inflow of hydropower plants is achievable as depicted in Figure 3.7. Since the installed capacity for a given reference year has two operating states – operating and planning, the inflow data set provided in this study can be allocated either by installed capacity or by the total value of installed and planned capacity.

Finally, the daily inflows are apportioned evenly across each hour, thereby deriving the hourly inflows.

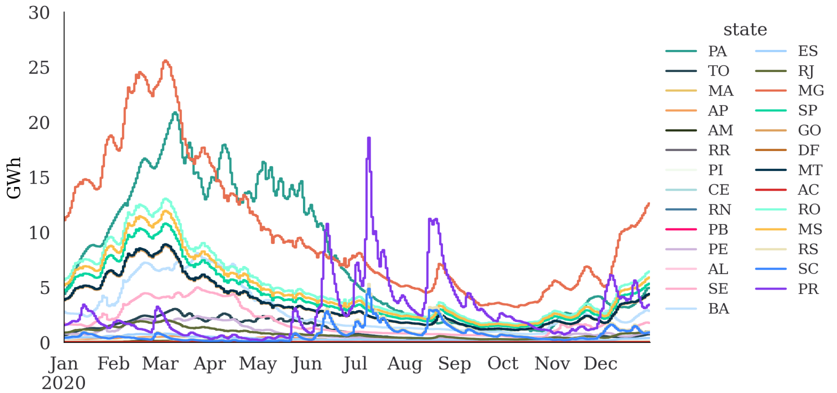

Figure 3.7: Per federal state inflow into hydropower plants for the reference year 2020. Note: allocation is based on the installed and operated capacities.

3.2.8 Variable renewable potentials (wind and solar)

For planning future energy systems, knowledge of the technical generation potential of vRES is essential. In particular, this includes geo-referenced data on the nominal installation capacity that can be installed in a specific area, along with an hourly generation time series due to the intermittent generation.

3.2.8.1 Data collection

The global resource assessment tool, EnDAT, assesses the renewable energy generation potential of different technologies such as PV, onshore, and offshore wind turbines. The methodology, as described in Scholz (2012) for the EU, is adapted for global application in Stetter (2014). So far, EnDAT is only available internally at the German Airspace Center (DLR). However, it is currently being revised, translated into Python, and prepared for open-source publication, slated for the first quarter of 2023. EnDAT requires inputs of weather resource maps at an hourly temporal resolution and a spatial resolution of $0.09° \times 0.09°$, along with static land cover maps at a resolution of $0.09° \times 0.09°$. As output, EnDAT provides

(i) spatially resolved maximum generation capacity and (ii) relative profiles of hourly power feed-in from wind and solar energy. The spatial output resolution of $0.09° \times 0.09°$is aggregated to the level of administrative regions, namely, the federal-state level.

For calculating the installable capacity, two sets of maps are used. One serves as areas of exclusion (cf. Table 3.16), while the other serves as suitability criteria to determine the share of the remaining available area (cf. Table 3.17). The spatial land cover maps are based on the Copernicus land cover data set (Buchhorn et al. 2020), the global lakes and wetland database (Lehner and Döll 2004), IUCN protected area categories (Dudley 2013), and a digital soilmap of the World (for dunes, glaciers, saltpans) (Land and Water Development Division, FAO 2020). The roughness length is calculated using the land cover maps and a roughness lookup table (Silva et al. 2007). Furthermore, spatio-temporally resolved maps from the ERA5 data set (Hersbach et al. 2020) are employed to generate the feed-in time series. It contains hourly resolved data for Global Horizontal Irradiance (GHI)[2], wind speed, and temperature at a 31 km spatial resolution.

3.2.8.2 Data processing

Geometric constraints are used to calculate the maximum installation density, i.e., taking into account the wake for wind, and using the maximum shading of the assumed module angle for PV during the winter solstice. The density is restricted by the available area, considering information on the land cover of the area, such as bare ground, crops, grasslands, mosses, shrubs, forests, urban area, and roughness, as well as excluded areas, such as distance from settlements, elevation, mining sites, protected areas, glaciers, slopes, wetlands, and water depth for offshore winds. An exclusion mask is defined if any exclusion criteria are met or any inclusion criteria are violated. This mask restricts the computations to

[2] Global Horizontal Irradiance (GHI) refers to the sum of the beam and the diffuse solar radiation on a surface (Duffie and Beckman 2013, p. 10).

Table 3.16: Utilisable areas for the EnDAT analysis. m denotes the value constrained according to the map, while the provided integer categories are excluded.

Criteria	Map	PV	Wind onshore	Wind offshore
inclusion	slope (°)	$m < 45°$	$m < 45°$	—
inclusion	distance to settlement (km)	$1 < m < 1000$	$1 < m < 1000$	—
inclusion	elevation (m)	$0 < m < 5000$	$m < 5000$	$-50 < m < 0$
inclusion	average wind speed (m/s)	—	0-50	0-50
inclusion	distance to coast (km)	—	—	$5 < m < 115$
inclusion	mining (0..1)	$m = 0$	$m = 0$	—
inclusion	salt/sand/ice (0..1)	$m = 0$	$m = 0$	—
exclusion	protected areas	$m \in \{1, \ldots, 6\}$	$m \in \{1, \ldots, 6\}$	$m \in \{1, \ldots, 6\}$
exclusion	wetland	$m \in \{1, \ldots, 10\}$	$m \in \{1, \ldots, 10\}$	—

Table 3.17: Suitability factors for the EnDAT analysis. The land cover maps are given in shares from 0 to 1 and are not mutually exclusive. Map data is taken from the Copernicus data set (Buchhorn et al. 2020).

Map	PV	Wind onshore	Wind offshore
bare	0.6	0.3	—
crops	0.24	0.15	—
grass	0.6	0.15	—
moss	0.6	0.3	—
shrub	0.6	0.15	—
forest	—	0.05	—
urban	0.024	—	—
marine water body	—	—	0.4

identified areas of interest during potential analysis, as meticulously illustrated in Table 3.16.

Next, suitability factors (cf. Table 3.17) are used to obtain the share of area available per land-cover type that can be used to install a particular technology. Therefore, for each power generation technology, a projection of the techno-economic parameters into the year 2050 is performed (cf. Table 3.18). The potential for PV capacities is determined for rooftops, facades, and other surfaces in urban and open areas where ground-mounted PV is installed. At the given resolution, one pixel can have more than one land cover type. Hence, the shares of each pixel are considered additive. The resulting installable capacity is an averaged value.

The subsequent evaluation of the feed-in time series is performed based on assessing the maximum generation capacity. Weather data are converted into power generation in each pixel and weighted by the spatial distribution of the installable generation capacities. For PV, feed-in time series are computed based on the module angle, orientation, and the hourly sun position at a temporally resolved GHI, Direct Normal Irradiance (DNI)[3], and temperature profile. ERA5 exclusively provides GHI. Hence, the Python library, pvlib (Holmgren et al. 2018), is utilised to derive the DNI from the GHI data. The wind feed-in time series considers the hourly wind speed (corrected at hub height using the local roughness) and power curves of turbines (Scholz 2012, Stetter 2014). Finally, generation capacities and time series are spatially aggregated to a defined region – Brazil's federal-state level.

The map of installable capacity (in $\mathrm{MW/km^2}$) and the annual power production map (in $\mathrm{MW\,h/km^2}$) illustrate the resource maps obtained from the Brazilian potential analysis. Figure 3.8 indicates PV generation and Figure 3.9 illustrates wind generation, where geographical features such as bodies of water or rain forests are visible.

[3] Direct Normal Irradiance (DNI), also termed as beam radiation, refers to the solar radiation received from the sun without having been scattered by the atmosphere (Duffie and Beckman 2013, p. 10).

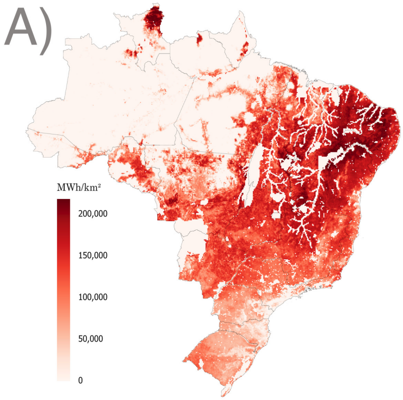

Figure 3.8: Maps of PV power generation potential for the reference year 2019 – A) annual generation, B) installable capacities. Each map combines the potential for urban and open field installation and generation.

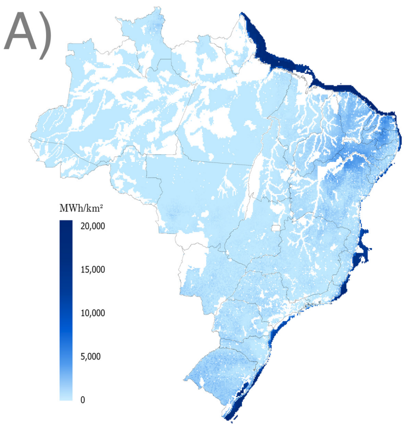

Figure 3.9: Maps of wind generation potential for the reference year 2019 – A) annual generation, B) installable capacities. Onshore wind and offshore wind are combined in each map.

Table 3.18: Technical parameters for the different generation technologies in EnDAT.

Category	Parameter	Unit	Value
PV	power reduction	1/K	-0.005
PV	η_{module}	—	0.26
PV	η_{rest}	—	0.91
PV	availability	—	0.98
all wind onshore	nacelle height	m	112
all wind onshore	rotor diameter	m	165
all wind onshore	distance factor	—	6
all wind onshore	wind shading loss	—	0.85
all wind onshore	availability factor	—	0.982
wind onshore weak	nameplate capacity	kW	3630
wind onshore medium	nameplate capacity	kW	5330
wind onshore strong	nameplate capacity	kW	10550
wind offshore	nacelle height	m	150
wind offshore	rotor diameter	m	200
wind offshore	distance factor	—	6
wind offshore	wind shading loss	—	0.85
wind offshore	availability factor	—	0.95
wind offshore	nameplate capacity	kW	10000

3.2.9 Cross-border electricity exchanges

In addition to the national electricity transmission, SIN connects Brazil to Uruguay, Argentina, and Venezuela for importing and exporting electricity to these countries. Annual power imports remain modest, accounting for only 0.04% (0.60 TWh) of total annual energy consumption, with most of the imports happening between May and November.

3.2.9.1 Data collection

ONS publishes hourly historical cross-border flows with Uruguay and Argentina, with the time series data available for the period 1999-2020 for Argentina-Brazil and 2000-2020 for Uruguay-Brazil (ONS 2021e) (the data set was obtained in July 2021).

3.2.9.2 Data processing

The cross-border power exchange data from ONS have gaps in time series. In particular, the data for Uruguay-Brazil have missing values for each year except 2018-2020. Most of the data are missing for 2000-2003, and 2.5% of values are missing in 2016 and 0.3% in 2014. The Argentina-Brazil data set has one or two missing values in each year except 2019-2020. For the years 2008, 2009, and 2016, the data exhibit missing value proportions of 6.6%, 12.1%, and 2.5%, respectively. To be consistent with the time frame of other data sets, only the time series for 2012-2020 are selected for further processing. Missing values are mainly filled with the value of the same point in time from the previous week, with the previous hour being used for the rest.

The substations of both transmission lines are situated within the Rio Grande do Sul (RS) in Brazil (ONS 2021f). Federal states are assigned two-character labels manually, whilst foreign nodes receive three-character designations (e.g., URU for Uruguay, ARG for Argentina). Thus, the transmissions receive the labels RS-URU and RS-ARG, as illustrated in Figure 3.10.

3.3 Data records

The data set provided in this dissertation is publicly available for download from the repository (Deng et al. 2022). The download file contains nine directories, each representing a subset. Figure 3.11 illustrates the folder structure. The data

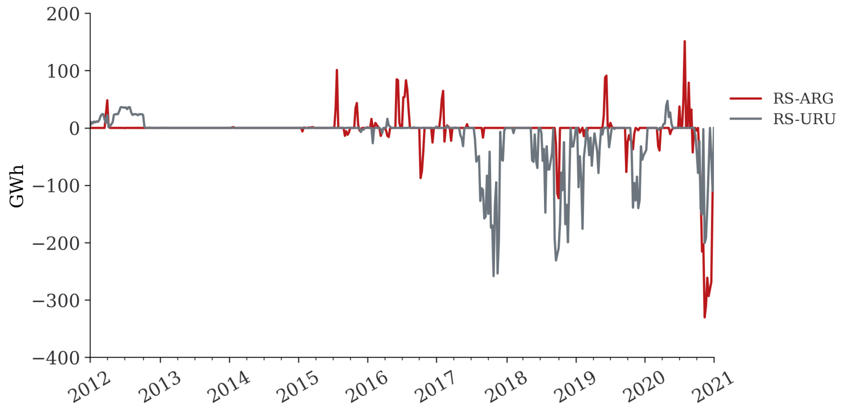

Figure 3.10: Weekly aggregation of the hourly cross-border electricity transmission from Brazil-Uruguay (RS-URU) and Brazil-Argentina (RS-ARG).

files within each directory are in a standard format of CSV, except for geospatial data for Brazil. All data are spatially resolved at the ISO 3166-2 level and temporally resolved in hours. The time series files are provided for the reference years from 2012 to 2020.

3.3.1 Geospatial data for Brazil

The `Geospatial Data for Brazil` folder contains a shapefile, which is a widespread geospatial vector data format suitable for use in geographic information system software. This shapefile employs the CRS with code EPSG:4087. A detailed description of the entities is available in Table 3.19. This data determines the nodes used for the entire data set provided in this dissertation, represented by abbreviations of the federal states (cf. Figure 3.1).

i. Geospatial data for Brazil
ii. Aggregated grid network topology
iii. Variable renewable potentials (wind and solar)
    - onshore
    - offshore
    - PV
iv. Installable capacity for biomass thermal plant
v. Inflow for the hydropower plants
    - by_hydropower_plants_operation
    - by_hydropower_plants_operation+planning
vi. Power plants
vii. Electricity load profiles
    - by_consumption
    - by_consumer
viii. Scenarios of energy demand
ix. Cross-border electricity exchanges

Figure 3.11: Folder structure of data records on Zenodo (Deng et al. 2022).

Table 3.19: Metadata of the records for Section 3.3.1.

node_epsg4087.shp		
field	***type***	***description***
name	string	Abbreviation of federal state
state_full	string	Full name of the federal state in Portuguese
x	number	The latitude of the polygon centre geometry of the federal state, and CRS is EPSG:4087
y	number	The longitude of the polygon centre geometry of the federal state, and CRS is EPSG:4087

3.3.2 Grid network topology

The data folder `Grid Network Topology` contains two files – one including only the topology of the operational network (file name: `EPEWebmap_equivalent_grid_aggregate_by_state_only_operation.csv`), and the other additionally covering the planned network (`EPEWebmap_equivalent_grid_aggregate_by_state_operation_and_planned.csv`). The attributes are shown in Table 3.20. The voltage is not shown here because it is an equivalent network for which the net transfer capacity is calculated.

Table 3.20: Metadata of the records for Section 3.3.2.

EPEWebmap_equivalent_grid_aggregate_by_state.csv		
field	***type***	***description***
node0	string	start node
node1	string	end node
transfer capacity	number	transfer capacity between the start and end nodes, in MW
efficiency	number	transmission efficiency between the start and end nodes, assuming an efficiency of 1 for HVDC lines
name	string	The data processing produces a string that helps to trace each transmission line in the original data set (EPE Webmap) by line name. The different line names are connected by the character "_".
length	number	length of the representative transmission between the start and end nodes
carrier	string	the type of the line, either AC or HVDC

3.3.3 Variable renewable potentials (wind and solar)

The data in this folder are organised in a directory structure containing CSV files. Three generation technologies (wind onshore, wind offshore, PV) are in three directories: onshore, offshore, and solar_pv.

These directories contain the installable potentials and the yearly time series. The installable potentials are named as EnDAT_<TECH_NAME>_installable_capacity.csv and the time series as EnDAT_<TECH_NAME>_per_unit_generation_weather_year_<YYYY>.csv. The text "YYYY" corresponds to the weather year. Each installable_capacity file contains the region abbreviation and the respective capacity in MW. The time zone of the time series is UTC+0.

The first column of the generation time series data represents the hourly timestamp in the format of YYYY-MM-DD HH:00:00. The subsequent columns are the unit generation for each federal state, and the column names are the abbreviations of the respective federal states.

3.3.4 Installable capacity for biomass thermal plants

Within the data folder, each file, titled biomass_geographic_potential_reference_year_<YYYY>.csv, represents the installable capacity records for each year. The text "YYYY" corresponds to the reference year. Table 3.21 reports the details of the information provided by each record.

3.3.5 Inflow of hydropower plants

The inflows to the hydropower plants in each federal state are obtained separately from two allocation parameters related to the operating status of the total installed capacity. Therefore, there are two subdirectories under this folder, namely, by_hydropower_plants_operation+planning and by_hydropower

Table 3.21: Metadata of the records for Section 3.3.4.

biomass_geographic_potential_reference_year_YYYY.csv		
field	***type***	***description***
state	string	abbreviation of federal states
value	number	the installable capacity, in MW
reference_year	number	reference year, i.e., `YYYY`
type	string	power plant type – “biomass”
phase	string	Operational status. All values here are “potential”, indicating the installable capacity, which is used to differentiate the status in the data of power plants.

`_plants_operation`. Each subdirectory includes nine files for each reference year. Each file lists the federal state in its columns, with each row representing the hourly inflow, measured in MWh, for that federal state throughout the year at the timestamp `YYYY-MM-DD HH:00:00`. The time zone of the time series is UTC-3 (Brasília Time).

3.3.6 Power plants

The information on the installed capacity of power plants in each federal state is recorded in relation to the reference year, with each file representing a record for a reference year. These values are given in a subsequent table within the folder. Data attributes are given in Table 3.22.

3.3.7 Electricity load profiles

The folder in the repository includes two subdirectories, `by_consumer` and `by_consumption`. This is related to the disaggregation of the original data set, as presented in the Section 3.2.5. Under each subdirectory are hourly load curves for each reference year, as Table 3.23 details.

Table 3.22: Metadata of the records for Section 3.3.6.

ANEEL_powerplants_per_state_per_type_reference_year_YYYY.csv		
field	***type***	***description***
state	string	abbreviation of federal states
type	string	the type of power plants type – biomass, solar_pv, on_wind, mini_hydro, small_hydro, hydro, nuclear, coal, gas, oil
phase	string	operation status – operation or planning
value	number	capacity in MW
reference_year	number	reference year, i.e., `YYYY`

Table 3.23: Metadata of the records for Section 3.3.7.

Hourly_electricity_demand_per_state_YYYY.csv		
field	***type***	***description***
time	string	the time stamp, `DD.MM.YYYY HH:00:00`, time zone is UTC-3 (Brasília Time).
state	string	abbreviation of federal state
value	string	load value in MW. Note: As this is derived from the grid operator ONS, it includes the physical loss of SIN.

3.3.8 Scenarios of energy demand

Energy demand data (XLSX format) aggregated by energy carrier and end-use sector for PNE2050 and COPPE as the attributes of the records are detailed in Table 3.24. Legal constraints permit only the display of IEA data, as demonstrated in Figure 3.6. For the sake of expediting data processing, the data are presented in a UTF-8 encoded CSV format.

Table 3.24: Metadata of the records for Section 3.3.8.

Energy_demand_scenarios_by_sector_by_energy_carrier.xlsx		
field[a]	***type***	***description***
Publication	string	the source of the data
Scenario	string	the full name of the scenario
Region	string	the name of the country
Category	string	the indication of the data category. As it is the data set of energy demand, it is “Energy”.
Product	string	the energy carriers with aggregation. Values are “Total”, “Electricity”, “Total liquids”, “Total gases”, and “Total solid fuels”. Note: “Total” is the sum of the remaining energy carriers.
Flow	string	end-use sectors with aggregation. Values are “Total final consumption”, “Transport”, “Buildings”, “Industry”, and “Other”. Note: “Total final consumption” is the sum of the remaining end-use sectors.
Unit	string	unit of the demand value, i.e., PJ.
Year	numeric	year. Values are “2010”, “2015”, “2030”, “2040”, and “2050”.
Value	numeric	value of the demand. The decimal point is written in “,”.
Alias	string	The alias of the scenario used for plotting. It has the format `XXXX_YYYY`. `XXXX` is the abbreviation of the study, i.e., “WEO2021”, “PNE2050”, “COPPE”. `YYYY` indicates the abbreviation of the scenario name, see Tables 3.12 to 3.14.

[a] The data attributes used in this dissertation closely resembles that of WEO21 data set (IEA 2021a).

3.3.9 Cross-border electricity exchanges

Under this folder, there is a single file named `international_transmission _RS-URU_RS-ARG_2012-2020_hourly.csv`. It stores records of cross-border electricity imports and exports between Brazil and its neighbours for the 2012-2020 timeframe. A description of the records on the file is presented in Table 3.25.

Table 3.25: Metadata of the records for Section 3.3.9.

Cross-border_transmission_RS-URU_RS-ARG_2012-2020_hourly.csv		
field	***type***	***description***
time	string	the hourly time stamp, `YYYY-MM-DD HH:00:00`, time zone is UTC-3 (Brasília Time).
node0	string	start node with Brazilian federal state abbreviation, namely, RS
node1	string	end nodes for neighbouring country abbreviations, i.e., ARG and URU
power	number	electricity exchanged, MW

3.4 Technical validation

Most of the original data sets are taken directly from the official Brazilian database. For this reason, the data sets have not undergone additional validation. However, it is necessary to note that spatially aggregating Brazil's power transmission network to a network model of interconnected federal states implies deviations in the resulting power flows. For validation, reference data from power-flow analyses of the fully-resolved network are required, ideally for a multitude of grid uses. Since these use cases strongly depend on the power plant dispatch and future load patterns, a validation would call for a power system model for the fully-resolved network. However, setting up such a model for validation has been beyond the scope and capacity of this dissertation.

Another exception requiring validation is the data set described in the Section 3.2.8. The technical validation is approached with two data sources: (i) observations of site-specific power generation from a set of real-world PV plants and wind farms in 2018 (ONS 2021b), and (ii) country-wide power generation indicators from global databases for 2019, namely the Global Wind Atlas (GWA) (Badger et al. 2019) and the Global Solar Atlas (GSA) (Solargis 2019).

3.4.1 Solar feed-in

The spatial distribution of PV plants is shown in Figure 3.4. The installed capacity for each PV park is collected based on ANEEL (2021b), ONS (2021a). Of the 17 PV parks, twelve have been selected for further analysis. The Pearson correlation is calculated to determine whether the temporal profiles generated by simulation and observation are similar. Table 3.26 presents the average correlation between the simulated data and the reference for each PV park, which is approximately 0.8. The deviation can be attributed to the inability to determine the orientation and inclination of the reference PV installation from available data sources, such as aerial images. Given that the effect of orientation under small module inclinations is minimal, this aspect is not considered in the assessment with EnDAT. By default, EnDAT calculates an ensemble of solar power plants with a southern orientation facing east and west at 60° away from the south.

The quantity for country-wide validation with the GSA (Solargis 2019) is performed by converting solar resources, namely DNI and GHI, into power generated per unit of capacity of pre-defined PV power plants over the long term, called PVOUT. The solar resources obtained by Solargis are compared to those from ERA5 reanalysis data used by EnDAT. Given that the GSA provides raster data with 1 km resolution, an upscaling is performed to match the 0.09° resolution of EnDAT, using the nearest neighbour method. The degree of overestimation or underestimation is evaluated using the mean bias error (MBE). The comparison of PVOUT derived from EnDAT and the GSA shows an MBE of -7% and -36% PV in urban and open areas, respectively. Especially the deviation increases with the

Table 3.26: Correlation between PV site power generation and EnDAT simulation results for these sites.

Plant name	$\mathrm{corr}_{\mathrm{Pearson}}$
Fontes Solar I	0.92
Fontes Solar II	0.92
Assu 5	0.87
Conjunto Fotovoltaico Bom Jesus	0.86
Conjunto Fotovoltaico Ituverava	0.88
Conjunto Fotovoltaico Lapa	0.85
Conjunto Fotovoltaico Pirapora 2	0.83
Conjunto Fotovoltaico Nova Olinda	0.86
Conjunto Fotovoltaico BJL Solar	0.62
Conjunto Fotovoltaico Floresta	0.82
Conjunto Fotovoltaico Horizonte MP	0.76
Conjunto Fotovoltaico Guaimbe	0.78

distance to the equator. The result indicates that EnDAT overestimates the PVOUT in comparison with GSA. The deviation can be attributed to the differences in solar resource data (Urraca et al. 2018) and is considered reasonable.

3.4.2 Wind feed-in

A validation data set consists of the observed hourly electricity production from several wind farms in 2018, as published by ONS (ONS 2021b). The installed capacity, hub height, location, and turbine type of each wind farm are gathered from ANEEL (2021b), ONS (2021a). Among the identified eleven Brazilian wind farms, seven are chosen for subsequent analysis due to inconsistencies in the data. As detailed in Table 3.27, the correlation between real-world wind farms and EnDAT-simulated generation time series ranges from 0.23 to 0.58. The deviation may be due to the fact that the potential analysis approach of EnDAT does not account for local wind effects caused by elevation, which could result in gaps in correlation. However, most existing wind farms are located in areas highly influenced by local wind phenomena. Several of the investigated wind parks are located on the coastline where hot winds can cause temperature differences between land and sea, superposed with nearby elevation changes inland of the wind parks. Other sites are located on plateaus in hilly terrain. The weather data used by EnDAT – wind speed – originates from the ERA5 reanalysis data, which has a resolution of 31 km at the equator and is represented as the grid average. On small geographical and temporal dimensions, however, observations of wind speed can differ due to the local terrain, vegetation, and built environments (Hersbach et al. 2020). The wind speed data from ERA5 may not accurately describe wind speed in highlands or valleys.

Table 3.27: Correlation of wind power generation between wind farm observations and EnDAT simulations.

Plant name	$\mathrm{corr}_{\mathrm{Pearson}}$
Praia Formosa	0.44
Icaraizinho	0.51
Malhadinha 1	0.23
Alegria II	0.32
Alegria I	0.38
Elebras Cidreira 1	0.58
Xangri-LA	0.52

The data of GWA 3.0 (Badger et al. 2019) is derived from the same reanalysis data as that of this dissertation. However, the GWA only provides average wind speed and average power density at five different heights (10 m, 50 m, 100 m, 150 m, and 200 m) and average Capacity Factors (CFs) for three turbine classes as defined by the International Electromechanical Commission (IEC). A comparison of the CFs for IEC Class I and III from GWA with EnDAT-simulated results necessitates upscaling the GWA data (with a spatial resolution of 250 m) to EnDAT's resolution of 0.09° for Brazil, using the nearest neighbour method. In contrast to GWA, the CFs for onshore wind appear lower, and for offshore wind, higher. This observation persists, aligning the technical specifications with the GWA's assumptions for this validation, featuring Vestas V112 turbines for IEC Class I and V136 turbines for IEC Class III. In particular, the MBE between CFs calculated for onshore wind between EnDAT and the GWA is 17% for IEC Class I and 18% for IEC Class III. The MBE for offshore wind is 17% in IEC Class I and 14% for IEC Class III. However, the identification of all factors contributing to the differences between the data processed in this dissertation and the GWA is hindered by barriers in accessing details on assumptions made for the GWA.

3.4.3 Conclusions

The simulations of this dissertation correlate better with real-world PV generation than onshore wind generation at a spatial resolution of 0.09°. EnDAT calculates a higher PV generation compared to GSA. The onshore wind power potential obtained by EnDAT is lower than the GWA, while the offshore wind power potential calculated by EnDAT is higher. It is essential to highlight that the data provided for PV and wind power is aggregated at the federal-state level. Appropriate validation data for this geographical dimension still needs to be included, as available validation data is limited and often site-specific. The data presented in this dissertation show better agreement with simulated data from GSA and GWA, which rely on much higher resolved resources data but only provide CFs instead of time series of power generation. However, downscaling may be necessary when using the regionalised results from EnDAT.

3.6 Usage notes

The provided data set consists of multiple CSV files and can be loaded using software capable of handling CSV files. The use of the data set is self-explanatory, which can serve as input to any energy system model. With its high-resolution (hourly and for the 27 federal states of Brazil), the data enables the emulation of the Brazilian power system and the representation of Brazil in a global energy system model at a sufficient resolution.

However, comparing historical annual trends in data where the installed capacity determines the reference year is inappropriate. This applies to data, for instance, Section 3.3.4 and Section 3.3.5. This is because most of the date information in the original data set is missing, as described in the Section 3.2.3.

To provide a reliable and open database for modelling the Brazilian power sector, the evolution of electricity consumption by sector until 2050 is available in the Section 3.2.6. It is necessary to learn the principal premises of each scenario to understand the dynamics of the evolution of electricity consumption, presented in Tables 3.12 to 3.14. For example, whether decarbonisation of the transport sector should rely on electrification or the adoption of biofuels is still open. Therefore, to better comprehend the role of electrification in each sector and the intersectoral dynamics, the evolution of the consumption of additional energy carriers in each sector until 2050 is also presented in complementary form (cf. Figure 3.6). It should be noted that the PNE2050 data may contain numerical deviations from the extraction of numbers from the charts.

Although the available data for 27 federal units contribute to the spatial resolution of the Brazilian energy system model compared to the data currently used, the intent of harmonisation may limit the study of energy systems at a higher resolution. Therefore, the code is made openly accessible and is documented to the best of the author's knowledge. Under the "resources" folder, users can find the processed data before aggregation to 27 nodes. For example, the data for power plants can be found in the project folder `power_plantsresourceconvert_ANEEL_geolocation_added_state_updated_2021_06.csv`.

3.7 Code availability

Direct use of the provided data sets is available on Zenodo (Deng et al. 2022). The source code used for data collection, processing and analysis is also on

Gitlab (Deng 2023a). The data processing is performed using Python 3.9 and the necessary toolboxes, such as Pandas and Geopandas. To facilitate the integration of the data set into energy system models, the most relevant information is provided by open-sourcing the code. Although step-by-step tutorials could also be helpful for this purpose, such information should be best conveyed through the source codes (Deng 2023a).

Regretfully, scripts for the vRES potential data cannot be provided now. The data of vRES potential is created by the EnDAT framework, which is in the process of being open-sourced.

4 Modelling a Carbon-neutral Brazilian Power System – PyPSA-Brazil

Contents of this chapter are based on

Y. Deng, K.-K. Cao, M. Wetzel, W. Hu, and P. Jochem. **E-kerosene Production and Export in Carbon-neutral Power Systems – A Solution for Sustainable Aviation?**. 2023. *Submitted to Journal of Scientific Reports*.

To answer the Research Question 1, a novel energy system model is built, described in detail in this chapter.

4.1 Model framework selection

This section discusses the criteria and processes employed to choose a suitable modelling framework for setting up an energy system model for this dissertation. It commences by outlining the model's scope, followed by an exposition of the methodology for framework selection.

4.1.1 Model scope

As highlighted in the literature review in Section 2.5, the development of a forward-looking open-source model for Brazil's energy system is urgently required to effectively tackle the imperative of decarbonisation in long-term planning. A model of this nature should be capable of regulating load fluctuations associated with the electricity generation from vRES, while also modelling an array of technologies such as enhanced power transmission, battery storage, or backup generators. Additionally, the model should be flexible enough to include other sectors, specifically addressing the demand and supply of kerosene.

This dissertation develops the model with an hourly temporal resolution and a spatial resolution corresponding to the Brazilian federal state. Such a granularity aims to make the model allow for a more detailed and accurate representation of the energy system compared to preceding models, while ensuring compatibility with personal computing devices for user-friendliness.

The high resolution of the model provides policymakers with insights into effective investments in renewable technologies, e-kerosene production units, transmission lines, and storage across federal states. These insights should assist policymakers in avoiding a sharp increase in electricity prices. Thus, the model's objective is cost optimisation of the operation and capacity expansion of the technologies.

4.1.2 Selection methodology

Energy models typically comprise data and assumptions specific to a particular research purpose. In contrast, energy modelling frameworks consist of architectures designed to provide reusable functionality when building models (Pfenninger et al. 2018). Given the availability of a few energy modelling frameworks, this dissertation builds on them to create an energy optimisation model for Brazil.

The selection procedure encompasses two steps: preselection and comparison. The information collected is evaluated and assigned a rating according to the satisfaction of the criteria: +2 for fully satisfied, +1 for partially satisfied, and 0 for rarely satisfied (cf. Table 4.3).

4.1.2.1 Preselection of modelling frameworks

Preselection criteria include open-source availability, high resolution in time and space, and the capability to analyse multiple energy sectors beyond the electricity sector (Chang et al. 2021, Prina et al. 2020). To this end, the selection has been narrowed in accordance with a study of 75 state-of-the-art models and modelling frameworks (Ringkjøb et al. 2018). The five preselected open-source modelling frameworks are Calliope, Oemof, PyPSA, OseMOSYS, and FINE (cf. Table 4.1). These frameworks allow building Linear Programming (LP) or MILP models with medium to high temporal and spatial resolution (multi-node approaches possible) while supporting the analysis of sectoral synergies and interconnections.

4.1.2.2 Framework comparison

The preselected frameworks are further compared based on model logic, techno-economic details, ease of use, popularity, and added value.

Model logic evaluations focus on the purpose and language of the frameworks that are compatible with the objective of this dissertation. Except for OseMOSYS, the other four frameworks meet the requirements for cost optimisation for operation and expansion (cf. “purpose” under “Model logic” in Table 4.1).

Modelling frameworks can be scripted in mathematical programming languages (e.g., GAMS, GNU MathProg, and Pyomo) or general-purpose programming languages (e.g., Python, Julia). While mathematical programming languages closely resemble mathematical models, general-purpose languages are more accessible to non-programmers (Pfenninger et al. 2018). The latter also facilitates data processing and analysis through packages such as Pandas, Numpy, and Matplotlib. For this reason, in the “language” column under “Model logic” in Table 4.1, a framework based on a general-purpose language is considered more beneficial.

Techno-economic details are essential for the application of modelling frameworks to create energy system models. In modelling the impact of increasing the share of vRES, large-scale production of e-kerosene, and alternate kerosene supply options, key attributes to consider include grid development, energy storage, and demand-side management (Ringkjøb et al. 2018). The modeller connects general functions, often called components, using specifications. They then add user-defined mathematical constraints where necessary. These attributes are the technical and economic parameters in the model components, including conventional or renewable generation technologies, energy storage, emissions, cost, and grid, which determine the level of technical-economic detail. A framework allowing for varying levels of techno-economic details is preferred for flexibility in balancing computational resources and the consequences of errors due to low resolution of techno-economic detail (Prina et al. 2020, Chang et al. 2021). While most of the available model components are similar across the five frameworks, it is the grid modelling that is noteworthy (cf. “Techno-economic details” in Table 4.2). OseMOSYS does not include grid modelling, Calliope and Oemof (SOLPH) use the Net Transfer Capacity (NTC) approach, while FINE builds on this supports linear power flows, as do power system analysis tools, and PyPSA further allows nonlinear power flows. Thus, PyPSA and FINE are preferred for their relatively great technical-economic details compared to other frameworks.

“Ease of use” is determined by the availability of comprehensive documents and tutorials. These materials should help entry-level modellers to understand the framework effectively (Pfenninger et al. 2018). From this perspective, the quality of online documentation, formulations, and tutorials is characterised as high, medium, or low based on the authors’ practical experience (summarised in Table 4.2 under the “Easy of use”).

The popularity of the framework indicates its sustainability and potential for widespread adoption (cf. “Popularity” in Table 4.2). The popularity is measured by a combination of factors, including the number of projects, publications, and the presence of an open community. Building a model on a popular framework can enhance its maintenance and likelihood of adoption by other researchers. Choosing a framework with an open community is also beneficial for modellers as it allows for peer-to-peer support and direct discourse with the core developers of the framework (Pfenninger et al. 2018). Evaluating the number of publications, along with the geographic distribution of the most prolific contributors, aids in assessing the international dissemination of the framework.

"Added-value" in Table 4.2 refers to additional algorithms or embedded libraries within the framework, which relieve modellers of the burden of creating specialised functionalities, such as space and time aggregation. Apart from OseMOSYS, other frameworks offer added value by incorporating additional algorithms or packages.

4.1.3 Selection outcome

Based on the information collected and shown in Table 4.1 and Table 4.2, each framework is scored according to its level of satisfaction with the underlying research criteria. Consequently, PyPSA (Brown et al. 2018a) emerges as the chosen framework due to its highest score (cf. Table 4.3).

Table 4.1: Five preselected open-source modelling frameworks based on the 75 state-of-the-art models in Ringkjøb et al. (2018)[a].

Model	**Resolution**		**Sector-coupling**		**Model logic**		
	in time	in space	commodity	demand sectors	language	methodology	purpose
Calliope[b]	UD[c]	UD	Electricity, heat, hydrogen, fuels	All sectors[d]	Python	LP[e]	Investment & Operation Decision Support
Oemof (SOLPH)[f]	UD	UD	Electricity, heat, hydrogen, fuels	Building, transport, industry	Python	LP, MILP	Investment & Operation Decision Support, Scenario
PyPSA[g]	Hourly	UD	Any commodity	All sectors	Python	LP	Investment & Operation Decision Support, Power System Analysis Tool
OseMOSYS[h]	UD	UD	Electricity[i]	All sectors	GNU MathProg[j]	LP	Investment Decision Support
FINE[k]	UD	UD	Any commodity	All sectors	Python	MILP	Investment & Operation Decision Support

[a] Even though FINE is not featured in Ringkjøb et al. (2018), the information about it is collected and presented in this dissertation. Some of this information is updated based on the official documentation of the modelling framework.
[b] Calliope is a model framework published by ETH Zürich (`https://www.callio.pe/`).
[c] "UD" refers to User-defined. Developers can use the framework to build energy systems with multiple regions (also known as nodes) and time steps at their request.
[d] "All sectors" indicates the common practice in the energy system model of combining demand/load based on power consumption across all sectors.
[e] MILP is under development.
[f] The **O**pen **E**nergy **Mo**delling **F**ramework, or Oemof, is an important element of this research published by Reiner Lemoine Institute/ZNES (`https://oemof.readthedocs.io/en/latest/`).
[g] PyPSA stands for **Py**thon for **P**ower **S**ystem **A**nalysis, published by FIAS (Brown et al. 2018a) (`https://pypsa.org/`).
[h] OseMOSYS stands for **O**pen **S**ource **E**nergy **Mo**delling **Sys**tem, published by KTH Royal Institute of Technology (`http://www.osemosys.org/`).
[i] While only "Electricity" is recognised in Ringkjøb et al. (2018, Table 3), the OseMOSYS online documentation indicates its application in the "Water-Food Nexus" project, suggesting the possibility of incorporating multiple commodities within OseMOSYS.
[j] GNU MathProg is a mathematical programming language for describing linear mathematical programming models. Additionally, the OseMOSYS model framework is implemented using languages such as GAMS and Pyomo.
[k] The **F**ramework for **In**tegrated **E**nergy System Assessment, or FINE, is published by Forschungszentrum Jülich GmbH (`https://vsa-fine.readthedocs.io/en/latest/index.html`).

Table 4.2: Comparison between the five preselected open-source modelling frameworks.[a]

Model	Techno-economic details[b]	Ease of use[c]	Popularity[d]			Added-value[e]
	(generation, storage, grid)	(docs, formulation, tutorial)	projects[f]	publications[g]	open community	
Calliope	(all[h], all[i], NTC[j])	(high, high[k], high)	EU, UK, Kenya, China, Italy, Bangalore, South Africa, Cambridge	39 (2019-2022), mainly EU + India	Gitter, 66 members	time clustering
Oemof (SOLPH)	(all, all, NTC)	(high, medium, low)	—	95 (2016-2022), mainly EU + China	—	`demandlib` for demand data, `feedinlib` for time series, and `TESPy` provides thermal energy systems for in-depth modelling
PyPSA	(all, all, non-linear/linear power flow[l] and NTC)	(high, medium, high)	EU, South Africa, China, Germany	148 (2017-2022), EU+US	Google group, 388 members	spatial clustering, `Atlite` for vRES generation potential
OseMOSYS	(all, all, None)	(medium, medium, low)	South America, EU, Global, Africa, Cypriot[m]	301 (2002-2022), US+EU	Google group, 381 members[n]	—
FINE	(all, all, linear power flow and NTC)	(low, medium, low)	—	73 (2018-2021), EU+China+US	—	`tsam` for time clustering

[a] The gathered information relies on examining framework documentation, relevant publications, and web sources, as outlined in the associated footnotes.
[b] The details provided come from the Ringkjøb et al. (2018) and FINE's documentation. For further information beyond Table 4.1, refer to Ringkjøb et al. (2018).
[c] The evaluation is conducted by examining the project's source code and documentation.
[d] The data collection phase lasted until October 2021.
[e] Algorithms available to modellers, aiding in workload reduction, are taken into consideration.
[f] The value presented reflects the number of open projects available.
[g] The number is identified through the citation of publications from the Scopus database, which are recommended in the online documentation.
[h] The "all" indicates that power generation technologies, whether conventional or renewable, can be modelled using the provided general functionality.
[i] The "all" signifies that all energy storage technologies, such as batteries, hydrogen, and thermal energy storage, can be modelled with the general functions provided.
[j] The NTC approach is popular in energy system modelling due to its simplicity and high accuracy.
[k] Calliope's clear explanation of its general functionality is particularly useful for developers in technology modelling.
[l] Power flow modelling proves more capable than the NTC approach in grid modelling, as it adheres closely to grid principles. Offering both power flow and NTC approaches is seen as a model selection advantage, providing modellers with more options (Brown et al. 2018a).
[m] The web documentation references more than five countries.
[n] Of note is the extensive use of OseMOSYS by a great academic community for teaching purposes.

Table 4.3: Results of the model frame selection. The orange cell is the preselection step (cf. Table 4.1), the green cell is the second step of comparison (cf. Table 4.2), and the obtained scores are listed in the "Total" column. The rating is given according to the level of satisfaction of the criteria, +2 for satisfied, +1 for partially, and 0 for rarely. As shown in the blue cells, PyPSA is the selected model framework.

Open source model	High resolution	Sector-coupling	Model logic	Techno-economic details	Subjective perception	Popularity	Added-value	Total
Calliope	+2	+2	+2	+1	+2	+1	+1	11
Oemof	+2	+2	+2	+1	+1	0	+1	9
PyPSA	+2	+2	+2	+2	+2	+2	+2	14
OseMOSYS	+2	+1	0	0	+1	+2	0	6
FINE	+2	+2	+2	+2	0	0	+1	9

4.2 Model

4.2.1 Optimisation model PyPSA-Brazil

PyPSA-Brazil is a novel model that uniquely positions the Brazilian energy system as being open-source and within the framework of substantial renewable energy feed-in. This model harnesses publicly accessible data sets, as explained in Chapter 3, and uses an open modelling framework PyPSA (Brown et al. 2018a).

The boundaries of the model are established to ensure the computational feasibility on personal computers, improve accuracy over the existing Brazilian models, and facilitate investigations into e-kerosene production within the Brazilian power system. As depicted in Figure 4.1, PyPSA-Brazil comprises 27 nodes, each symbolising one of the 26 federal states or the federal district of Brasília. PyPSA-Brazil aims to achieve a cost-optimal equilibrium and regulates the hourly dispatch and infrastructure expansion across the year to accommodate exogenously designated electricity and kerosene demand, while respecting technical and physical constraints. This objective is set as a linear optimisation problem that factors in short-term dispatch and long-term investments, and is solved using the commercial solver Gurobi (Gurobi Optimization 2021).

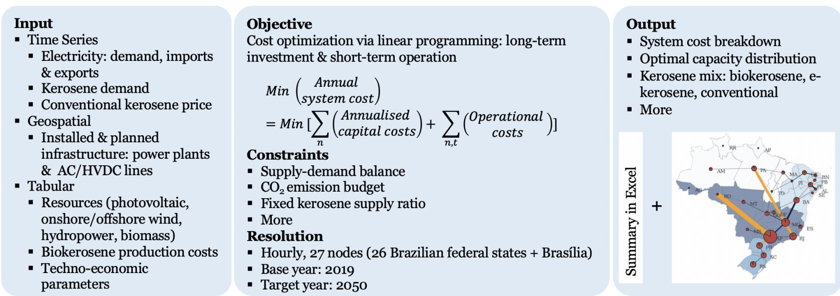

Figure 4.1: Overview of the PyPSA-Brazil model.

The starting point for optimisation is the 2019 power system, including existing transmission infrastructure, hydroelectric, biomass, wind, PV facilities, but excludes other existing assets (partial greenfield approach). The model assumes hydropower capacity expansion aligns with the National Ten-Year Expansion Plan (EPE 2020c). See Section 3.2.3 for details.

Most countries will start to witness the impact of e-fuels on GHG emissions reductions only from 2030 (Ueckerdt et al. 2021). Given Brazil's pledge to reach climate neutrality by 2050 (UNFCCC 2022), this dissertation employs scenario analysis for 2050 to evaluate the potential contribution of e-kerosene production to Brazil's energy system. This assessment presumes long-term perfect competition and foresight in markets as described by Neumann et al. (2022), disregarding intermediate accumulation steps leading up to 2050.

The parameterisation of the model deliberately avoids favouring certain technologies so that the model selects system components solely based on cost-effectiveness and technology characteristics. The Section 4.2.4 details assumptions for the e-kerosene production chain, which can vary according to feedstocks and principal technologies (Brynolf et al. 2018).

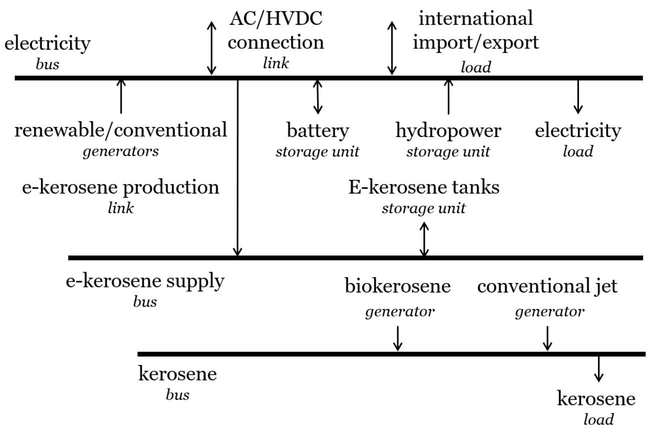

Figure 4.2: Energy flow at one node in the PyPSA-Brazil model.

The application of the PyPSA framework in modelling the technologies in PyPSA-Brazil is depicted in Figure 4.2, where energy flow at a single node is illustrated. Italicised terms like `Bus`, `Link`, and `Generator` denote reusable functionality in PyPSA, while arrows represent the flow of energy carriers (PyPSA developers 2023). Each horizontal line represents a bus of energy carriers, such as electrical power and kerosene, where an hourly energy balance must be maintained. Every federal state comprises two buses, representing the power and aviation sectors. Sections 4.2.2 to 4.2.3 offer a comprehensive mathematical description of the model.

4.2.2 Optimisation problem

The objective is to minimise the annual system costs. This includes the annualised capital costs – attributed to the expansion of generation capacities, transmission capacities, storage capacities, and energy conversion capacities – and the variable costs associated with the dispatch of generation, storage, and energy conversion. Equation (4.1) presents the mathematical expression for this objective:

$$\min_{G,E,F,P,g,e,f,p} \Bigg\{ \sum_{n,r} c_{n,r} \cdot G_{n,r} + \sum_{n,s} c_{n,s} \cdot E_{n,s} + \sum_{l} c_l \cdot F_l + \sum_{n,k} c_{n,k} \cdot P_{n,k} + \sum_{n,r,t} o_{n,r} \cdot g_{n,r,t} + \sum_{n,s,t} o_{n,s} \cdot e_{n,s,t} + \sum_{l,t} o_l \cdot f_{l,t} + \sum_{n,k,t} o_{n,k} \cdot p_{n,k,t} \Bigg\} \tag{4.1}$$

where c_* represents the capital costs, while o_* signifies variable costs. The indices r, s, l, and k label the generation technologies, storage technologies, transmission lines, and energy conversion technologies, respectively. The symbols G, F, E, and P correspond to the expanded capacity of generation, transmission, storage, and energy conversion technologies, respectively. Additionally, g, f, e, and p indicate the dispatch of the respective elements across various time snapshots, denoted as t and expressed in hours. The index n stands for each node within the system with $n \in \mathcal{N}$, $\mathcal{N} = 1, 2, \ldots, 27$. Transmission lines serve as bus connectors, while specific nodes are equipped with converters that are capable of converting one energy carrier into another. Both transmission lines and converters are modelled using `Link` component, as illustrated in Figure 4.2.

The cost of the entire system is derived by summing the annualised capital expenditures, encompassing the annuity payment required and fixed operating expenses, in addition to variable costs, which include variable operating expenses and fuel costs. The equivalent annuity payment is calculated using the capital investment and the capital recovery factor. This approach aligns with the method demonstrated by Hörsch et al. (2018a), which follows the formula stipulated in Short et al. (1995, Equation 2-12, p. 14), taking into consideration the lifetime and discount rate of each technology.

$$\mathcal{A} = \frac{\mathcal{I}}{\frac{(1+i)^N - 1}{i \cdot (1+i)^N}} \tag{4.2}$$

where

$\mathcal{A}$: equivalent annuity payment

$\mathcal{I}$: capital investment

i : annual discount rate

N : lifetime of the technology in years.

Modelling the physical process entails adopting linear eligibility as a standard assumption.

4.2.3 Constraints

The system cost minimisation is subject to a set of applied constraints.

Energy balance

The fundamental constraint for optimisation is ensuring that the energy supply of each federal state within Brazil covers the local demand – power and kerosene – for every hour of the year.

$$\sum_{r} g_{n,r,t} + \sum_{s} e_{n,s,t} + \sum_{l} \alpha_{n,l} \cdot f_{l,t} + \sum_{k} \alpha_{n,k} \cdot p_{n,k,t} = d_{n,t} \quad \leftrightarrow \quad \lambda_{n,t} \quad \forall\, n, t \tag{4.3}$$

where

- $g_{n,r,t}$: generation dispatch
- $e_{n,s,t}$: storage dispatch
- $\alpha_{n,*}$: flow direction and efficiency on bus connectors – time-independent values – $\alpha_{n,l}$ for transmission lines and $\alpha_{n,k}$ for the production of e-kerosene
- $f_{l,t}$: power flow
- $p_{n,k,t}$: the dispatch of energy conversion
- $d_{n,t}$: hourly demand at node n, either electricity ($d_{n,t}^{\text{electricity}}$) or kerosene ($d_{n,t}^{\text{kerosene}}$)
- $\lambda_{n,t}$: Karush-Kuhn-Tucker (KKT) multipliers associated with the equality constraints of the supply-demand balance. The value of $\lambda_{n,t}$ at the optimal point is an output of the optimisation.

The KKT multiplier represents the marginal price of the respective energy carrier at which the node n fulfils more demand at time t, also known as the Local Marginal Price (LMP) (Schlachtberger et al. 2017).

The model's hourly resolution significantly lengthens the computation time needed, but it allows for a more accurate system description that considers the synergy effects of various system components or sectors.

Transmission

Between the nodes, the energy can be transferred from one to another through transmission lines. The maximum power flowing through the links at any time is limited by the maximum physical capacity F_l:

$$\underline{f}_l \cdot F_l \leqslant f_{l,t} \leqslant \overline{f}_l \cdot F_l \quad \forall\, l, t \tag{4.4}$$

where the $\underline{f}_l = -0.7$ and $\overline{f}_l = 0.7$ denote an additional unit security margin for line capacity. These values ensure approximate N-1 security and reserve capacity for lines while allowing both import and export between neighbouring nodes (Schlachtberger et al. 2017, Hörsch et al. 2018a).

The physical capacity of the line F_l is constrained ($\underline{F}_l \leqslant F_l \leqslant \overline{F}_l$) and can be expanded during the optimisation, depending on the cost-effectiveness. In this study, the lower bound $\underline{F}_l$ is the nominal transfer capacity of lines obtained from Section 3.2.2. The upper bound $\overline{F}_l$ is set to infinite. However, the expansion of the transmission lines is limited by a global constraint:

$$\sum_l \ell_l \cdot F_l \leqslant \Gamma_{\text{line volume}} \quad \leftrightarrow \quad \mu_{\text{line volume}} \tag{4.5}$$

where $\Gamma_{\text{line volume}}$ is the sum of transfer capacities F_l of the line l multiplied by their lengths ℓ_l (referred as line volume and measured in MWkm withing the model) for existing lines with a variable multiplier. Should Equation (4.5) be binding, the KKT multiplier $\mu_{\text{line volume}}$ is expected to be positive, which represents the marginal value of the increase in line volume to the system. Otherwise, it indicates the cost per MWkm essential for the optimal solution to have the line volume $\Gamma_{\text{line volume}}$ (Schlachtberger et al. 2017). For the analysis at hand, the multiplier is set to an infinite value, thus making $\Gamma_{\text{line volume}}$ infinite as well.

Using Kirchhoff's formulation, a linear optimal power flow is applied that ignores the effect of impedance on the flows. It solely requires nodal power balance according to Kirchhoff's Current Law (KCL) (Hörsch et al. 2018b).

Generation

The dispatch of the generators for every hour $g_{n,r,t}$ is constrained by:

$$\underline{g}_{n,r,t} \cdot G_{n,r} \leqslant g_{n,r,t} \leqslant \overline{g}_{n,r,t} \cdot G_{n,r} \quad \forall\, n, r, t \tag{4.6}$$

where

$G_{n,r}$: optimum installed capacity of generators

$\underline{g}_{n,r,t}$: lower bound of the availability. For all types of generators, this value is set to zero ($\underline{g}_{n,r,t} = 0$), which indicates that must-run operation is not required.

$\overline{g}_{n,r,t}$: upper bound of the availability, [0, 1]. The value for wind and solar energy depends on time and location. This value refers to the availability per unit capacity. The multiplication value ($\overline{g}_{n,r,t} \cdot G_{n,r}$) indicates the maximum producible energy per hour, which can be derived from the reanalysis weather data. In the context of fossil-fuelled power plants, a default value of 1 signifies high flexibility, devoid of any ramp-up, ramp-down, start-up or shutdown costs.

The installed capacity for generators can be expanded and is limited by the following:

$$\underline{G}_{n,r} \leqslant G_{n,r} \leqslant \overline{G}_{n,r} \quad \forall\, n, r \tag{4.7}$$

where

$\underline{G}_{n,r}$: lower bound of capacity expansion. For onshore wind, PV, and biomass thermal power plants, the value is set to be the installed capacity of the base year 2019 provided by Section 3.2.3.

$\overline{G}_{n,r}$: upper bound of capacity expansion. The value for wind and solar energy is the technical generation potential estimated by geometric and environmental constraints obtained from Section 3.2.8. For biomass thermal power plants, it is the sum of existing and planned capacity for the base year 2019 and the economic potentials presented in Section 3.2.4.

The PyPSA-Brazil model does not permit the expansion of fossil power plants, and the calculated capital cost is set to zero. However, fossil and nuclear power plants are excluded from the scenario analysis in this dissertation.

Storage

The state-of-charge of the storage should equal the dispatch at each hour:

$$soc_{n,s,t} = \eta_{s,0} \cdot soc_{n,s,t-1} + e^{\text{inflow}}_{n,s,t} + \eta^{\text{charge}}_{s} \cdot e^{\text{charge}}_{n,s,t} - \frac{e^{\text{discharge}}_{n,s,t}}{\eta^{\text{discharge}}_{s}} \quad \forall\, n, s, t \quad (4.8)$$

where

$soc_{n,s,t}$: state-of-charge of every storage

s : storage technology, $s \in \{\text{battery, reservoir hydropower plant, e-kerosene tank}\}$

$\eta_{s,0}$: standing loss per hour to the state-of-charge. For battery, $\eta_{s,0}$ is constant, while for reservoir hydropower plant and e-kerosene tank, no standing losses are assumed ($\eta_{s,0} = 0$).

$e^{\text{inflow}}_{n,s,t}$: natural inflow to the storage. Only reservoir hydropower plant has time-dependent inflow for each node (cf. Section 3.2.7).

η^{charge}_{s} : charging efficiency. A reservoir hydropower plant operates under the setting of $\eta^{\text{charge}}_{s} = 0$, while a constant value applies to both battery storage and the e-kerosene tank.

$e^{\text{charge}}_{n,s,t}$: dispatch of power charging at node n

$\eta^{\text{discharge}}_{s}$: discharging efficiency – set to a constant value

$e^{\text{discharge}}_{n,s,t}$: dispatch of power discharging at node n.

η^{charge}_{s} and $\eta^{\text{discharge}}_{s}$ determine losses and signify that storage is only charged during periods of excess system power supply and depleted during periods of insufficient power production by generators and import options (Schlachtberger et al. 2017).

In PyPSA-Brazil, the storage energy capacity, represented by $h^{\text{max}}_{s} \cdot E_{n,s}$, is optimised depending on the storage power capacity $E_{n,s}$. The Energy to Power (E2P) ratio, denoted as h^{max}_{s}, is the fixed duration during which the stored energy can be fully charged or discharged at maximum power (Moseley and Garche 2015).

$$0 \leqslant soc_{n,s,t} \leqslant h^{\text{max}}_{s} \cdot E_{n,s} \tag{4.9}$$

The power capacity of the storage $E_{n,s}$ can be expanded but should be within the upper and lower limits:

$$\underline{E}_{n,s} \leqslant E_{n,s} \leqslant \overline{E}_{n,s} \tag{4.10}$$

where

$\underline{E}_{n,s}$: lower bound. For battery and e-kerosene tanks, $\underline{E}_{n,s} = 0$ is set. For hydro reservoirs, however, $\underline{E}_{n,s}$ signifies the installed capacity of all sizes of hydropower plants in the base year, derived from Section 3.2.3.

$\overline{E}_{n,s}$: upper bound. $\overline{E}_{n,s} = \infty$ is designated for battery and e-kerosene tanks. For reservoir hydropower, $\overline{E}_{n,s}$ represents the sum of the installed and planned capacity from the Brazilian Ten-Year Energy Plan (EPE 2020c) (cf. Section 3.2.3).

Due to the annual periodicity of demand and seasonal generation patterns, it makes sense to assume cyclic states of charge when optimising a full year (Schlachtberger et al. 2017). In this way, storage can be used efficiently at the beginning of the modelled time horizon and avoid the depletion in the end, $soc_{n,s,t=0} = soc_{n,s,t=T} \quad \forall\, n, s$.

E-kerosene generation

The modelling of e-kerosene production employs the `Link` component in PyPSA framework. It is assumed that the capacity expansion of the e-kerosene production unit relies exclusively on a cost basis, setting $0 \leqslant P_{n,k} < \infty \quad \forall\, k$.

The dispatch of e-kerosene generation is not only constrained by its rated capacity but may also be limited by conditions under which it must operate and the availability:

$$\underline{p}_{n,k,t} \cdot P_{n,k} \leqslant p_{n,k,t} \leqslant \overline{p}_{n,k,t} \cdot P_{n,k} \quad \forall\, n, k, t \tag{4.11}$$

where

k : energy conversion technology, $k \in \{$e-kerosene production unit$\}$

$P_{n,k}$: capacity of energy conversion

$p_{n,k,t}$: dispatch of energy conversion

$\underline{p}_{n,k,t}$: must-run factor. It is set to 0, $\underline{p}_{n,k,t} = 0$, implying that the conversion from electricity to e-kerosene is a unidirectional process, without any mandatory operational levels.

$\overline{p}_{n,k,t}$: availability factor. It is set as $\overline{p}_{n,k,t} = \eta_k$, where η_k denotes the conversion efficiency of the e-kerosene production unit.

Supply of biokerosene and conventional kerosene

In the model, the supply of biokerosene and conventional kerosene is represented using the `Generator` component in PyPSA framework. It is assumed that there are no capacity limits, hence, setting $0 \leqslant G_{n,r} < \infty$ (cf. Equation (4.7)). This implies that the supply amount per hour depends entirely on the marginal cost of providing biokerosene and conventional kerosene, which is measured in €/MWh.

Additional constraints

The constraints in Equations (4.3) to (4.11) primarily represent technical restrictions. However, to ensure that the optimisation problem produces feasible solutions, additional constraints can be implemented.

One such constraint involves limiting the total CO_2 emissions ensuring that they do not exceed a specified budget, denoted as Γ_{CO_2}:

$$\sum_{n,r,t} \frac{1}{\eta_{n,r}} \, g_{n,r,t} \cdot \rho_r \leqslant \Gamma_{CO_2} \quad \leftrightarrow \quad \mu_{CO_2} \tag{4.12}$$

where

r : technology, $r \in \{\text{fossil generators, conventional kerosene supply}\}$.

$\eta_{n,r}$: generator efficiency at node n for technology r

$g_{n,r,t}$: generator dispatch at time t

ρ_r : fuel-specific emissions, measured in units of $CO_2\ \mathrm{t/MWh}$. This emission rate is assumed to apply only to the supply of conventional kerosene.

Γ_{CO_2} : predetermined budget of CO_2 emissions

μ_{CO_2} : KKT multiplier, also referred to as the shadow price. It indicates the marginal cost of emitting an additional tonne of CO_2. It can also be interpreted as the additional cost required to achieve the CO_2 emissions reduction target.

In the scenario analysis conducted in this dissertation, there is an option to limit the contribution of e-kerosene to a specific fraction of the total kerosene demand. This results in a constraint where the combined supply of biokerosene and conventional kerosene must exceed a certain proportion (γ) of the total kerosene demand, $d_{n,t}^{\text{kerosene}}$:

$$\sum_{n,t} g_{n,r,t} = \gamma \cdot \sum_{n,t} d_{n,t}^{\text{kerosene}} \tag{4.13}$$

where $r \in \{\text{conventional kerosene supply, biokerosene supply}\}$. For instance, in the "100% e-kerosene supply" scenario, $\gamma = 0$ is set.

4.2.4 Assumptions on e-kerosene production route

The e-kerosene production chain has a wide choice of technologies that correspond to each processing step, namely, the provision of H_2 and CO_2, the synthesis and upgrading (Schmidt and Weindorf 2016). This section outlines herein the assumptions and simplifications employed in the modelling of e-kerosene production within the PyPSA-Brazil model, which this dissertation refers to as the "e-kerosene production link" in Figure 4.2.

This dissertation utilises a simplified representation of the e-kerosene production plant, as opposed to the detailed component modelling delineated in Sherwin (2021). The model relies on conversion efficiencies and techno-economic parameters derived from Schmidt et al. (2016) to emulate the technical behaviour. The plant features a conversion efficiency from electricity to e-kerosene of 0.42 and includes a plant configurations of low-temperature electrolysis (AEL or PEM), hydrogen storage, CO_2 sourced from DAC, and a FT pathway comprising FT synthesis, Reverse Water-gas Shift (rWGS), and hydrocracking/isomerisation.

In the provision of CO_2, fossil CO_2 using CCU is elected not to be used, as it falls short as a long-term, carbon-neutral solution (Ueckerdt et al. 2021). Additionally, while CO_2 could be obtained from concentrated sustainable sources such as biomass combustion, organic residues, and bio-ethanol production from sustainably produced sugars or starches (Gabrielli et al. 2020), these options call for access to extensive biomass data. As such, this dissertation assumes that CO_2 is sourced exclusively from the atmosphere via DAC and is universally available in Brazil.

The assumption is made that high-purity water needed for FT-based e-kerosene production is readily available in Brazil and may not pose a technological challenge in Brazil. This is due to the relatively lower water demand compared to biokerosene production by HEFA process or ATJ (Schmidt and Weindorf 2016). The ready availability of both groundwater (Gleeson et al. 2016) and surface water (Pekel et al. 2016), coupled with Brazil's status as one of the world's leading nations in terms of seawater availability (Stockli 2009) and the successful water scarcity management (Alves et al. 2020), implies that the pre-treatment process of water or the cost thereof is deemed negligible.

The FT synthesis pathway is the focus of this dissertation, a process prevalent in large-scale industrial applications for producing liquids from natural gas or coal (Drünert et al. 2020). Although methanol synthesis is capable of yielding e-kerosene, so far, the first-of-its-kind aviation fuel specification, ASTM D7566 standard, exclusively specifies this synthetic kerosene derived from the FT process (ASTM 2018). A noteworthy assumption in this dissertation is the potential for altering future blending ratios of e-kerosene with crude oil-based kerosene (ICAO 2022b, Breyer et al. 2022), speculating that they may no longer be limited to the 50%[1] currently prescribed by the ASTM regulations.

This dissertation explicitly models the energy system with generation, storage, transmission and demand for electricity supply for e-kerosene production using PyPSA-Brazil model. By considering the dynamics of the system, the cost of electricity supply is calculated endogenously at the federal-state level in Brazil.

The PyPSA-Brazil model posits that the e-kerosene production results in an ERF of 100%. Emissions Reduction Factor (ERF) measure the net life-cycle CO_2 benefits of SAFs by accounting for the CO_2 savings from feedstock production or growth, and incorporating the emissions incurred during fuel production (ATAG 2021). 100% ERF indicates that there is no net carbon loss between the stages of emissions and capture, which is also referenced by Micheli et al. (2022). However, Micheli et al. (2022) adopt a more conservative stance, assuming 5% loss within the closed carbon cycle. Such a loss translates to emissions ranging from 0.9-4.0 $\mathrm{g\,CO_2e/MJ}$, on the condition that electricity is sourced from wind or solar energy. In addition, ATAG explores sustainable trajectories for aviation by assuming ERFs of 70-100% for SAF (ATAG 2021). This is indicative of the industry's direction towards mitigating carbon emissions.

It is imperative to underscore that focusing solely on achieving a closed carbon cycle with regard to CO_2 emissions does not address the broader environmental impacts. Specifically, aircraft emissions in the upper atmosphere, including water vapour, aerosols, and nitrogen oxides (NOx), have a significantly more detrimental effect on the climate compared to CO_2 emissions at lower altitudes (Stratton et al. 2011, Braun-Unkhoff et al. 2017). These non-CO_2 impacts, often overlooked, merit greater consideration and are already discussed in Chapter 1.

[1] It refers to the volume-matched blending ratio with conventional petroleum-derived jet fuel.

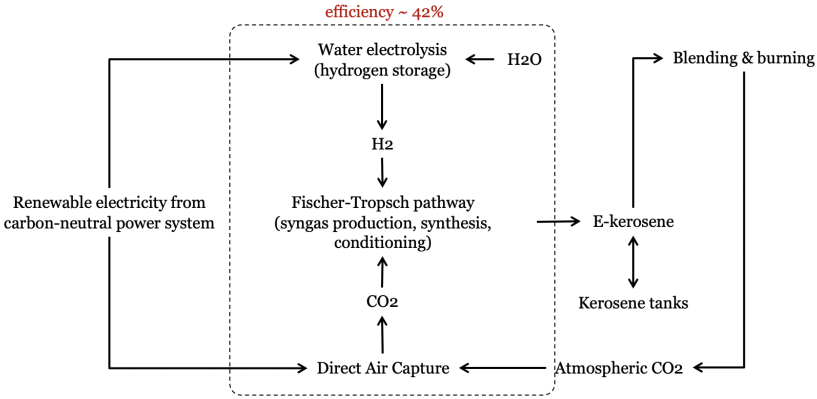

Figure 4.3: E-kerosene production unit considered (own illustration inspired by Schmidt and Weindorf (2016), König et al. (2015), Drünert et al. (2020)).

4.3 Data

4.3.1 Power sector

The inputs and the assumptions for modelling the Brazilian power system are detailed in Chapter 3, introducing the open, spatially resolved, harmonised data set of the Brazilian energy system. PyPSA-Brazil adopts 2019 as the base year, ensuring that all input data are from that year.

Stored capacity for reservoir hydropower plant

Hydropower plants, assumed to be of the reservoir type, base their energy capacity on both power capacity and the Energy to Power (E2P) ratio (cf. Equation (4.9)). The E2P ratio is derived from the data set of stored energy capacity for each electric region in SIN, and as released by ONS (ONS 2022c). The stored capacity of hydropower[2] is about 357,548,409 MWh. This regional storage energy capacity then undergoes conversion to the federal-state level:

$$h_s^{\max} = \frac{E_{n,s}}{\sum_n E_{n,s}} \cdot \frac{\mathcal{S}_{R,s}}{\sum_n E_{n,s}} \tag{4.14}$$

where

$h_s^{\max}$: E2P ratio assumed, in the unit of h

s : storage technology, $s \subseteq$ reservoir hydropower plant

n : node of the model – Brazilian federal state, $n \in \mathcal{N}, \mathcal{N} = 1, 2, \ldots, 27$

$E_{n,s}$: power capacity at federal state n, in unit of MW

R : electric regions defined by SIN (cf. Table 3.2)

$\mathcal{S}_{R,s}$: stored energy capacity at the region R, in unit of MWh.

4.3.2 Cost assumptions

The financial and technical assumptions, such as investment costs, Variable Operation and Maintenance (VOM) costs, Fixed Operation and Maintenance (FOM) costs, efficiency, and lifetime, are based on insights from the scientific literature and are presented in Table 4.4. The capital investment of each technology is annualised with a discount rate of 8% over the economic lifetime used in Equation (4.2).

Capital investment in transmission lines comes from historical auctions with units of R$\$/\mathrm{MW}/\mathrm{km}$ (ANEEL 2021a). The capital investment costs are derived by interpolating representative line lengths for AC and HVDC lines, considering the cost of converters and transformers for each historical auction.

2 The stored capacity of hydropower is given daily for each of four electric regions in MWmês. Conversion to MWh is applied: 1 MWmês = 720 $\mathrm{MWh}/\mathrm{month}$.

Table 4.4: Technology cost and lifetime assumptions for 2050 (VOM, FOM).

Technology	Parameter	Value	Unit	Source
Unit conversion	discount rate[1]	0.08	per unit	EPE and MME (2020)
	jet fuel density[2]	775	kg/m^3	ASTM (2018)
	jet fuel heat	42.8	MJ/kg	ASTM (2018)
	euro to dollar[3]	1.119	$/€	European Central Bank (2022a)
	euro to real[3]	4.413	R$/€	European Central Bank (2022b)
	ton to kg	1,000	kg/t	Newell and Tiesinga (2019)
	m^3 to L	1,000	L/m^3	Newell and Tiesinga (2019)
	MWh to MJ	3,600	MJ/MWh	Newell and Tiesinga (2019)

Continued on next page

Technology	Parameter	Value	Unit	Source
Solar PV[4]	FOM[5]	1.6	%/year	DEA (2020b)
	VOM[6]	0.01	€/MWh	Hörsch et al. (2018a)
	investment	490,000	€/MW	DEA (2020b)
	lifetime	40	years	DEA (2020b)
Offshore wind[7]	FOM[8]	1.8	%/year	DEA (2020b)
	VOM	2.4	€/MWh	DEA (2020b)
	investment[9]	1,780,000	€/MW	DEA (2020b)
	lifetime	30	years	DEA (2020b)
Onshore wind[10]	FOM[11]	1.2	%/year	DEA (2020b)
	VOM	1.22	€/MWh	DEA (2020b)
	investment[12]	960,000	€/MW	DEA (2020b)
	lifetime	30	years	DEA (2020b)
Hydro reservoir	FOM	2	%/year	Schröder et al. (2013)
	efficiency	0.9	per unit	Schröder et al. (2013)
	investment[13]	1,565,000	€/MW	Schröder et al. (2013)
	lifetime	80	years	Schröder et al. (2013)

Continued on next page

Technology	Parameter	Value	Unit	Source
	max hour[14]	18	h	ONS (2021g)
Biomass thermal	FOM[15]	1.7	%/year	EPE and MME (2020)
	VOM	2.1	€/MWh	DEA (2020b)
	investment[15]	1,200,000	€/MW	EPE and MME (2020)
	lifetime	25	years	DEA (2020b)
	efficiency[16]	0.39	per unit	Bogdanov et al. (2019)
	fuel	7	€/MWh	IEA (2021a)
AC line	investment[17]	6286.5	R$/MW/km	ANEEL (2021a)
	FOM	2	%/year	Hagspiel et al. (2014)
	lifetime	40	years	Hagspiel et al. (2014)
HVDC line	investment[17]	864.56	R$/MW/km	ANEEL (2021a)
	FOM	2	%/year	Hagspiel et al. (2014)
	lifetime	40	years	Hagspiel et al. (2014)

Continued on next page

Technology	Parameter	Value	Unit	Source
Battery storage[18]	investment[19]	75,000	€/MWh	DEA (2020a)
	max hour[20]	6	h	Bogdanov et al. (2019)
	loss[21]	0.004	per unit	DEA (2020a)
	lifetime[22]	30	years	DEA (2020a)
Battery inverter[23]	charge efficiency[24]	0.985	per unit	DEA (2020a)
	discharge efficiency	0.975	per unit	DEA (2020a)
	lifetime[22]	30	years	DEA (2020a)
	FOM[25]	0.9	%/year	DEA (2020a)
	VOM	1.6	€/MWh	DEA (2020a)
E-kerosene unit[26]	investment[27]	2,000,000	€/MW	Schmidt et al. (2018)
	VOM[28]	7.4	€/MWh	DEA (2020b)
	lifetime[29]	25	years	DEA (2021)
	efficiency[30]	0.42	per unit	Schmidt et al. (2018)
Jet fuel	CO_2 emissions[31]	3.16	$kg\,CO_2/kg$ Jet	EPA (2022)
Kerosene tank[32]	efficiency	0.9	per unit	Maurice (2021)

Continued on next page

Technology	Parameter	Value	Unit	Source
	investment	0.098	€/L	[33]
	lifetime	30	years	Maurice (2021)
	max hour	144	h	Moriarty and Kvien (2021)

[1] The value is sourced from EPE and MME (2020, Anoexos, p. A-3).
[2] The value represents the lower limit of aviation fuel density, ranging from 775-840 kg/m^3.
[3] The 2019 annual average is used.
[4] The value comes from “sheet 22 Photovoltaics medium”.
[5] The value results from dividing “Fixed O&M” by “Specific investment, total system” in the raw data.
[6] A value of 0.01 adjusts the curtailment order of renewable technology (Hörsch et al. 2018a).
[7] The value originates from “sheet 21 Large wind turbines offshore”.
[8] This is a ratio of “Fixed O&M” to “Variable O&M” derived from the original data.
[9] The value is obtained by deducting “Nominal investment grid connection costs” from “Investment costs”.
[10] The value is sourced from “sheet 20 Large wind turbines on land”.
[11] This is a ratio of “Fixed O&M” to “Nominal investment” as observed in the raw data.
[12] This refers to “Nominal investment”.
[13] This refers to “Reservoir repowered” from Schröder et al. (2013, p. 27, 2.5 Hydro).
[14] The PyPSA-Brazil model updates this threshold for each state based on stored capacity.
[15] The value originates from EPE and MME (2020, p. A-6).
[16] This value is extracted from the “Biomass CHP” in the supplementary material.
[17] This value is derived from the source data by dividing the investment cost (in R$) by transfer capacity (in MW) and line length (in km). For multiple capacities, the smallest is chosen, ignoring voltage differences.
[18] The value comes from “sheet 180 Lithium-ion battery”.
[19] This refers to the “Energy storage expansion cost (0.075 M€2015/MWh)” from the raw data.
[20] This refers to the E2P ratio.
[21] The value of “Energy losses during storage(%/day)” from the raw data is divided by 24 for consideration.
[22] This refers to “Technical lifetime”.
[23] The value is sourced from “sheet 180 Lithium-ion battery”.
[24] This refers to the “Round trip efficiency DC (discharge) charging efficiency (%)”.
[25] The ratio is derived from “Fixed O&M” to “Output capacity expansion cost investment·100” in the raw data.
[26] This considers a range of technologies and processes, including low-temperature electrolysis (AEL or PEM), H_2 storage, CO_2 from DAC, FT pathway (FT synthesis, rWGS and hydrocracking, isomerization).
[27] The value is a division of “Total[M€]” and “Fuel output” in Schmidt et al. (2018, Table 2.).
[28] The value combines “Fix O&M” and “Variable O&M” from “sheet 102 Power to Jet Fuel”.
[29] This refers to the “Technical lifetime” from “sheet 102 Power to Jet Fuel”.
[30] The value is sourced from “Efficiency[%]” from Schmidt et al. (2018, Table 2.).
[31] The value is sourced from EPA (2022, Table 1). The GHG emissions is 3.166 $kg\,CO_2e/kg$ Jet.
[32] This is assumed to be of an aboveground petroleum storage tank type.
[33] The original value of £7,266 (Fuel Tank Shop 2023) is converted from GBP to EUR based on the 2019 annual average (European Central Bank 2023), and then divided by 100,000L to be the desired value.

4.3.3 Aviation sector

4.3.3.1 Kerosene demand

In the model, aviation kerosene demand for 2050 is an hourly time series of historical federal-state kerosene demand statistics scaled up to projected national fuel demand in 2050.

The model incorporates kerosene demand from both domestic and international flows at civil airports in 2019. Brazil's National Civil Aviation Agency (Portuguese: Agência Nacional de Aviação Civil) (ANAC) publishes extensive air transport statistics, consisting of 110 variables (ANAC 2021). These variables capture critical parameters such as the number of passengers, cargo and postal traffic, distance flown, and fuel consumption, among others, for each stage of flight and each airline. These variables include key industry indicators: Revenue Tonne Kilometer (RTK), Revenue Passenger Kilometers, Available Seat Kilometers, and Available Tonne Kilometers.

The model assumes flights departing from Brazilian airports refuel within Brazil, thereby constituting the kerosene demand for each airport. As a result, four attributes of the original air transport data set (as detailed in Table 4.5) are used. By accounting for the location of the refuelling airport, the kerosene demand is aggregated by each federal state. The model presumes that the departure time of the aircraft corresponds to the refuelling date, which yields a daily kerosene demand pattern. This daily time series is then averaged out to derive an hourly demand profile (presented in Figure 4.4).

In 2019, the kerosene demand is 4,286.6 ML (approximately 39.5 TWh), with the highest demand found in the federal state of SP(39.9%), followed by RJ and DF (7.9% each), PE (5.2%), BA (4.8%), CE (4.5%), MG (4.4%), RS and PR (3.2% each). Historical kerosene demand is available for 2000-2020, but the model only employs the time series for the base year 2019 (cf. Figure 4.5).

The ANAC releases official annual demand forecasts for domestic and international flights up to 2050, distinguished by two scenarios: "without mitigation"

Table 4.5: Attributes used in PyPSA-Brazil from the air transport statistics (ANAC 2021).

PyPSA-Brazil	Original data set	Unit	Type	Explanation
`origin_state_name`	`sg_uf_origem`	—	string	abbreviation of Brazilian federal state, in total 27 federal units
`departure_date`	`dt_partida_real`	—	string	time stamp of the real take-off date of the state, `yy:MM:dd hh:mm:ss`
`fuel_consumption`	`lt_combustivel`	L	float	the kerosene demand

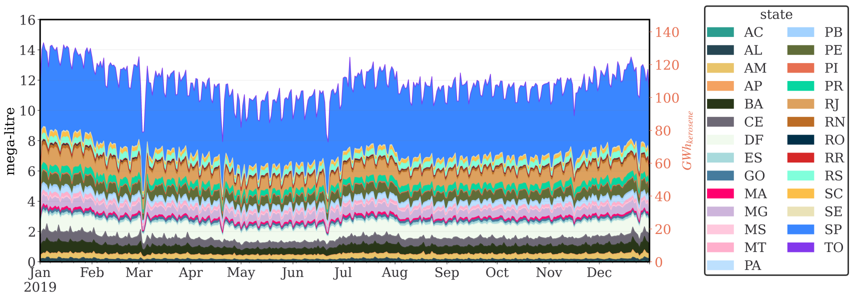

Figure 4.4: 2019 kerosene demand by federal states. The left y-axis is in units of the original data, and the right axis is in units converted to GWh according to Table 4.4.

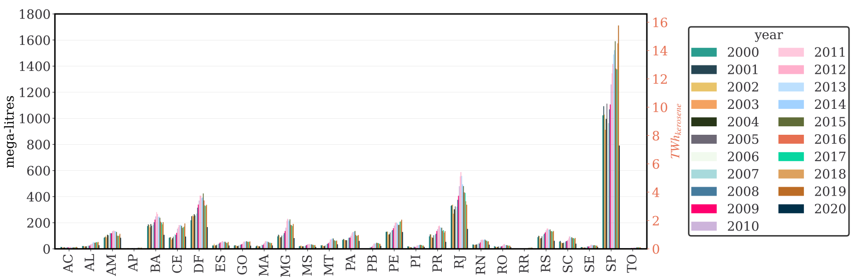

Figure 4.5: Two-decade kerosene demand by federal states (2000-2020): dual y-axis display of original and converted units (TWh) as per Table 4.4.

and "with mitigation" (Ministry of Infrastructure 2019). The projection for the period 2019-2050 on total annual national kerosene demand is determined using monthly RTK and kerosene consumption statistics from 2010-2018, as well as the anticipated progress in fuel efficiency (ICAO 2019b). In the "with mitigation" scenario, Brazil's total kerosene consumption is expected to reach 13.2 million tons in 2050 (Ministry of Infrastructure 2019), representing an overall growth of 217.5% and an average annual growth of 3.7% from 2018 to 2050. This projection of kerosene consumption of 13.2 million tons (around 157 TWh) for 2050 is integrated into the PyPSA-Brazil model, which is approximately four times higher than the consumption level in the base year of 2019.

4.3.3.2 Kerosene supply

According to Figure 4.2, the aviation sector consumes kerosene that is synthetically produced with e-kerosene, fossil origin, or biokerosene.

Supply of conventional kerosene

The supply of conventional kerosene depends purely on the cost of supply.

The National Agency for Petroleum, Natural Gas and Biofuels (Portuguese: Agência Nacional do Petróleo, Gás Natural e Biocombustíveis) (ANP) regularly updates the fuel distribution prices at a national, regional, and federal state level[3] (ANP 2022). The state-level data are incorporated into PyPSA-Brazil, using regional data when values are absent for certain states such as SE and AP. It is assumed that the conventional kerosene price (R$/L) in 2019 is the marginal production cost in each state in 2050. An average hourly price is then determined from the monthly prices (cf. Figure 4.6) since PyPSA-Brazil considers a time-dependent marginal cost. With the carbon emissions from conventional kerosene generation, a carbon price is introduced for Brazil to achieve carbon neutrality (cf. Section 4.3.5).

[3] The data are stored in XLSX format.

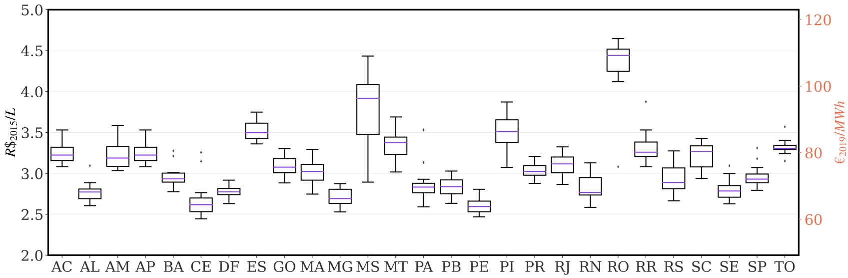

Figure 4.6: Box plot of monthly kerosene distribution price across federal states in 2019: input data of PyPSA-Brazil model processed from original source (ANP 2022), with the raw and converted units of €/MWh (cf. Table 4.4).

Supply of biokerosene

PyPSA-Brazil model posits that the biokerosene potential for 2050 is measured by its production cost, as appraised by Cervi et al. (2020). This assessment employs TEA and spatial data analysis to examine the potential of 13 distinct production routes in 2030 at a spatial resolution of 5 km. These routes comprise eight first-generation biomass: maize, sugarcane, sorghum, eucalyptus, soybean, sunflower, palm, and macaw; and five conversion pathways, including ATJ, HEFA, FT, Direct Fermentation of Sugars to Hydrocarbons (DSHC), and Hydrotreated Depolymerized Cellulosic Jet (HDCJ). Cervi et al. (2020) assume that the land used for biokerosene production is leftover – it is not utilised for other purposes, such as forest plantations and urbanisation, and it is not set aside for conservation areas.

Cervi et al. (2020) provide data in $\$/\mathrm{t}$, which is converted to €/MWh for integration into PyPSA-Brazil. The resolution provided by Cervi et al. (2020) for the cost of biokerosene production is 5 km, whereas PyPSA-Brazil utilises a coarser spatial resolution corresponding to federal states. In PyPSA-Brazil, the production cost of biokerosene for each federal state is determined by calculating 10%, 25%, 50% percentile of the cost within $5\,\mathrm{km} \times 5\,\mathrm{km}$ cell, as depicted in Figure 4.7. For scenario analysis, the input to the model indicates that the production cost at the federal-state level ranges from 69.5-149.2 €/MWh at a low level, 104.2-234.6 €/MWh at a medium level, and 147.8-725.6 €/MWh at a high level.

As the biomass used in Cervi et al. (2020) (maize, sugarcane, sorghum, eucalyptus, soybean, sunflower, palm and macaw) is of the biogenic type, the life-cycle GHG emissions of biokerosene are set to be carbon neutral (Prussi et al. 2021), signifying its environmental sustainable character.

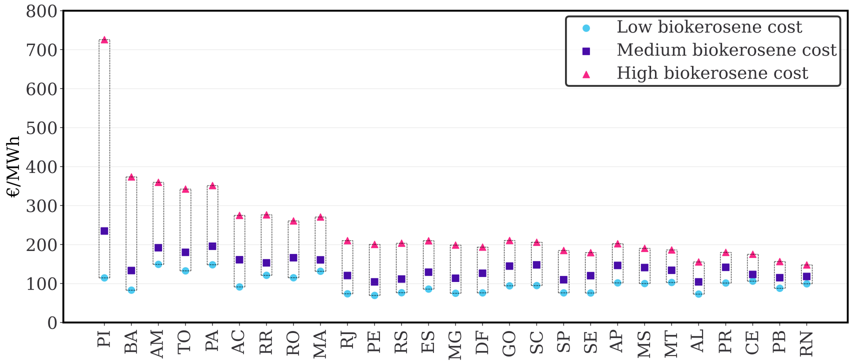

Figure 4.7: Input assumptions of biokerosene production costs for the federal states used in PyPSA-Brazil. Each marker represents the input assumption – the percentile of biokerosene production costs for pixel points within the federal state. The lower the percentile, the lower the presumed production cost. The range of variation orders the values.

4.3.4 Carbon emission cap

In PyPSA-Brazil, total carbon emissions across sectors are limited so as not to exceed a predetermined budget, represented by Γ_{CO_2} as shown in Equation (4.12). In compliance with Brazil's Intended Nationally Determined Contributions (iNDC), the nation is committed to cutting GHG emissions to 50% below the levels recorded in 2005 by the year 2030, and further attaining climate neutrality by

2050 (UNFCCC 2022, p. 1). This commitment translates into an average annual reduction rate of 2%. The scarcity of sector-specific statistics and emission budgets, however, necessitates certain assumptions for modelling purposes.

As a reference, in 2006, the power sector was responsible for the emissions of 26.42 Mt CO_2e (EPE 2011). Since data for 2005 are not available, this dissertation assumes a consistent 2% reduction rate from 2006 to 2050. This assumption yields an 88% reduction by 2050 based on 2006 emissions, setting a budget of 3.17 Mt CO_2e. This budget represents GHG emissions, and in the context of PyPSA-Brazil, it is regarded as the carbon emission budget for the power sector.

Regarding the aviation sector, the ANAC has estimated the carbon emissions for the period 2019-2050, drawing upon the projected kerosene consumption for domestic and international flights. This calculation, underpinned by the assumption of kerosene demand being exclusively met by conventional kerosene, applies a carbon emission factor of $3.16\,\mathrm{kg}\,CO_2/\mathrm{kg}$ Jet (Ministry of Infrastructure 2019, p. 32). Consistent with the global mitigation measure to secure carbon-neutral growth in aviation from 2020, and net-zero carbon emissions by 2050 (ICAO 2019c, p. 1-2), the PyPSA-Brazil model postulates that Brazil adopts an emissions budget for 2050 equivalent to the projection for 2020 (Ministry of Infrastructure 2019), amounting to 14.2 million tonnes. This budget of 14,221,089.4 tonnes pertains to carbon emissions. Consequently, the model permits up to 34% of the demand to be satisfied by conventional kerosene, assuming a total kerosene consumption of 13.2 million tonnes in Brazil by 2050.

4.3.5 Carbon pricing range

Carbon pricing is a policy tool that charges on GHG emissions, encouraging governments and industries to modify their production, consumption, and investment habits in favour of low-carbon growth (World Bank 2022). As of 2022, Brazil has been evaluating the introduction of carbon pricing, though it has not yet been established (World Bank 2022, p. 12, 55). Notably, the current carbon pricing in effect regulates only the CO_2 emissions from aviation (Lee et al. 2021). For instance, the European Union (EU)'s Emission Trading System (EU ETS) focuses on CO_2 emissions because the scientific understanding of non-CO2 effects (such as NOx, water vapour, soot, sulphates, and contrails) is not yet sufficiently mature to formulate comprehensive policies (European Commission 2020, Lee et al. 2021). For this reason, PyPSA-Brazil limits the application of carbon budgets and carbon pricing to CO_2 emissions.

In the scenario analysis of this dissertation, carbon pricing is primarily applied to the combustion of jet fuel, which leads to CO_2 emissions. The analysis begins with the implementation of a carbon emissions budget (cf. Section 4.3.4), and in PyPSA-Brazil, this corresponds to an initial carbon price of 160 €/t.

The analysis explores a range of carbon prices for the year 2050, extending from 160 €/t to 1000 €/t. This range includes specific price points such as 200 €/t, 260 €/t, 320 €/t, and 500 €/t. The assumed range of carbon prices is in line with the IPCC's mitigation pathway of limiting the median warming to below 1.5 °C by 2100. The selected carbon prices fall within the range specified by two IPCC scenarios: the "low overshoot pathway", which holds a 50-67% likelihood of a temporary early overshoot of 1.5 °C, and the high overshoot pathway, having an over 67% probability of an early temporary overshoot (IPCC 2022b).

4.4 Scenario definitions

This dissertation dissects the economic feasibility of the production of e-kerosene within a future carbon-neutral Brazilian power system. It also investigates Brazil's prospects for exporting carbon-neutral kerosene. The scenarios predominantly align with the Research Questions 3.1 to 3.4.

To address the Research Question 3.1, this dissertation conducts an analytical comparison, using input data, between electricity demand and generation potential.

Two scenarios are considered in response to Research Question 3.2. The first, “only power system”, posits a carbon-neutral Brazilian power system by 2050 without resorting to fossil and nuclear power plants. The second, “100% e-kerosene supply”, envisages that Brazil completely meets its kerosene demand with e-kerosene by 2050. This spotlights the potential upper boundaries of such a system design.

Research Question 3.3 delves into the cost competitiveness of e-kerosene by juxtaposing it with biokerosene and fossil-derived jet fuel. This comparison accounts for all options of kerosene supply, stepping away from the aforementioned discussed ceiling scenario confined to e-kerosene alone. The model favours e-kerosene, biokerosene and fossil-derived jet fuel based on their cost effectiveness, with the rise in biokerosene production costs and carbon pricing acting as potential catalysts for e-kerosene uptake. The scenario analysis accommodates assumptions on biokerosene inputs (low, medium, and high, cf. Section 4.3.3.2). Additionally, it considers varying carbon prices (160 €/t, 200 €/t, 260 €/t, 320 €/t, 500 €/t, and 1000 €/t, refer to Section 4.3.5). The model, in return, determines the potential shares of e-kerosene, biokerosene, and conventional kerosene in the total jet fuel demand.

For Research Question 3.4, this dissertation relaxes the 2050 domestic demand for aviation fuel to consider the potential export expectations. From the findings of Research Question 3.3, a carbon price is determined, which encourages the system to supply carbon-neutral alternatives (biokerosene and e-kerosene), irrespective of biokerosene production costs. The model runs through each level of biokerosene production costs with a projected total domestic kerosene demand (i.e., 157 TWh). Running the model would yield a set of baseline scenarios for subsequent comparative analyses. Following this, the domestic demand is scaled proportionally across Brazil’s federal states with additional increments (50%, 100%, 150%, 200%, 400%, 500%), representing an increased demand for kerosene intended for export.

4.5 Equations for analysis

4.5.1 Average system cost

In this dissertation, the Average System Cost (ASC) is employed as a metric that quantifies the average optimised total system cost per unit of energy generated within an energy system (Schlachtberger et al. 2017, Fig. 2). Employing ASC as a metric enables the insightful comparison of the relative costs associated with energy supplies across various system designs through a given equation:

$$\text{ASC} = \frac{\mathcal{C}^*}{\Gamma^*} \tag{4.15}$$

where

$\mathcal{C}^*$: optimised total system cost, €, computed as outlined in Equation (4.1)

Γ^* : optimised total dispatch, MWh. It includes the amount of energy produced by renewable generation technologies and the supply of kerosene in the system.

4.5.2 Levelised cost of electricity

The Levelised Cost of Electricity (LCOE) assesses the costs associated with electricity generation from a single technology, with the costs being the net present sum of investment, fuel, operational and maintenance costs (Brown and Reichenberg 2021, Short et al. 1995). This dissertation uses LCOE to compare the generation cost for each technology among studies through the equation:

$$\text{LCOE}_r = \frac{\sum\limits_{n} c_{n,r} \cdot G^*_{n,r} + \sum\limits_{n,t} o_{n,r} \cdot g^*_{n,r,t}}{\sum\limits_{n,t} g^*_{n,r,t}} \tag{4.16}$$

where

LCOE_r	: levelised cost of electricity for technology r
r	: generation technology
n	: node
$c_{n,r}$	: annualised capital costs for technology r
$G^*_{n,r}$	: optimised installed capacity of generators
$o_{n,r}$	: variable costs
$g^*_{n,r,t}$	: optimised generation dispatch, MWh.

4.5.3 Levelised cost of fuel

The Levelised Cost of Fuel (LCOF) refers to the supply of e-kerosene, which is essential for determining its economic viability:

$$\text{LCOF} = \frac{\sum_n \left\{ \sum_{k,t} (c_{n,k} \cdot P_{n,k} + o_{n,k} \cdot p_{n,k,t}) + \sum_{s,t} (c_{n,s} \cdot E_{n,s} + o_{n,s} \cdot e_{n,s,t}) + \overline{\lambda_n^{\text{electricity}}} \cdot \Gamma_n^{\text{electricity}} \right\}}{\sum_n \Gamma_n^{\text{e-kerosene}}} \tag{4.17}$$

where

n : node, $n \in \mathcal{N}, \mathcal{N} = 1, 2, \ldots, 27$
k : energy conversion technologies, $k \in \{\text{e-kerosene production unit}\}$
t : hour
$c_{n,*}$: annualised capital expenditures
$P_{n,k}$: installed capacity of technology k at node n
$o_{n,*}$: variable operational expenditure
$p_{n,k,t}$: e-kerosene dispatch at hour t at node n
s : storage technology, $s \in \{\text{e-kerosene tank}\}$
$E_{n,s}$: power capacity of storage technology s at node n
$e_{n,s,t}$: storage dispatch of e-kerosene tank
$\overline{\lambda_n^{\text{electricity}}}$: median KKT multiplier of electricity at node n (cf. Equation (4.3))
$\Gamma_n^{\text{electricity}}$: total electricity consumption for e-kerosene production at node n
$\Gamma_n^{\text{e-kerosene}}$: total e-kerosene supply at node n.

4.5.4 Export cost

The cost of export is defined as the relative deviation compared to the reference scenario without export:

$$\mathcal{E}_{\beta,\delta} = \frac{\mathcal{C}_{\beta,\delta} - \mathcal{C}^{\text{Ref.}}}{d_{\beta,\delta}^{\text{kerosene}} - d^{\text{Ref.,kerosene}}} = \frac{\mathcal{C}_{\beta,\delta} - \mathcal{C}^{\text{Ref.}}}{\delta \cdot d^{\text{Ref.,kerosene}}} \tag{4.18}$$

where

$\mathcal{E}_{\beta,\delta}$: export cost for the scenario given β, δ

β : level of production cost for biokerosene, $\beta \in \{\text{low, medium, high}\}$

δ : additional kerosene demand for export,
$\delta \in \{50\%, 100\%, 150\%, 200\%, 400\%, 500\%\}$

$\mathcal{C}_{\beta,\delta}$: total system cost of the scenario given β, δ

$\mathcal{C}^{\text{Ref.}}$: total system cost of the reference scenario

$d^{\text{kerosene}}_{\beta,\delta}$: total kerosene demand of export scenario given β, δ,
$d^{\text{kerosene}}_{\beta,\delta} = (1 + \delta) \cdot d^{\text{Ref.,kerosene}}$

$d^{\text{Ref.,kerosene}}$: total kerosene demand in the reference scenario, i.e., $157\ \mathrm{TWh}$.

4.5.5 Export amount of e-kerosene

The amount of the e-kerosene for export is the absolute difference in the amount of e-kerosene supply between the export scenario and the reference scenario.

$$\mathcal{P}_{\beta,\delta} = p_{\beta,\delta} - p^{\text{Ref.}} \tag{4.19}$$

where

$\mathcal{P}_{\beta,\delta}$: e-kerosene for export given β, δ

$p_{\beta,\delta}$: generation of e-kerosene given β, δ

$p^{\text{Ref.}}$: generation of e-kerosene in the reference scenario.

5 E-kerosene Production and Export in Carbon-neutral Power Systems – A Solution for Sustainable Aviation?

Contents of this chapter are based on

Y. Deng, K.-K. Cao, M. Wetzel, W. Hu, and P. Jochem. **E-kerosene Production and Export in Carbon-neutral Power Systems – A Solution for Sustainable Aviation?**. 2023. *Submitted to Journal of Scientific Reports*.

This chapter presents the results of the scenario analysis to address Research Question 2 and Research Question 3.

5.1 Results

5.1.1 Availability of renewable energy in Brazil for comprehensive e-kerosene production

This section evaluates the assumptions concerning demand and generation potentials within the PyPSA-Brazil model, in light of Research Question 3.1. It particularly focuses on the potential for renewable energy generation and the projected energy demand in Brazil by 2050, with a special emphasis on e-kerosene.

Table 5.1 compiles the technical potential for renewable energy generation and contrasts it with statistics on electricity generation for the year 2019. The inclusion of 2019 data acts as a yardstick to show the plausibility of model results and offers a snapshot of the renewable energy generation status in Brazil that year. Additionally, Table 5.2 reveals how much energy Brazil could need by the year 2050, including electricity, kerosene (converted into TWh), and annual electricity exchanges.

Table 5.1: Renewable electricity generation potential assumed in PyPSA-Brazil.

Technology	**Status in 2019 (TWh) (ONS 2021b)**	**Potential (TWh) (Chapter 3)**
Offshore wind	—	3,552.9
Onshore wind	53.4	3,114.0
PV	5.0	513,669.2
Hydropower	405.6	2.0[a]
Non-biomass thermal	73.3	—
Biomass thermal	14.5	222.5[b]
Nuclear	16.1	—
Total	567.9	520,560.6

[a] The computation represents the product of the allowed expansion capacity and the E2P ratio, presented in h.
[b] The value is the multiplication outcome of the allowed expansion capacity (set at 25.4 GW) and the cumulative hours of the year, which amount to 8,760 hours.

A noteworthy observation is that the estimated renewable electricity generation stands at a substantial 520,561 TWh, far surpassing the maximum total demand of 1,322 TWh. Given an e-kerosene production efficiency at 0.42 (cf. Table 4.4 and Section 4.2.4), meeting the entire kerosene demand through e-kerosene would theoretically impose an additional burden of 374 TWh. This amount corresponds to 32% of the future electricity demand under the $\text{COPPE}_{\text{lowBECCS}}$ scenario. Hence, the main obstacle to building adequate infrastructure to harness the generating

Table 5.2: Energy demand in 2050 assumed in PyPSA-Brazil.

Demand type	**Input scenario**	**Value (TWh)**
Kerosene	ANAC "with mitigation"	157.0
Electricity (Section 3.2.6)	$\text{COPPE}_{\text{2Deg2030}}$	779.4
	$\text{COPPE}_{\text{BAU}}$	748.1
	$\text{COPPE}_{\text{lowBECCS}}$	1,167.8
	$\text{PNE2050}_{\text{ECS}}$	885.3
	$\text{PNE2050}_{\text{SS}}$	620.8
Electricity import/export[a]	import/export from neighbouring country	1.87
Maximum total demand[b]	—	1,321.93

[a] The value represents electricity import/export from neighbouring countries. Positive values indicate Brazil importing energy, while negative values indicate Brazil exporting energy. The assumption is based on the electricity trade patterns observed in the base year 2019.

[b] The value is calculated as the sum of kerosene demand and electricity demand of $\text{COPPE}_{\text{lowBECCS}}$, subtracting electricity imports/exports.

potentials would principally revolve around economic feasibility and the societal acceptance of renewable power plants.

This dissertation takes into account the limitations in expanding current hydropower facilities due to environmental and societal considerations, as highlighted by Nogueira et al. (2014). Therefore, it is assumed that hydropower expansion follows the trajectory laid out in the Brazilian Ten-Year Energy Plan (cf. Section 3.2.3). Looking ahead, the Brazilian energy system may increasingly rely on wind and solar energy sources (cf. Section 1.5). Integrating e-kerosene production for the aviation sector into Brazil's energy mix requires strategic decision-making regarding locations and timings for electricity and kerosene production, with consideration of the aforementioned constraints and potentials.

5.1.2 Future carbon-neutral power system with and without e-kerosene production

In response to Research Question 2 and Research Question 3.2, this section offers an analysis of Brazil's future carbon-neutral power system, with a particular focus on the incorporation of e-kerosene production. Two scenarios are compared based on three key parameters: annual total system costs, the distribution of optimal installed capacity, and nationally aggregated electricity generation.

5.1.2.1 Annual total system costs

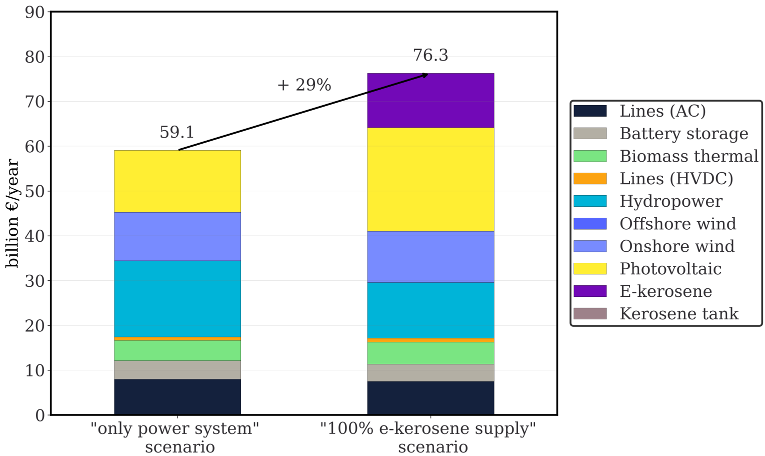

Figure 5.1: Breakdown of annual total system costs in Brazil's carbon-neutral power system scenarios without ("only power system") and with e-kerosene production integration ("100% e-kerosene supply").

The PyPSA-Brazil model outcomes, displayed in Figure 5.1, indicate a rise in total system costs, which is driven by the additional provision of e-kerosene (increasing from 59.1 to 76.3 billion €/ year, by 29%). The main contributor to this increase is the further investment in PV installations, which provides 317 TWh. In contrast, hydropower remains relatively stable, while wind onshore (additionally 35 TWh) and biomass (additionally 38 TWh) energy see an uptick. E-kerosene production offers some load-balancing flexibility, leading to a slightly reduced investment in battery storage.

5.1.2.2 Distribution of optimal installed capacity

The efficient allocation of generation capacities across different energy sources and regions can help in minimising costs and ensuring a reliable energy supply. In this context, considering the regional differences between the two scenarios, PV installations display the most pronounced impact with a surge of 213 GW (cf. Figure 5.2). The federal states of São Paulo, Minas Gerais, Distrito Federal and Goiás are expected to be the focal regions for PV installations.

In conjunction with PV, the expansion of installed onshore wind power capacity is necessary, especially in the Northeast and South regions of Brazil. The state of Rio de Janeiro shows a prominent increase with a total installed capacity of 16.11 GW. The disparity in biomass thermal plant installations is relatively modest at 0.64 GW. To exclusively fulfil the kerosene demand of both domestic and international airlines refuelling at Brazilian civil airports with e-kerosene by 2050, Brazil would have to install a total of 49.54 GW of e-kerosene production units. São Paulo is expected to host the bulk of these installations. The incorporation of e-kerosene into the energy mix calls for an extra 387 GWh of battery storage and 6,601 GWh of kerosene tank capacity compared to the scenario with only a carbon-neutral power system. To realise a fully decarbonised power system, the grid is set to grow beyond its size as of 2019. This expansion rises to 29.5% when including e-kerosene production to meet the projected kerosene demand in 2050.

A remarkable outcome from integrating e-kerosene is its ability to decrease the Average System Cost (ASC), defined as the total system cost divided by total energy generated (cf. Equation (4.15)), from 50.3 €/MWh in the "only power system" scenario to a lower value, a 13.8% decrease. This decrease can be

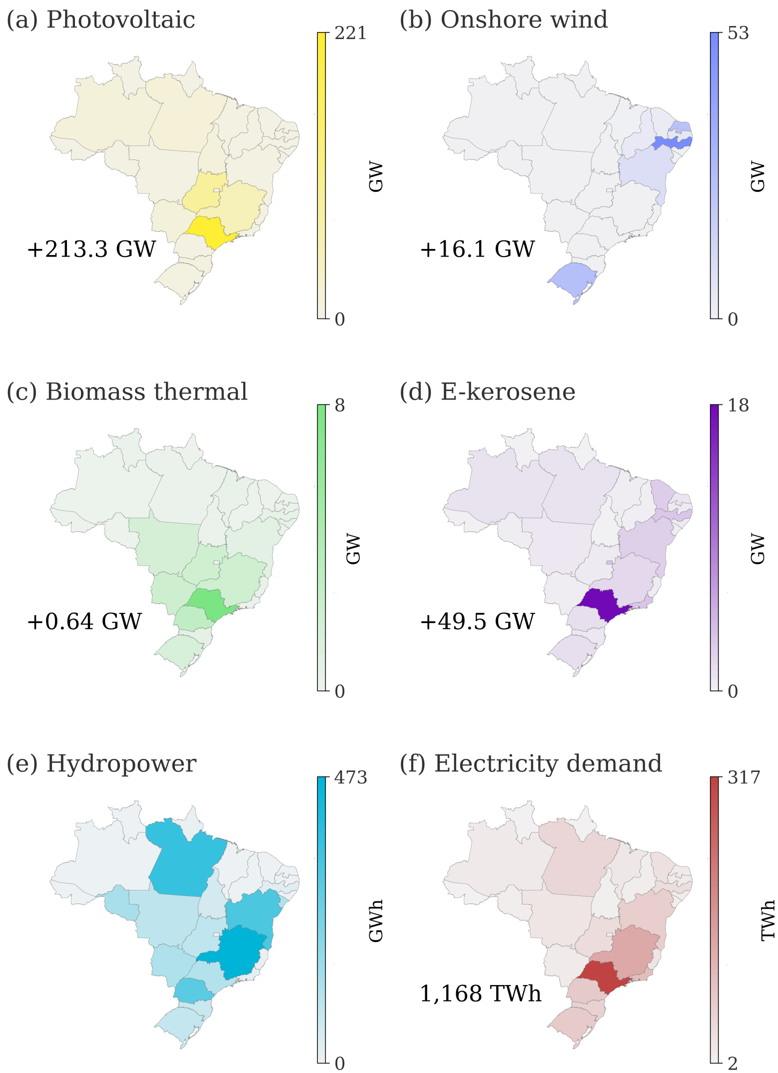

Figure 5.2: Distribution of installed capacities of selected technologies for the "100% e-kerosene supply" scenario obtained from PyPSA-Brazil. The values indicate the differences compared to the "only power system" scenario. Note that, unlike the other subplots, (f) electricity demand is an input to the model and is included here for reference.

attributed to a reduction in the curtailment[1] of biomass thermal power plants (falling from 50.5% to 22.5%). Concurrently, offshore wind power generation also experiences a reduction in curtailment (from 10.8% to 6.3%), as does PV power plants (from 0.9% to 0.3%). The exception is onshore wind, which observes a slight increase of 1%. Therefore, the integration of e-kerosene production contributes to improving the overall efficiency of the power system.

5.1.2.3 Annual electricity generation

Figure 5.3 illustrates the additional electricity generation required for producing e-kerosene in a carbon-neutral power system. Specifically, the results accentuate the substantial contribution from PV generation. This is complemented by 35 TWh from onshore wind and 39 TWh from biomass thermal energy. While hydropower experiences a slight rise, contributing to 2 TWh, it pales in comparison to the aforementioned technologies. Offshore generation also contributes but has a minimal impact in both scenarios.

5.1.3 Shares of e-kerosene in Brazil under uncertain biokerosene costs and carbon prices

This section addresses the Research Question 3.3 and evaluates the cost-effectiveness between e-kerosene, biokerosene, and conventional jet fuel. It reveals the proportions would need to attain to satisfy kerosene demand across Brazil's federal states in 2050.

According to the model results, e-kerosene constitutes between 2.7% and 18.5% of the fuel mix in most scenarios. These scenarios are differentiated by biokerosene production costs and carbon prices. In the case where both biokerosene production costs (cf. Section 4.3.3.2) and carbon prices (cf. Section 4.3.5) are high, there is

[1] Generation curtailment is defined as a decrease in the output of a generator compared to its potential production, given available resources such as wind or sunlight.

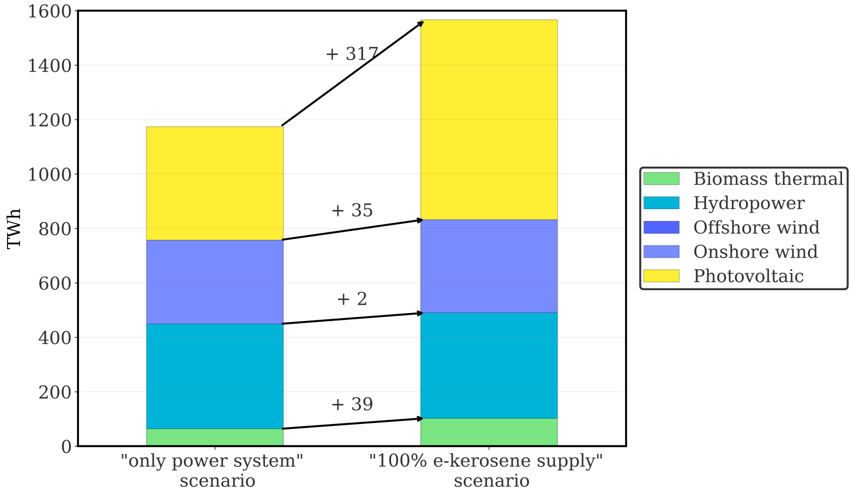

Figure 5.3: A comparison of annual electricity generation in Brazil's energy system under carbon-neutral scenarios without ("only power system") and with the integration of e-kerosene production ("100% e-kerosene supply").

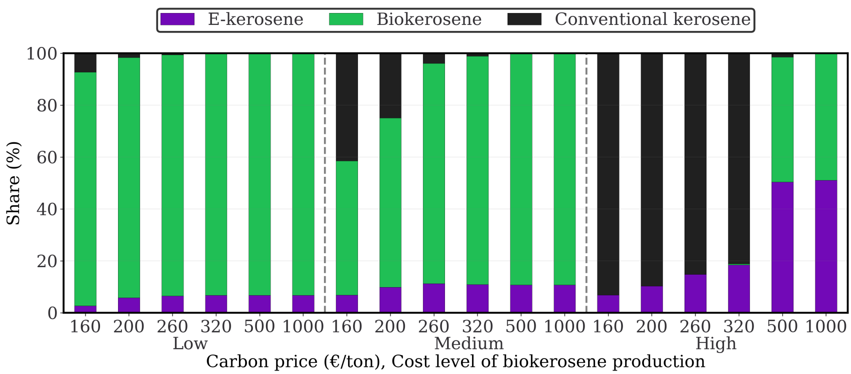

Figure 5.4: Supply shares of e-kerosene, biokerosene, and conventional kerosene, adjusted according to biokerosene production costs and carbon pricing associated with conventional kerosene production.

a sharp substantial increase to 50.4-51.1% in the share of e-kerosene, as shown in Figure 5.4. This outcome indicates a positive correlation between the share of e-kerosene and the production costs of biokerosene alongside carbon pricing.

Figure 5.1 compares the "100% e-kerosene supply" scenario, wherein the entire kerosene supply is assumed to be e-kerosene, against a carbon-neutral power system scenario. Table 5.3 extends this analysis with further details, contrasting scenarios in which kerosene demand is exclusively met by conventional kerosene at various carbon prices (0 €/t, 500 €/t, and 1000 €/t), or by biokerosene with different production costs (low, medium, and high). Under the assumption that e-kerosene is the only source to meet the kerosene demand by 2050, the total system cost rises by 29.1%. This is only more cost-intensive than scenarios where kerosene demand is completely fulfilled by low-cost biokerosene (22.5%) or carbon-free priced conventional kerosene (19.3%). Therefore, if the conventional kerosene costs remain as they are today and the biokerosene costs stay low in the future, their economic competitiveness may discourage the production of e-kerosene.

5.1.4 Export costs of carbon-neutral kerosene from Brazil

The cost-benefit analysis in previous section finds that when the carbon price reaches 1000 €/t, only carbon-neutral kerosene – comprising biokerosene and e-kerosene – is integrated into the supply, regardless of how the biokerosene production costs vary (cf. Figure 5.4).

Building on this finding, this section explores the additional burden imposed by exporting carbon-neutral kerosene, in response to Research Question 3.4. The export costs of carbon-neutral kerosene, as elaborated in Section 4.5.4, tend to remain stable despite increasing export demand. However, these export costs range from 78 €/MWh to 181 €/MWh, depending on whether the production costs of biokerosene are low or high. It is also noteworthy that, at a high production

Table 5.3: Comparison of additional theoretical costs on a carbon-neutral power system basis when the total domestic kerosene demand in 2050 (157 TWh) is covered by conventional kerosene, biokerosene and e-kerosene[a].

Kerosene options		**Absolute difference (billion€/year)**	**Relative difference[b] (%)**
Conventional	No carbon price	11.4	19.3
	Carbon price: 500 €/t	32.3	54.7
	Carbon price: 1000 €/t	53.2	90.0
Biokerosene	Low costs	13.3	22.5
	Medium costs	19.3	32.7
	High costs	33.3	56.3
"100% e-kerosene supply" scenario		17.2	29.1

[a] Results are obtained by post-processing, except for the "100% e-kerosene supply" scenario.
[b] The "only power system" scenario projects a system cost of 59.1 billion€/year.

cost of biokerosene, the export cost is approximately equivalent to the situation when only e-kerosene is allowed to be produced.

For a deeper understanding, Figure 5.5 presents the model outcomes of e-kerosene generation for export (cf. Section 4.5.5 for definition) as an illustrative demonstration of its contribution at various cost levels of biokerosene production. For contextual reference, results from the hypothetical scenario where the supply is solely composed of e-kerosene are also exhibited, concurrent with the rising demand for kerosene export. The results indicate that production of e-kerosene for export remains restrained, stabilising below 25 TWh, when the biokerosene production costs are in the low to medium range. The greater cost competitiveness of biokerosene production, particularly in meeting the additional export demand, accounts for this trend over e-kerosene production.

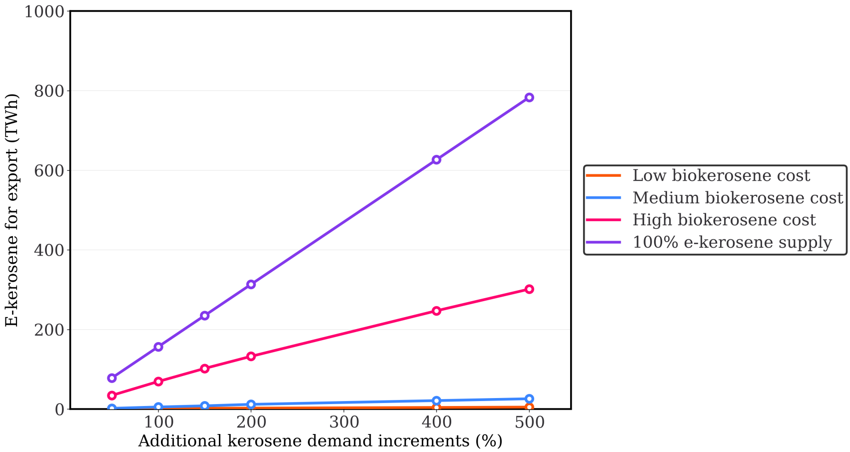

Figure 5.5: E-kerosene generation for export at different cost levels of biokerosene production, assuming a carbon price of 1000 €/t.

5.2 Discussions

5.2.1 Feasible e-kerosene productions in Brazil from abundant renewable potentials

This dissertation found that attaining a fully decarbonised power system with e-kerosene in Brazil is not only feasible but also demonstrates higher efficiency compared to merely targeting a carbon-neutral power system by 2050. In the Brazilian context, such a system necessitates the deployment of new PV capacities, particularly in the federal states of Minas Gerais, Goiás, and Distrito Federal, with a special emphasis on São Paulo.

As shown in Table 5.4, São Paulo emerges as the dominant federal state in terms of electricity and kerosene demand, given its stature as the country's largest economy and the most populous state. In contrast, Rio de Janeiro and Distrito Federal have relatively high population densities. São Paulo's low population density might contribute positively in lessening social acceptance issues linked to land use for

PV expansion. Distrito Federal, characterised by the highest population density, predominantly relies on importing electricity from neighbouring states. Adjacent to Distrito Federal, Goiás displays moderate electricity demand and relatively low kerosene demand. The lower population density in Goiás positions it favourably for PV expansion and for acting as an electricity conduit or even a powerhouse to other federal states. Minas Gerais follows São Paulo in electricity and kerosene demand, and its low population density might result in fewer social acceptance issues regarding new PV installations. Lower population density can be a factor in diminishing local acceptance conflicts, albeit not a definitive solution (Fitiwi et al. 2020, Bertsch et al. 2016).

Table 5.4: GDP, population, area, and population density in 2018.

Federal state	GDP (thousand R$) (IBGE 2018c)	Population (IBGE 2018b)	Area (km^2) (IBGE 2018a)	Population density ($people/km^2$)
São Paulo	2,210,561,949	45,538,936	248,219	184
Goiás	195,681,724	6,921,161	340,125	20
Distrito Federal	254,817,204	2,974,703	5760	516
Minas Gerais	614,875,819	21,040,662	586,521	36
Rio de Janeiro	758,859,046	17,159,960	43,750	392

Owing to Brazil's substantial solar potential and the relatively low cost of PV installations, this potential could lead the way in Brazil's quest for a carbon-neutral power system. Other cost assumptions, such as those made by Dranka and Ferreira (2018), lead to diverse outcomes. However, the LCOE for PV in 2050 is estimated at approximately $33\,€/MWh$, which is in alignment with findings by IEA (2021a) and IRENA (2022). The LCOE of other renewable energy technologies, such as biomass thermal plants and onshore wind power, are observed in the same order of magnitude (IRENA 2022). An exception to this finding is offshore wind, with LCOE estimated at around 59 €/MWh, which is lower than the anticipated range of 71.6-115.3 €/MWh[2].

5.2.2 Consistent system benefits from e-kerosene production

This study demonstrates that the production cost of e-kerosene can be competitive with biokerosene and carbon-priced fossil jet fuel and can make up 2.751.1% of the fuel mix. However, an increase in carbon pricing does not invariably result in a linear increment in the share of e-kerosene. The future production cost of biokerosene stands as a determinant shaping the contribution of e-kerosene within the Brazilian aviation sector. Biokerosene costs are held constant over time in this analysis, with the exploration of three cases – low, medium, and high – which vary by the federal states in Brazil.

The analysis is founded on the assumption that Brazil is to implement a carbon price in 2050, from 160 €/t. Within this parameter, the production of e-kerosene consistently emerges as cost-beneficial, as per PyPSA-Brazil. When the biokerosene production costs are low to medium, the contribution of e-kerosene is present yet minimal. In such a scenario, the continuous use of conventional jet fuel may also be cost-effective, if carbon pricing is not high enough.

The extent of e-kerosene's contribution to the Brazilian aviation sector markedly intensifies only when biokerosene's production cost is high, and the use of conventional jet fuel is restricted, such as by well-established carbon price or carbon emissions budgets. This finding needs to be interpreted with caution as it is primarily impacted by assumptions on the production cost of biokerosene. Although PyPSA-Brazil considers biokerosene supply as carbon neutral, indirect GHG emissions, land use, and competition with food would prevent it from being available at scale.

[2] The estimate stems from a conversion of the value 0.064-0.103 ¢/kWh, as suggested by IRENA (2022) for China, into Euro using the exchange rates from Table 4.4.

In addition, Cervi et al. (2020) conclude a wide range of production costs for biokerosene, depending on the pathways and biomass types. The minimal production cost for pixels (5 $\mathrm{km} \times 5$ km) lies at 79.2-384 $€_{2019}/\mathrm{MWh}$[3]. The potential overestimation of biokerosene cannot be overlooked, particularly given the assumption of unlimited quantity and season-independent availability to maintain data integrity. This calls for further examination in the assessment of biomass potential.

5.2.3 Insights into e-kerosene's mild contribution

The economic practicability of e-kerosene supply, as portrayed in Table 5.3, might lead one to expect its extensive incorporation in the fuel mix. However, an unexpected observation emerges from Figure 5.4, which reveals that even amidst high carbon pricing and biokerosene cost, e-kerosene accounts for a maximum of 51.1% of the total supply in the scenarios studied. For clarification, Figure 5.6 illustrates the allocation of biokerosene and e-kerosene across federal states, considering high biokerosene costs and carbon prices. The data in Figure 5.6 indicate that, in the majority of federal states, e-kerosene assumes the larger portion of the fuel supply. São Paulo, however, deviates from this trend, exhibiting a marked inclination for biokerosene, thus magnifying its cumulative share in fulfilling the kerosene demand.

A deeper examination of costs in São Paulo sheds light on prominence of biokerosene. Within PyPSA-Brazil, the biokerosene production cost in São Paulo is assumed to be 184.8 $€/\mathrm{MWh}$, lower than the e-kerosene LCOF (about 215.4 $€/\mathrm{MWh}$). An essential point of note is that the production cost of biokerosene is considered constant, whereas the cost of e-kerosene varies over time as calculated by PyPSA-Brazil. Consequently, e-kerosene's contribution is optimised during periods wherein its supply proves more economically efficient compared to biokerosene, which explains its modest share.

[3] The original value is 20-97 $\$_{2015}/\mathrm{GJ}$ (Cervi et al. 2020, supplementary), and converted using the data in Table 4.4.

São Paulo's reliance on biokerosene has an overall impact on the fuel landscape in Brazil. The economic barriers that e-kerosene faces in competing with biokerosene are illustrated by the entrenched dominance of biokerosene in São Paulo, the state with the highest kerosene demand. To strengthen the market position of e-kerosene, efforts should be made to reduce its production costs or policy reforms should be made to create an enabling environment for e-kerosene.

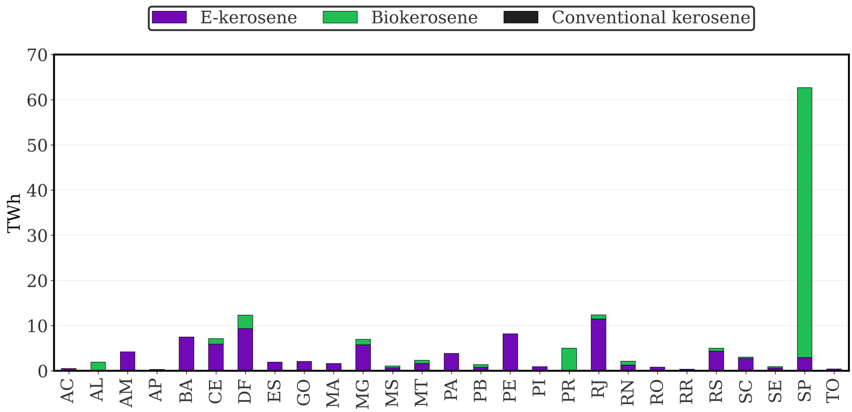

Figure 5.6: Supply of kerosene at federal state given the carbon price of 1000 €/t and biokerosene production level at high.

5.2.4 Supporting e-kerosene production through exporting scenarios in Brazil

The PyPSA-Brazil model delineates a range of export costs from 78-181 €/MWh for the prospect of bolstering e-kerosene production within an export context in Brazil. The results reveal a noteworthy dynamic: as the production costs of biokerosene rise, e-kerosene begins to take a more prominent role. This relationship is evident because when e-kerosene production exclusively satisfies both domestic and export demands, the export costs are almost identical to those in scenarios of high biokerosene production cost.

To place these findings in a broader context, the results in this dissertation are compared with the research by Hampp et al. (2023) on FT fuels export. The maximum export cost identified in this dissertation ($181\,€/\mathrm{MWh}$) is comparable with those reported by Hampp et al. (2023) for exports from Australia and Spain to Germany, yet exceed those for Argentina, Egypt, Morocco, and Saudi Arabia. It is worth noting that the methodologies and focuses concerning export product in the two works are different. Hampp et al. (2023) concentrate on H_2 export demand, assessing the competitive supply between FT fuels and other chemical carriers, such as Power-to-gas (PtG)-induced H_2. Such perspective may overestimate the export costs of FT fuels, especially given the lower efficiency involved in producing FT fuels from H_2 and then converting them back into H_2.

5.2.5 Biokerosene's impact on Brazil's role as an exporter of carbon-neutral kerosene

Section 5.1.4 explores Brazil's potential to become an exporter of carbon-neutral kerosene. As exhibited in Figure 5.5, the contribution of e-kerosene appears relatively modest when biokerosene production costs are low to medium. In those scenarios, biokerosene remains the primary export due to its affordability and presumed carbon-neutrality in PyPSA-Brazil. However, as the costs of biokerosene production increase, e-kerosene becomes more noticeable. A corresponding marked influence of biokerosene costs on the export costs and e-kerosene's export prominence is observable in Section 5.1.4.

Assessing the likelihood of biokerosene production becoming high-cost within Brazil's geographic context is intricate due to various dynamic factors (Kaltschmitt and Neuling 2018). However, biokerosene production demands substantial water and land resources, which could contribute to cost augmentations in the future (Schmidt et al. 2018).

Additionally, the environmental sustainability of biokerosene is called into question by the risk of indirect GHG emissions arising from land-use changes. For instance, the HEFA pathway using cooking oil as feedstock, despite being cost-effective (Schmidt and Weindorf 2016), may emit as much as 27-67.4 $g\,CO_2/MJ$ (De Jong et al. 2017, ICAO 2021a). Although such levels of emissions are compliant with the sustainability criteria for SAF[4] (ICAO 2021b), they cast doubts on the complete climate neutrality of biokerosene. The imperative to restrain biomass cultivation to safeguard biodiversity (Kaltschmitt and Neuling 2018), mitigate indirect GHG emissions (World Bank 2022), and ensure responsible land use (Kaltschmitt and Neuling 2018) makes the presumption of limitless biokerosene production improbable. These factors could subsequently lead to a more conservative deployment of biokerosene at scale and, conversely, higher cost levels.

In light of these considerations, the ambition for Brazil to establish itself as an exporter of carbon-neutral kerosene may act as a catalyst for heightened investments in e-kerosene production. This would signify a progression from mere pursuit of a self-sufficiency in kerosene supply in 2050 to engaging proactively in global kerosene markets towards carbon-neutral aviation. The implications of such a transition could extend beyond economic considerations to involve broader sustainability objectives (Bergero et al. 2023). Harnessing the potential of e-kerosene could position Brazil as a leader in the transition towards carbon-neutral kerosene, while concurrently supporting its commitments to climate change mitigation. This strategic approach would enable Brazil to strike a balance between economic, environmental, and societal interests, contributing significantly to the global endeavour of creating a sustainable aviation sector (Bergero et al. 2023).

5.2.6 Comparisons with relevant literature

This section compares the results of this dissertation with existing studies in terms of three parameters: (i) the electricity supply cost in a fully decarbonised Brazilian

[4] It refers to reducing the life-cycle GHG emissions 10% below to the conventional kerosene.

power system, (ii) the production cost of e-kerosene, and (iii) the capacity factor of the e-kerosene supply.

5.2.6.1 Electricity supply cost in carbon-neutral scenarios

This section evaluate carbon-neutral Brazilian energy systems from this dissertation and contrasts them with alternative designs presented in existing literature, focusing on electricity supply cost, represented by ASC (cf. Equation (4.15)).

The results from the "only power system" scenario in this dissertation indicate an ASC of 50.3 €/MWh. This is lower than the 70.6 $€_{2019}$/MWh posited by Dranka and Ferreira (2018) for a 100% renewable power system across four Brazilian regions in 2050. The 70.6 €/MWh is converted from the original 78.99 $/MWh using 2019 exchange rates as indicated in Table 4.4. The discrepancy in ASC between this dissertation and Dranka and Ferreira (2018) can be explained by differences in system designs. First, Dranka and Ferreira (2018) assume a higher rate of electrification, resulting in an electricity demand of 1,571.5 TWh, while this dissertation estimates a more conservative demand of 1,164.8 TWh ($COPPE_{lowBECCS}$ scenario presented in Table 5.2). Secondly, Dranka and Ferreira (2018) suggest a total power generation capacity of 623 GW, much larger than the 523 GW identified in this work. Furthermore, their study estimates hydropower to contribute 50% of energy supply, approximately 800 TWh, which is almost twice as much as Brazil's hydropower production capacity in 2019. In comparison, this dissertation suggests a smaller share of 32.8% for hydropower (386-388 TWh, akin to the levels in 2019) and a higher share of 35.5% for PV.The capital costs and lifetime assumptions for PV also differ. Dranka and Ferreira (2018) lean less on solar power due to a permissive technology and economic parameterisation – their annualised capital costs of 187,357.6 €/MWh, nearly three times higher than the 48,931.5 €/MWh observed in this dissertation.

Comparisons can also be made with Barbosa et al. (2016), which examines potential fully decarbonised Brazilian power systems with applications of renewable electricity for other end use. They report a decrease in ASC from 61 €/MWh to $53\,€/\mathrm{MWh}$ when adding 25% more electricity demand for water desalination and synthetic gas production. In a similar vein, this dissertation includes e-kerosene production, which leads to a 32% increase in additional electricity demand under the "100% e-kerosene supply" scenario. Consequently, the ASC of the system in this dissertation dips from $50.3\,€/\mathrm{MWh}$ to $44.2\,€/\mathrm{MWh}$. One of the key factors for the lower ASC in this dissertation is the inclusion of interstate transmission in the PyPSA-Brazil performed, in contrast to the coarser spatial resolution in four regions adopted by Barbosa et al. (2016). Furthermore, while Barbosa et al. (2016) include pumped and run-of-river hydropower plants and allows hydropower capacity to expand significantly – 200% of the installed capacity, this dissertation assumes reservoir types with limited expansion capabilities, in line with Brazil's National Ten-Year Energy Plan (cf. Section 3.2.3). This assumption, although seemingly conservative, is based on Brazil's objective to diversify its energy generation portfolio, mitigating risks associated with dependency on hydropower, especially considering the environmental sensitivities in the Amazon region (cf. Section 1.5).

In summary, this dissertation unveils carbon-neutral power system designs for Brazil, which largely concur with those found in the existing literature. Notably, it employs the high-granularity PyPSA-Brazil model, integrating interstate transmission benefits even in the face of hydropower expansion constraints. Through this approach, a refined analysis is enabled, capitalising on Brazil's geographically diverse renewable resources. Consequently, this dissertation presents a more cost-effective system than previously estimated in alternative literature, reducing the average system cost and affirming carbon neutrality as an attainable and economically viable goal for Brazil's power sector, whilst incorporating e-kerosene production.

5.2.6.2 Capacity factor of e-kerosene production unit

Apart from securing a low electricity supply cost, a high capacity factor for the e-kerosene production unit is indispensable to ensure its economic feasibility (Batteiger et al. 2022). Echoing this perspective, Agora Energiewende (2018) present a comparison between scenarios with varying operation hours of electrolysers and synthesis, specifically 2,000 and 8,000 hours. In addition, Breyer et al. (2022) highlight the considerable impact that the operation hours of FT synthesis have on economic viability as they assume baseload-like DAC operating for 8,000 hours. This dissertation aligns with these findings, demonstrating that the capacity factor for e-kerosene production fluctuates between 0.7 and 0.9 – a range that supports its economic feasibility.

5.2.6.3 Levelised cost of fuel for e-kerosene supply

This section positions Brazil in the context of global studies on the levelised costs for e-kerosene. The LCOFs calculated for Brazil in this dissertation are compared with those reported from various global regions. The analysis is limited to projections for the year 2050 and integrates production chains for carbon-neutral e-kerosene that are consistent with the plant design outlined in Section 4.2.4. A compilation of LCOF findings from seven TEA studies, along with their respective contexts and assumptions, is provided in Table 5.5.

For Brazil, the LCOFs for e-kerosene derived in this dissertation range from 113.3 €/MWh to 215.5 €/MWh, assuming different carbon prices, biokerosene production costs, and Brazil's self-sufficiency in kerosene. Incorporating demand from exports extends this range to 117.9 €/MWh to 227.3 €/MWh.

These findings can be compared with the German and Spanish context, where the reported LCOF values vary more widely. For instance, Batteiger et al. (2022) estimate the LCOF for Germany to be 186.9 €/MWh, while the Spanish LCOF is slightly lower at 148.2 €/MWh. Drünert et al. (2020) indicate an even wider range for Germany, between 188.4 €/MWh to 284.3 €/MWh. The variability is likely attributable to disparities in methodologies, electricity costs, and assumptions surrounding the e-kerosene production process.

The research by Batteiger et al. (2022), for instance, uses an e-kerosene plant configuration similar to the one employed in this dissertation. However, they assume electricity costs of 43 €/MWh for Germany and 35 €/MWh for Spain.

In scenarios where a decarbonised power supply is considered within the EU energy system, Schlachtberger et al. (2017) anticipate electricity costs between 64.8 €/MWh to 84.1 €/MWh, despite a 5.1% contribution from gas power plants. The range in electricity costs is contingent upon either a ninefold expansion of the grid or its maintenance at 2013 levels, both of which could lead to a sharp rise in the production costs of e-kerosene when ensuring a carbon-neutral power sector.

Meanwhile, the results obtained for Brazil are relatively high compared to the estimates by Agora Energiewende (2018) and Breyer et al. (2022) for North Africa, the US and the EU-27 region, respectively. These studies report values below 100 €/MWh, which can be attributed to assumptions of lower electricity supply costs in spots with higher renewable energy generation potential. Moreover, sourcing electricity from renewable resources at high generation potentials without grid expenses and accommodating for final kerosene demand also contribute to these lower values.

The LCOF for the US, as calculated by Sherwin (2021), is at 84.8 €/MWh, lower than that of Brazil. This discrepancy is primarily due to their consideration of a more flexible and cost-effective e-kerosene production chain, including lower renewable electricity costs and higher efficiency in converting electricity to e-kerosene.Specifically, Sherwin (2021) assumes a renewable electricity costs of 10 €/MWh for solar, 16 €/MWh for wind and 54.6 €/MWh for grid electricity. Those assumptions are more ambitious than the figures obtained in this dissertation for Brazil, where the LCOE is 33 €/MWh for PV, 35 €/MWh for onshore wind and 70 €/MWh for grid electricity. Sherwin (2021) also assumes a higher efficiency in converting electricity to e-kerosene at 0.53, while this dissertation assumes an efficiency of 0.42.

Conversely, Becattini et al. (2021) report the highest LCOF range (217.0 - 434.1 €/MWh) without specifying a particular country. This indicates the upper limit of costs associated with achieving net-zero CO_2 emissions in e-kerosene production, depending on production processes and electricity expenses. The lower limit of this range (217.0 €/MWh) is marginally above the LCOF identified in this dissertation (214.7 €/MWh) where carbon-neutral e-kerosene exclusively fulfils the kerosene demand within a fully decarbonised power system.

In summary, the LCOF for e-kerosene production in Brazil in 2050 exhibits a competitive yet varied range depending on several factors. While Spain and Morocco demonstrate slightly lower LCOFs, Germany's LCOF figures span a range that overlaps with or exceeds Brazil's. The US, EU-27, and North Africa demonstrate substantially lower LCOFs, indicating greater competitiveness. Local renewable energy potential and electricity costs are key determinants in these observations (Ueckerdt et al. 2021). Brazil, with its potential to transition to a fully decarbonised power system, emerges as a promising player in e-kerosene production, poised to become a favourable contender for e-kerosene exporting.

Table 5.5: LCOF for e-kerosene in 2050 as reported in the literature.

Study	**Country**	**LCOF[a] (€$_{2019}$/MWh)**	**Notable factors influencing cost**
This dissertation[b]	Brazil	214.7	Fully decarbonised power system with e-kerosene meeting 100% of the kerosene demand ("100% e-kerosene supply" scenario).
This dissertation	Brazil	113.3 – 215.5	Scenarios excluding exports, considering variable biokerosene production costs (low, medium, and high) and carbon prices (160 €/t, 200 €/t, 260 €/t, 320 €/t, 500 €/t, 1000 €/t).
This dissertation	Brazil	117.9 – 227.3	Scenarios including various export demand levels (50%, 100%, 150%, 200%, 400%, and 500%) with fixed high carbon prices at 1000 €/t, considering biokerosene production costs (low, medium, and high) and exclusive e-kerosene.
Batteiger et al. (2022)	Germany	186.9	The value, initially 2186 €/t, is based on electricity supply cost at 43 €/MWh (Batteiger et al. 2022, Table 13), employing the identical e-kerosene plant setup as the dissertation.

Continued on next page

Study	**Country**	**LCOF[a] (€$_{2019}$/MWh)**	**Comment**
Drünert et al. (2020)	Germany	244.8 – 284.3	The value ranges from 2.91 €/kg to 3.38 €/kg. Power-to-liquid (PtL) process with low-temperature electrolysis, CO_2 from ambient air and renewable electricity cost varying from 35 €/MWh to 55 €/MWh (Drünert et al. 2020, Table 7). This cost is the cost of electricity used to meet a specific e-kerosene demand, driven by the specific process, process efficiency and carrier requirements (e.g. CO_2).
Drünert et al. (2020)	Germany	188.4 – 227.1	This range, originally 2.24 €/kg to 2.7 €/kg) (Drünert et al. 2020, Table 7). Similar to the previous entry but using high-temperature electrolysis.
Gonzalez-Garay et al. (2022)	Spain	188.4 - 416.4	This range (Gonzalez-Garay et al. 2022, Figure 7) relies on the electricity source (renewable or grid) and the incorporation of emissions costs. Utilising renewable electricity, the LCOF is estimated at 2.3 €/kg without emission cost and increase to 4.95 €/kg when considering the emission costs. Grid-sourced electricity results in a smaller increment due to emissions costs (from 2.24 €/kg to 2.8 €/kg). The study utilises a MILP approach to optimise the total system cost of the e-kerosene supply chain at 36 nodes.
Batteiger et al. (2022)	Spain	148.2	Based on FT synthesis with DAC and electricity supply cost at 35 €/MWh, the original value is 1762 €/t (Batteiger et al. 2022, Table 13).
Batteiger et al. (2022)	Morocco	145.9	Similar to Spain but with electricity supply cost at 32 €/MWh. The original value was 1735 €/t (Batteiger et al. 2022, Table 13).

Continued on next page

Study	Country	LCOF[a] ($€_{2019}/\mathrm{MWh}$)	Comment
Agora Energiewende (2018)	North Africa	75 – 137.5	The range, 75 €/MWh to 137.5 €/MWh (Agora Energiewende 2018, Figure 21, 2050, 100%), indicates the site of liquid synthetic fuel production and import to Germany, which includes transport costs. Note that e-kerosene is not explicitly mentioned as the final product.
Breyer et al. (2022)	EU-27	75	In this study, FT-derived kerosene is produced using DAC with electricity sourced from hourly PV and wind energy generation. Electricity costs are calculated without grid expenses. The valued is from Breyer et al. (2022, Table 11).
Breyer et al. (2022)	US	69	The assumptions mirror the EU-27 scenario, but this scenario is conducted for the US, which has a different renewable energy generation potential.
Sherwin (2021)	US[c]	84.8	The raw value is converted from 0.99 $/L_*gasoline equivalent* to $/MWh using density and heat value of gasoline of 0.755 kg/L and 13 kWh/kg) from Sherwin (2021, page F). The study employs grid electricity at 65 $/MWh,[d] wind supply at 19 $/MWh, and solar supply at 11.8 $/MWh.[e]
Becattini et al. (2021)	—	217.0 – 434.1	The range (2-4 €/L) in the study represents a scenario in 2050 where CO_2 from DAC and H_2 from water electrolysis are combined to produce synthetic fuels using renewable electricity, supplied based on LCOE at 61 €/MWh (Becattini et al. 2021, Figure 11, 2050 DAC-CCU scenario).

[a] Unit conversion details are elaborated in Table 4.4.
[b] The formulation details can be found in Equation (4.17).
[c] The data on supply costs of electricity originate from the US.
[d] Sherwin (2021) states that grid power not necessary for green power generation.
[e] The data are derived from the supplementary materials.

5.3 Conclusions

This chapter evaluates the feasibility of e-kerosene supply in a prospective carbon-neutral power system for potential domestic use and export. The methodology encompasses a comprehensive energy system model explicitly tailored for Brazil, dissecting three aspects: (i) the fulfilment of aviation fuel demand through e-kerosene, (ii) the synergies of attaining a fully decarbonised power system whilst producing e-kerosene, and (iii) the trade-offs between supplying e-kerosene and alternate options, such as biokerosene and conventional kerosene. For investigating these elements, the research leverages publicly accessible data and the open-source energy system optimisation model, PyPSA-Brazil. This tool proves a beneficial planning instrument across a 27-node network with hourly resolution.

The findings reveal Brazil's potential to achieve the dual goals: establishing a carbon-neutral power system and becoming a prime exporter of carbon-neutral kerosene by 2050. Such a vision is bolstered by system designs where PV assumes the lead technology. A comparison with biokerosene and fossil-derived kerosene highlights that e-kerosene becomes a cost-effective solution when carbon pricing schemes are in place, effectively punishing conventional kerosene supply. The significance of this observation becomes more apparent in scenarios where Brazil actively exports carbon-neutral kerosene. Intriguingly, the research underlines a potent interdependence between the cost of biokerosene provision and the share of e-kerosene supply, positioning e-kerosene as a preferable option when biokerosene production costs climb.

The dissertation steps away from traditional narratives, offering Brazil's first quantitative outcomes for e-kerosene production. By enlarging the scope of the best renewable energy sites to cover a fully decarbonised energy system for e-kerosene production, it imparts valuable insights for fostering the production of e-kerosene. Applying the PyPSA-Brazil model and the associated analysis may serve as a blueprint for other countries.

5.4 Code availability

This section describes the complete data acquisition, modelling, and scenario analysis. The code for PyPSA-Brazil is published at GitLab (Deng 2023b). Note: Access to the code will be available upon acceptance of the paper. The PyPSA-Brazil model is compatible with PyPSA version 0.22.0 and is performed using Python 3.9 and the necessary toolboxes such as Pandas and Geopandas.

6 Limitations and Outlook

6.1 Critical appraisal

6.1.1 Open Brazilian energy data

A multitude of data sets have been collected and processed to enable its use in the PyPSA-Brazil model for designing future cost-optimal energy systems at hourly and 27-node geographical resolution. However, the model's accuracy relies heavily on data availability and accuracy. Undoubtedly, the harmonised data sets presented in this dissertation represent a significant milestone in facilitating research into the Brazilian energy system, offering a valuable foundation for scholars and practitioners alike. Nonetheless, it must be acknowledged that they are merely a stepping stone towards a more comprehensive and refined understanding of this system, and thus present an opportunity for further improvement.

Concerning spatial resolution, models with even higher spatial resolutions could be desired, e.g., to conduct transmission expansion planning studies or to have more flexibility for defining user-specific spatial aggregations. The actual grid topology used in the model includes only the aggregated transmission network, ignoring the distribution network and resulting in a lack of consideration for power flows within federal states. The quality of the grid topology is heavily dependent on the quality of the three processing steps, notably the algorithm for "spatial join at the closest distance" (cf. Section 3.2.2). Ideally, data on transmission lines and connected substations would be available, eliminating the need for assumptions about topology.

The data include both existing and planned power plant infrastructure up to the year 2029 (cf. Section 3.2.3), but crucially lacks specific details on the timing of installations, retrofits, and decommissioning. The absence of clear specifications on these factors complicates studies on decarbonisation pathways, as the need to make assumptions can introduce significant uncertainty into modelling efforts. The geographical coordinates of power plants taken from the original ANEEL-SIGA data set were reconciled with the grid network from ONS and aggregated at the federal-state level. For this reason, modelling infrastructure at the level of transmission lines and individual power plants requires matching ANEEL-SIGA and ONS power plants, an issue that remains unaddressed in this dissertation. This undertaking poses significant challenges as both data sources are managed by governmental institutions and are regarded as reliable for Brazil. To proceed, the researchers must extend the available information by continuing to look for official documents that clarify differences in information or apply assumptions.

The demand time series of all end-use sectors are aggregated. This can be a limitation in cases when researchers wish to model decarbonisation in a particular sector rather than a whole sector, such as industry, residential, or even more granular sectors, such as ground transport, rather than the whole transport sector.

6.1.2 Modelling

Within the modelling framework of this dissertation, linearisation is assumed to ensure computational manageability. However, using linearisation brings about specific limitations, especially in the simulation of battery storage, tank storage, hydro reservoirs, and power transmission. For instance, PyPSA-Brazil may not perfectly capture transmission losses and non-linearity in storage systems, as indicated by Victoria et al. (2019), Hörsch et al. (2018b). In addition, the representation of power flow between nodes, for instance, is predicated on the “copper plates” assumption. In this approach, inter-state transmission is depicted as an aggregation of multiple cross-border lines, and losses and lengths are averaged. Such a simplification, while computationally expedient, inevitably disregards the inherent imperfections in power flow distribution and does not account for internal bottlenecks within states (Soroudi 2017).

The modelling of hydropower generation reveals discrepancies, as the generation is approximated at 386-388 TWh, which is around 5% lower than the 405.6 TWh recorded in the reference year 2019 (cf. Table 5.1). The PyPSA-Brazil model recognises that the depiction of hydropower plants cascades is basic due to the linearisation and constraints of data availability (cf. Sections 3.2.7 and 4.2.3). The data regarding water inflow, pivotal in modelling the behaviour of hydropower plants, lack the requisite granularity. The inclusion of detailed information regarding the distribution and technical specifications of individual hydropower stations would enable more accurate calculations of natural inflows in accordance with hydrological conditions following ENTSO-E (2019). Data sets from ONS (2022a), ANA (2022), Lehner et al. (2011) could be employed for refined modelling with assistance from Liu et al. (2019).

In the case of e-kerosene production, the model assumes that production operates with full flexibility, not considering constraints such as plant start-up and shutdown times or associated costs (Soroudi 2017, Chapter 5). The hypothesis, although advantageous for the overall system, may not be congruent with the technical and economic specifications of the individual plants (Peters et al. 2003, p. 394-401). Moreover, the model omits the selection or dimensions of critical components such as the electrolyser, synthesiser, DAC units, and CCU with various carbon sources (Wassermann et al. 2022, Sherwin 2021, MacDowell et al. 2010). This exclusion limits the depth of our insights into the feasibility of e-kerosene production at specific sites.

In terms of demand projections, the dissertation combines time series data from 2019 with annual predictions to estimate the demand curve for electricity and kerosene in 2050 (cf. Sections 3.2.5, 3.2.6, 4.3.3.1 and 5.1.1). This method rests on the assumption that demand patterns in 2050 will resemble those the reference year 2019, which might not capture the temporal variability intrinsic to the scenario year. Moreover, this approach might not be efficacious in extrapolating the demand curve into the distant future, as it does not consider evolving factors such as GDP, population, and others (Mattsson et al. 2021).

While the optimisation modelling in this dissertation is focused on minimising total system costs, this approach might not capture the complex objectives present in real-world energy supply scenarios (Bertsch and Fichtner 2016). Consideration of additional objectives would enable a more comprehensive analysis such as: (i) the environmental impact of land use (Kaltschmitt and Neuling 2018), water (Schmidt and Weindorf 2016), life-cycle GHG emissions (Micheli et al. 2022), and raw materials of the technologies (de Souza et al. 2018), (ii) the desire for security of supply against volatile political situations on the national and international level, unexpected outages of energy infrastructures (Vyhmeister et al. 2018), and (iii) the complex and hard-to-anticipate societal issues like the uneven evolution of equality of gender, income level, and ethnics (Cremonez et al. 2015, ICAO 2022b, 2018b).

This life-cycle carbon emissions of e-kerosene and biokerosene are assumed to be zero in this dissertation, representing an idealised scenario where these fuels are carbon-neutral [1]. However, in practice, there are considerable technological hurdles to achieving truly carbon-neutral e-kerosene and biokerosene. The production of e-kerosene, for instance, requires renewable-source hydrogen, which may not be entirely life-cycle carbon neutral (Gonzalez-Garay et al. 2022). Biokerosene production in Brazil could also involve well-to-tank life-cycle GHG emissions ranging from 1.4-37.6 gCO_2e/MJ (Capaz et al. 2020). Additionally, non-CO_2 emissions such as NOx, which significantly contribute to climate change[2], are not accounted for in this model. Comprehensive strategies that incorporate technological, economic, social, and political dimensions are required to address aviation emissions effectively (Bergero et al. 2023). Future research should attempt to

[1] This assumes no CO_2 loss between capture and binding in e-kerosene (Becattini et al. 2021) and net-zero life-cycle CO_2 emissions in biogenic-kind biokerosene due to full offsetting between combustion and carbon sequestration during feedstock growth (ICAO 2022a, p. 4).

[2] NOx emissions contribute to the formation of ozone and contrail-induced cloudiness at high altitudes, resulting in a net warming effect (Lee et al. 2009).

incorporate more realistic emissions data, including non-CO_2 emissions (De Jong et al. 2017), to build upon the foundation set by this study.

6.1.3 Scenario analyses

This dissertation uses a normative scenario analysis to offer insights into achieving strategic objectives in a techno-economically feasible way. A limitation of this approach is that it does not include transition pathways for moving from the current energy system to the envisioned target system. Consequently, it falls short in providing concrete timelines for infrastructure construction or decommissioning, or in assessing technology learning curves. Given the urgency of decarbonisation, modelling the near-future energy system is crucial to facilitate intermediate decision-making and ensure a smooth transition (Conejo et al. 2016). Thus, it is imperative to consider an efficient pathway for producing and utilising biokerosene and e-kerosene.

Additionally, the dissertation does not explore an alternative scenario that considers the persistent usage of fossil jet fuel while offsetting the resulting CO_2 emissions through the application of DAC and subsequent permanent storage, as demonstrated by Becattini et al. (2021).

This dissertation considers export perspectives, but exclusively from the exporter's standpoint. This perspective could be enriched by incorporating trade relations between Brazil and potential importers such as China, Japan, and Europe. Assessing the dynamics of international trade and preferences of importing countries would bolster the comprehensiveness of the scenario analysis.

6.2 Future directions

The research presented in this dissertation provides many starting points for future analysis and improvement. The following briefly outlines some potential areas for further research.

6.2.1 Improving Brazilian open energy data

To enhance the quality and accessibility of energy-related information in Brazil, one potential strategy would be to optimise the country's open energy data by incorporating more statistical data and reducing assumptions.

Statistical data sets can be examined on the PDA (Federal Government of Brazil 2023), which, contains information from 227 of Brazil's 227 government branches and over 12,000 data sets. However, as the PDA covers a vast number of data sets beyond the scope of energy system modelling, it is imperative to conduct further inquiries to filter the pertinent data sets and scrutinise the metadata for missing attributes or ambiguous information. It is also highly advisable to retain the processed version of the original data procured from the PDA. This dissertation has observed inconsistencies and errors across different versions of the original data set, as discussed in Chapter 3.

The data set by EPE (2020b), used to emulate the Brazilian energy system for Brazil's National Ten-Year Expansion Plan (EPE 2020c), merits further exploration. Such endeavours are of utmost importance to rectify incomplete technical and economic assumptions pertaining to Brazil-specific energy systems in this dissertation. Given the absence of metadata and the requisite Portuguese language skills necessary for comprehending the nuances of the Brazilian energy system, collaborations with domain experts and authorities are recommended.

To achieve higher resolution and harmonised topology for infrastructure data on power plants and transmission lines, OpenStreetMap (OpenStreetMap conbributors 2023) can be a source. This is similar to the data set of SciGrid Medjroubi et al. (2017) and PyPSA-Earth (Parzen et al. 2023), provided that the data from Brazil is complete, accurate, and of high quality.

Improving the electricity demand time series for the scenario year holds promise and is an avenue for future research. This enhancement can be achieved by using machine learning methods and incorporating features such as annual per capita electricity demand, purchasing power adjusted GDP, hourly temperature profiles, annual average temperature levels, as described in Mattsson et al. (2021).

While this dissertation provides most data sets, it lacks temperature data for the geographical level of federal states.

By streamlining the harmonised energy data sets and making them readily accessible through user-friendly interfaces, data visualisation tools, and cutting-edge technologies, policymakers, researchers, and other stakeholders could make more informed decisions regarding energy consumption, production, and conservation. Such accessibility, in turn, could facilitate greater transparency, accountability, and collaboration among various stakeholders, ultimately spurring further advancements in Brazil's energy sector.

6.2.2 Biokerosene generation potential, cost, and environmental impacts

In this dissertation, the potential of biokerosene is estimated based on the production cost study for 2030 by Cervi et al. (2020), which only considers the first generation of biomass as feedstocks for biokerosene production in Brazil. However, Cervi et al. (2021) have extended the scope of the study to include the second generation of biomass for biokerosene production. Future research could be conducted by acquiring the potential data from Cervi et al. (2020) to better measure the supply of biokerosene. Additionally, including the second and third-generation biomass for biokerosene production would provide a more comprehensive evaluation of biokerosene potential in Brazil. However, as the models used by both Cervi et al. (2020) and Cervi et al. (2021) are not openly accessible, efforts should be made to create a spatio-temporal techno-economic assessment for biokerosene generation potential that is open-sourced and includes all three generations of biomass, generation at different time intervals, and incorporates environmental considerations such as land-use, water use, and emissions.

6.2.3 In-depth modelling of material flows

Further refinement of the material flow modelling in e-kerosene production is achievable through the integration of sector-coupling technologies into the energy system model. This incorporation offers invaluable insights into the long-term benefits of flexibly operating PtG and PtL applications in facilitating better integration of renewable generation. Moreover, future research could shed light on the intricacies of hydrogen generation, storage, and transportation, as well as the energy demand sector and mobility.

With respect to the feedstocks for e-kerosene production, the modelling in this dissertation focuses primarily on electricity. This means it assumes ambient air serves as the sole carbon source and high-purity water is readily available. However, there are alternative carbon sources, including biogenic CO_2 captured from point source emitters such as agricultural crop residues, waste animal fats, and algae. These sources can be used as feedstocks, and industrial point sources might offer opportunities for applications tailored to specific regions or industries. For pathways that are not carbon-neutral, carbon emissions can be offset by afforestation and reforestation (IPCC 2022a). Furthermore, an examination of nationwide water potentials can be an insightful addition to future research, alongside the integration of e-kerosene and biokerosene production with water desalination processes, particularly when utilising saline water sources.

Regarding the products of the syncrude refinery process, it is worthwhile note sub-products such as oxygen and waxes. Nonetheless, producing these sub-products in adequate quantities could result in difficulties in their utilisation. Hence, a post-assessment of the sub-products could set further restrictions on the optimisation problem. An alternative approach entails marketing these sub-products to increase the cost-effectiveness of e-kerosene, thereby yielding revenue and lowering the production cost.

6.2.4 Scenario with continuous use of conventional kerosene

By including DAC and Carbon Capture and Storage (CCS) technologies that absorb and store emitted CO_2 permanently, conventional kerosene could potentially become carbon-neutral (Becattini et al. 2021). Incorporating such an aspect could have different implications for the contribution of e-kerosene production in Brazil and the need for a carbon pricing scheme.

6.2.5 Kerosene demand projection

The representation of kerosene demand projections in the scenario year can be improved by leveraging machine learning techniques. Although the current method of jet fuel demand prediction relies on statistical methods, this approach only yields annual demand. Hence, it lacks the granularity necessary for forming hourly or daily patterns for the depicted year (as summarised in Table 6.1).

The untapped potential of machine learning in this regard is significant, especially considering its proven track record in generating synthetic hourly electricity demand time series (Antonopoulos et al. 2020, Mattsson et al. 2021). However, the practical application of this technique to anticipate local kerosene demand with sufficient granularity for energy system modelling is a relatively unexplored field in Brazil.

Applying machine learning to model kerosene demand can offer more accurate estimates of balancing cost estimates, specifically within systems like PyPSA-Brazil. It also enables the creation of consumption profiles for arbitrary scenario years. This enhancement, in turn, supports more thorough scenario analysis of alternative kerosene consumption growth paths, from a gradual ascent to following the business-as-usual trajectory. However, choosing the appropriate machine learning algorithms and interpreting the results necessitates prudent judgement, as underscored by Frey (2021).

Table 6.1: A review of literature on aviation fuel demand prediction.

Study	Methodology	Geographical scope	Temporal scope	Variables
Ministry of Infrastructure (2019)	Apply ICAO's manual (ICAO 2006, 2019b) to forecast RTK and fuel efficiency. The future kerosene consumption is calculated by combining these forecasts.	Brazil	2019-2050, annual	(2000-2018, monthly) Statistics of RTK and kerosene consumption
Melikoglu (2017)	Use linear, quadratic, and exponential semi-empirical models	Turkey	2013-2023, annual	(1984–2010, annual) Historical jet fuel demand from EIA[a]
Chai et al. (2014)	Univariate time series forecasting using EST[b] and ARIMA[c] models, together with Bayesian multivariate linear regression models to address the effects of changes in aviation fuel consumption, aviation fuel costs and aviation fuel efficiency.	China	2012-2020, annual	(1979-2011, annual statistics) Product of the number of passengers and the transport distance in passenger kilometres, the product of the freight tonnage and the transport distance in tonne-kilometres, the maximum flying distance of an aeroplane per litre of fuel measured in kgtonne km, the ratio of the real load capacity with the maximum load capacity of an on-schedule aeroplane, the number of flight hours per day, the proportion of all the cities and towns residents in total population, the ratio of the real GDP with the total population, members of civil aviation airports, the number of air routes used for civil aircraft aviation activities, aviation fuel price, and airline passenger numbers

Continued on next page

Study	Methodology	Geographical scope	Temporal scope	Variables
Chèze et al. (2011)	Utilise dynamic panel-data econometric for air traffic projection and convert to jet fuel demand following the IPCC method	8 geographic zones	2025	(1980-2007, annual) Air traffic data, (1980-2006, annual) jet fuel consumption data
Mazraati and Alyousif (2009)	Employ a log-linear model using ordinary least squares	OECD and developing countries	2006–2030, annual	(1980–2005, annual) GDP, jet fuel price, urban population, passenger kilometres
Mazraati and Faquih (2008)	Apply a constant elasticity logarithmic model through ordinary least squares	US, China	2008-2025, annual	(1990–2007, annual) Passenger kilometres, tones kilometres, jet fuel price, average passenger load factor, consumer price index, GDP, population
Future direction	Use machine learning models such as decision tree, support vector machine, and random forest	Brazil	2050	(2002-2018, daily per federal state except 2007 and 2010) Year, month, day, passengers revenue, payload capacity, flown hour, distance, number of departing airlines,[d] GDP, population, airfare[e]

[a] “EIA” denotes the US Energy Information Administration.
[b] “EST” denotes Exponential Smoothing Technology.
[c] “ARIMA” denotes Autoregressive Integrated Moving Average.
[d] This figure is the result of aggregating data up to the federal-state level.
[e] Although airfare data is resolved monthly, raw data for population and GDP are yearly. These figures are assumed to be constant throughout the year for analysis purposes.

7 Summary, Conclusions, and Implications

7.1 Summary

The key contribution of this dissertation lies in the comprehensive data set for the Brazilian energy system, its implementation in PyPSA, and the integration of e-kerosene production into the energy system optimisation model. A novel open-source methodological framework is introduced that amalgamates an extensive assortment of publicly accessible data to build a model of Brazil's future energy landscape. This model explores Brazil's decarbonisation process, with an emphasis on sustainable e-kerosene production for the aviation sector.

This framework could notably simplify the exploration of the Brazilian energy system for fellow researchers. Furthermore, the dissertation envisions and examines a variety of kerosene production scenarios for their economic implications at the energy system level. These insightful findings may equip policymakers with a sturdy knowledge base for informed decisions on investing in e-kerosene production technologies. This could potentially position Brazil as a front-runner in curtailing aviation sector CO_2 emissions and as a green energy carrier exporter.

In the literature review, outlined in Chapter 2, this dissertation highlights gaps in empirically assessing the feasibility of producing e-kerosene and its export under the use of renewable energy sources. It also identifies the scarcity of energy system models tailored to assist in enlightened policy formulation for the incorporation of e-kerosene production in a decarbonised energy system. From these identified gaps, three main research questions arise.

Addressing the Research Question 1 entails the development of a Brazilian energy system model capable of balancing GHG emission-neutral electricity and e-kerosene production. The dissertation conducts an empirical study to find suitable modelling frameworks for energy scenarios served for the research purpose, as elaborated in Chapter 4. Following thorough comparison, PyPSA emerges as the preferred choice, leading to the development and introduction of PyPSA-Brazil.

The Research Question 2 concerns the design of a carbon-neutral Brazilian energy system in 2050. For this, the energy potentials of renewable energy sources such as hydro, wind, and solar, are a fundamental cornerstone. Data from various data sources are collected and harmonised to identify the most relevant ones for Brazil's high-resolution energy system optimisation model, as detailed in Chapter 3. The resulting data sets include nine subcategories, namely: (i) map of the 27 defined regions, (ii) aggregated grid network topology, (iii) local vRES potentials – profile and installable generation capacity, (iv) geographically installable capacity of biomass thermal plants, (v) hydropower plants inflow, (vi) existing and planned power generators with their capacity, (vii) electricity load profile, (viii) scenarios of sectoral energy demand, and (ix) cross-border electricity exchanges. With this data, researchers can replicate the Brazilian energy system, perform scenario analyses or improve the integration of Brazil's energy system into global energy models. The ready-to-use data set is then fed into PyPSA framework to set up the energy system optimisation model PyPSA-Brazil, as described in Chapter 4.

In the Research Question 3, the PyPSA-Brazil model is employed to analyse the interdependencies and trade-offs that arise from pursuing a carbon-neutral power system and the integration of e-kerosene production, as detailed in Chapter 5. A set of thirty-four scenarios has been selected for probing: (i) the dual goal of achieving net-zero emissions from the Brazilian power system and providing additional electricity for e-kerosene, (ii) the trade-offs between varying supply shares of biokerosene, conventional kerosene, and e-kerosene at different biokerosene production costs and carbon prices, and (iii) the export costs and e-kerosene volumes that emerge from different kerosene export targets.

Table 7.1 summarises the research questions and corresponding findings in this study, providing a clear overview of the main outcomes and serving as a valuable reference for readers interested in the key takeaways of this investigation.

Table 7.1: Summary of research questions and findings.

RQ 1: How can the scale-up of sustainable e-kerosene production be modelled without jeopardising the 100% renewable target for Brazilian electricity generation? A model named PyPSA-Brazil has been developed for a cost-optimal energy system. This model allows a dual balance of GHG emission-neutral electricity and e-kerosene production (cf. Chapter 3 and Chapter 4).
RQ 2: How would a carbon-neutral Brazilian power system appear at high temporal and spatial resolution? By 2050, a carbon-neutral power system for Brazil is feasible with an averaged electricity generation cost at 50.3 €/MWh, including production, transmission, and storage. Half of the energy would come from wind and solar generation (cf. Section 5.1.2 and Section 5.2.1).
RQ 3: What could be the local impacts of e-kerosene production in Brazil, and what constraints and opportunities might arise from its expansion in the energy system? • *RQ 3.1: Could renewable energy be sufficient for electricity generation when e-kerosene completely meets Brazil's kerosene demand in 2050?* It is feasible to have a fully decarbonised power system with e-kerosene in Brazil by 2050, with renewable energy supply significantly exceeding demand (cf. Section 5.1.1 and Section 5.2.1). • *RQ 3.2: What could a future carbon-neutral power system look like with and without e-kerosene production?* The addition of e-kerosene production to a fully decarbonised power system in Brazil is more efficient than simply aiming for a carbon-neutral power system. This will require new PV installations in areas such as Minas Gerais, Goiás, Distrito Federal, and São Paulo (cf. Section 5.1.2). • *RQ 3.3: In light of uncertain biokerosene production costs and carbon prices, what might be the share of e-kerosene in Brazil?* The share of e-kerosene varies widely across scenarios (2.7% - 51.1%) and is highly influenced by biokerosene production costs and carbon pricing. Even in a scenario with a low biokerosene production cost, e-kerosene production can still offer benefits. A carbon pricing scheme should be implemented to penalise the supply of conventional kerosene for such a system design (cf. Section 5.1.3 and Section 5.2.2). • *RQ 3.4: What could be the export cost if Brazil becomes an exporter of carbon-neutral kerosene?* The export cost of carbon-neutral kerosene depends mainly on the biokerosene production costs and ranges from 78 €/MWh to 181 €/MWh, depending on biokerosene production costs (cf. Section 5.1.4 and Section 5.2.4).

7.2 Conclusions and implications

This dissertation set out to assess Brazil's potential for transitioning into a producer and prospective exporter of carbon-neutral kerosene without jeopardising a carbon-neutral power system.

The research has identified that the integration of e-kerosene production enhances the efficiency of the energy system, diversifies the generation mix, and reduces dependence on hydroelectricity, compared to a sole aim on carbon neutrality of power system. However, this vision led to a slight increase in system costs. In addition, specific federal states such as Minas Gerais, Goiás, Distrito Federal, and São Paulo, also need to deploy additional PV installations.

The research has also shown that e-kerosene could compete cost-effectively with biokerosene and conventional kerosene supplies in 2050. The share of e-kerosene in meeting the kerosene demand is sensitive to biokerosene production costs and carbon pricing applied to conventional kerosene, ranging from 2.7% to 51.1% across various scenarios.

Moreover, the export cost of carbon-neutral kerosene is primarily influenced by biokerosene production costs, which is estimated to be between $78\,€/\mathrm{MWh}$ to $181\,€/\mathrm{MWh}$. The levelised cost of e-kerosene production in Brazil for 2050 oscillates between $113.3\,€/\mathrm{MWh}$ to $227.3\,€/\mathrm{MWh}$, subject to factors such as carbon pricing, biokerosene production costs, and export intention.

The evidence presented in this dissertation convincingly advocates the feasibility of Brazil developing a fully decarbonised power system in 2050 alongside scaling up sustainable e-kerosene production to harness its abundant renewable energy sources. In addition, replacing fossil-based kerosene with renewable e-kerosene presents a compelling opportunity for a seamless transition to a sustainable aviation future. Success in this transition, however, hinges on the establishment of a carbon pricing scheme that incentivizes e-kerosene production. The findings suggest that Brazil possesses the potential to establish itself as a prospective supplier of carbon-neutral kerosene by betting on investment in e-kerosene production.

Utilising the energy system optimisation model, PyPSA-Brazil, this dissertation highlights light several implications vital for decision-makers, industry, bankers and scientists seeking guidance on the feasibility of starting and betting on e-kerosene production in Brazil and the advantages of promoting Brazil's transition to an exporter of carbon-neutral kerosene.

- E-kerosene could stand poised to rival biokerosene and conventional kerosene in cost-competitiveness in Brazil in 2050. Nevertheless, the extent to which this SAF can contribute to the aviation supply depends on sustained policies. To level the playing field for e-kerosene, Brazil needs to implement carbon pricing, a measure yet to be instituted. The trajectory of biokerosene remains nebulous at the local echelon, and its production and pricing influence e-kerosene's role. As a result, the size of the national e-kerosene market future remains indeterminate.
- In light of Brazil's pledge under the NDC and its nascent deployment of solar and wind energy, investment in e-kerosene production for aviation emerges as viable strategy to pursue alongside efforts to achieve a carbon-constrained power sector. While prioritising only the latter may seem sufficient, such a strategy overlooks the potential benefits of timely e-kerosene deployment in achieving carbon neutrality in both power and aviation sectors, notwithstanding e-kerosene's initial scarcity and long-term uncertainty as an innovative fuel.
- Anticipating the widespread availability of carbon-neutral e-kerosene, Brazil is called upon to endorse national or international cooperation with industry to hasten technological advancements in renewable energy generation, electrolysis, and DAC – process elements that are pivotal in making e-kerosene a cost-effective product.
- Amidst the fervent discourse surrounding green energy carriers for export, Brazil should be positioned to capitalise on an export niche by trading e-kerosene with densely populated countries such as Japan, Germany, and South Korea, which grapple with limited renewable energy and fossil fuel

resources. However, the international trade of e-kerosene requires the formulation of a comprehensive trade framework and coordination of its growth on a global scale, a task rendered formidable by geopolitical intricacies and divergent interests of the nations involved.

- PyPSA-Brazil and Open Brazilian Energy Data could serve as potent tools for shaping policy and formulating strategies concerning e-kerosene production and export in Brazil. By leveraging this open model and data set, nations with a vested interest in e-kerosene research can rapidly adopt the resulting analyses. Moreover, this model is easily adaptable to extend its relevance to an array of research domains, such as hydrogen and methane, allowing for even greater versatility in addressing critical energy issues.

List of Figures

List of Tables

List of Publications

Journal articles

Y. Deng, K.-K. Cao, W. Hu, R. Stegen, K. von Krbek, R. Soria, P. R. R. Rochedo, and P. Jochem. Harmonized and Open Energy Dataset for Modeling a Highly Renewable Brazilian Power System. *Scientific Data*, 10(1):103, 2023a. doi: 10.1038/s41597-023-01992-9.

Y. Deng, K.-K. Cao, M. Wetzel, W. Hu, and P. Jochem. E-kerosene Production and Export in Carbon-neutral Power Systems - A Solution for Sustainable Aviation?, 2023b. *Submitted to Journal of Scientific Reports*.

Y. Deng, C. Jardim Reis Souza, K.-K. Cao, T. Pregger, and P. Jochem. Biokerosene Production in Brazil: A Spatio-temporal Techno-economic Assessment. *Manuscript in progress*, 2023c.

W. Hu, Y. Scholz, M. Yeligeti, and Y. Deng. Projecting future electricity demand in the context of climate change: a temperature-dependent dynamic regression model, 2023a. *Manuscript in an internal review. Submit to Journal of Energy*.

W. Hu, Y. Scholz, M. Yeligeti, L. von Bremen, and Y. Deng. Downscaling era5 wind speed data: A machine learning approach considering topographic influences. *Environmental Research Letters*, 18:094007, 2023b. doi: 10.1088/1748-9326/aceb0a.

Conference contributions

Y. Deng, K.-K. Cao, and B. Wanke. Designing a Brazilian energy system model for studying energy planning at high spatial and temporal resolution. In *Volume 24: Sustainable Energy Solutions for a Post-COVID Recovery towards a Better Future: Part VII*, volume 24, page 6. Energy proceedings, 2021. ISBN 2004-2965. URL https://doi.org/10.46855/energy-proceedings-9781.

Bibliography

Agora Energiewende. The Future Cost of Electricity-Based Synthetic Fuels. Technical report, Agora Energiewende, Berlin, Germany, 2018. URL `https://www.agora-energiewende.de/en/publications/the-future-cost-of-electricity-based-synthetic-fuels-1/`.

R. P. Allan, C. Cassou, D. Chen, A. Cherchi, L. Connors, F. J. Doblas-Reyes, H. Douville, F. Driouech, T. L. Edwards, E. Fischer, G. M. Flato, P. Forster, K. M. AchutaRao, B. Adhikary, E. Aldrian, and K. Armour. Summary for Policymakers. In *Climate Change 2021: The Physical Science Basis. Contribution of Working Group I to the Sixth Assessment Report of the Intergovernmental Panel on Climate Change*, pages 3–32. Cambridge University Press, Cambridge, United Kingdom and New York, NY, USA, 2021. doi: 10.1017/9781009157896.001.

R. Altman. Sustainable aviation biofuels—A development and deployment success model. In *Bioenergy*, pages 621–647. Elsevier, 2020. doi: 10.1016/B978-0-12-815497-7.00030-0.

K. d. F. Alves, E. P. Andrade, J. P. Savioli, A. V. Pastor, M. C. B. de Figueirêdo, and C. M. L. Ugaya. Water scarcity in Brazil: part 2—uncertainty assessment in regionalized characterization factors. *The International Journal of Life Cycle Assessment*, 25(12):2359–2379, 2020. doi: 10.1007/s11367-020-01739-3.

ANA. Sistema Interligado Nacional, 2022. URL `https://www.ana.gov.br/sar/sin/sistema-interligado-nacional`.

ANAC. Dados Estatísticos do Transporte Aéreo no Brasil: Microdados, 2021. URL `https://www.gov.br/anac/pt-br/assuntos/regulados/empre` sas-aereas/Instrucoes-para-a-elaboracao-e-apresentacao-das-demonstracoes-contabeis/envio-de-informacoes/microdados. Básica.

E. P. Andrade, A. B. De Araújo Nunes, K. De Freitas Alves, C. M. L. Ugaya, M. Da Costa Alencar, T. De Lima Santos, V. Da Silva Barros, A. V. Pastor, and M. C. B. De Figueirêdo. Water scarcity in Brazil: part 1—regionalization of the AWARE model characterization factors. *The International Journal of Life Cycle Assessment*, 25(12):2342–2358, 2020. doi: 10.1007/s11367-019-01643-5.

ANEEL. Resultado do Leilão de Transmissão, 2021a. URL https://www.aneel.gov.br/documents/654791/20589082/Resultado+do+Leil%C3%A3o+de+Transmiss%C3%A3o/0ac53811-f890-9274-1ba9-4bee7cab9723.

ANEEL. Sistema de Informações de Geração da ANEEL- SIGA, 2021b. URL https://app.powerbi.com/view?r=eyJrIjoiNjc4OGYyYjQtYWM2ZC00YjllLWJlYmEtYzdkNTQ1MTc1NjM2IiwidCI6IjQwZDZmOWI4LWVjYTctNDZhMi05MmQ0LWVhNGU5YzAxNzBlMSIsImMiOjR9.

ANP. RESOLUÇÃO ANP Nº 17, DE 26.7.2006, DOU 27 DE JULHO DE 2006, 2006. URL https://atosoficiais.com.br/anp/resolucao-n-17-2006-regula-o-exercicio-da-atividade-de-distribuicao-de-combustiveis-de-aviacao?origin=instituicao&q=17/2006.

ANP. RESOLUÇÃO ANP Nº 37, DE 1º12.2009, DOU 2 DE DEZEMBRO DE 2009, 2009. URL https://atosoficiais.com.br/anp/resolucao-n-37-2009?origin=instituicao&q=37/2009.

ANP. RESOLUÇÃO DE DIRETORIA RD Nº 506/2013, 2013. URL https://atosoficiais.com.br/anp/resolucao-de-diretoria-n-506-2013-minuta-de-resolucao-que-aprova-o-regulamento-de-licitacoes-de-blocos-sob-regime-de-partilha-de-producao-em-areas-do-pre-sal-e-em-areas-estrategicas?origin=instituicao&q=506/2013.

ANP. RESOLUÇÃO ANP Nº 63, DE 5.12.2014, DOU 8 DE DEZEMBRO DE 2014, 2014. URL https://atosoficiais.com.br/anp/resolucao-n-63-2014?origin=instituicao&q=63/2014.

ANP. Preços de distribuição de combustíveis: Combustíveis de aviação, Mensais, 2022. URL https://www.gov.br/anp/pt-br/assuntos/precos-e-defesa-da-concorrencia/precos/precos-de-distribuicao-de-combustiveis.

I. Antonopoulos, V. Robu, B. Couraud, D. Kirli, S. Norbu, A. Kiprakis, D. Flynn, S. Elizondo-Gonzalez, and S. Wattam. Artificial intelligence and machine learning approaches to energy demand-side response: A systematic review. *Renewable and Sustainable Energy Reviews*, 130:109899, 2020. doi: 10.1016/j.rser.2020.109899.

ASTM. D7566-18: Specification for Aviation Turbine Fuel Containing Synthesized Hydrocarbons. Technical report, ASTM International, 2018. URL http://www.astm.org/cgi-bin/resolver.cgi?D7566-18.

ASTM. D1655: Specification for Aviation Turbine Fuels. Technical report, ASTM International, 2022. URL https://www.astm.org/standards/d1655.

ATAG. Waypoint 2050: An Air Transport Action Group Project. Technical report, ATAG, Geneva, Switzerland,, 2021. URL https://aviationbenefits.org/media/167417/w2050_v2021_27sept_full.pdf.

J. Badger, I. Bauwens, P. Casso, N. Davis, A. Hahmann, S. B. K. Hansen, B. O. Hansen, D. Heathfield, O. J. Knight, and O. Lacave. Global Wind Atlas 3.0, 2019. URL https://globalwindatlas.info. World Bank Group.

L. B. Baptista, R. Schaeffer, H. L. van Soest, P. Fragkos, P. R. Rochedo, D. van Vuuren, R. G. Dewi, G. Iyer, K. Jiang, M. Kannavou, N. Macaluso, K. Oshiro, C. Park, L. J. Reedman, G. Safonov, S. Shekhar, U. Siagian, K. Surana, and C. Qimin. Good practice policies to bridge the emissions gap in key countries. *Global Environmental Change*, 73:102472, 2022. doi: 10.1016/j.gloenvcha.2022.102472.

L. d. S. N. S. Barbosa, J. F. Orozco, D. Bogdanov, P. Vainikka, and C. Breyer. Hydropower and Power-to-gas Storage Options: The Brazilian Energy System Case. *Energy Procedia*, 99:89–107, 2016. doi: 10.1016/j.egypro.2016.10.101.

V. Batteiger, P. Schmidt, K. Ebner, A. Habersetzer, L. Moser, W. Weindorf, and T. Rakscha. Power-to-Liquids – A scalable and sustainable fuel supply perspective for aviation. Technical report, German Environment Agency, 2022. URL `https://www.umweltbundesamt.de/en/publikationen/power-to-liquids`.

A. Bauen and L. Nattrass. Sustainable Aviation Biofuels: Scenarios for Deployment. In M. Kaltschmitt and U. Neuling, editors, *Biokerosene*, pages 703–721. Springer Berlin Heidelberg, Berlin, Heidelberg, 2018. doi: 10.1007/978-3-662-53065-8_27.

A. Bauen, N. Bitossi, L. German, A. Harris, and K. Leow. Sustainable Aviation Fuels: Status, challenges and prospects of drop-in liquid fuels, hydrogen and electrification in aviation. *Johnson Matthey Technology Review*, 2020. doi: 10.1595/205651320X15816756012040.

V. Becattini, P. Gabrielli, and M. Mazzotti. Role of Carbon Capture, Storage, and Utilization to Enable a Net-Zero-CO_2 -Emissions Aviation Sector. *Industrial & Engineering Chemistry Research*, 60(18):6848–6862, 2021. doi: 10.1021/acs.iecr.0c05392.

C. Bergero, G. Gosnell, D. Gielen, S. Kang, M. Bazilian, and S. J. Davis. Pathways to net-zero emissions from aviation. *Nature Sustainability*, 2023. doi: 10.1038/s41893-022-01046-9.

V. Bertsch and W. Fichtner. A participatory multi-criteria approach for power generation and transmission planning. *Annals of Operations Research*, 245 (1-2):177–207, 2016. doi: 10.1007/s10479-015-1791-y.

V. Bertsch, M. Hall, C. Weinhardt, and W. Fichtner. Public acceptance and preferences related to renewable energy and grid expansion policy: Empirical insights for Germany. *Energy*, 114:465–477, 2016. doi: 10.1016/j.energy.2016.08.022.

D. Bogdanov, J. Farfan, K. Sadovskaia, A. Aghahosseini, M. Child, A. Gulagi, A. S. Oyewo, L. d. S. N. S. Barbosa, and C. Breyer. Radical transformation pathway towards sustainable electricity via evolutionary steps. *Nature Communications*, 10(1):1077, 2019. doi: 10.1038/s41467-019-08855-1.

BP. bp Statistical Review of World Energy: 2022 | 71th edition. Technical report, The British Petroleum Company (BP), 2022. URL `https://www.bp.com/en/global/corporate/energy-economics/statistical-review-of-world-energy.html`.

R. Bramstoft, A. Pizarro-Alonso, I. G. Jensen, H. Ravn, and M. Münster. Modelling of renewable gas and renewable liquid fuels in future integrated energy systems. *Applied Energy*, 268:114869, 2020. doi: 10.1016/j.apenergy.2020.114869.

M. Braun-Unkhoff, U. Riedel, and C. Wahl. About the emissions of alternative jet fuels. *CEAS Aeronautical Journal*, 8(1):167–180, 2017. doi: 10.1007/s13272-016-0230-3.

C. Breyer, M. Fasihi, M. Micheli, A. S. Oyewo, P. Schmidt, and W. Weindorf. E-kerosene for Commercial Aviation: From Green Hydrogen and CO_2 from Direct Air Capture – Volumes, Cost, Area Demand and Renewable Energy Competition in the United States and Europe from 2030 to 2050. Technical report, Deutsche Energie-Agentur (dena), 2022. URL `https://www.dena.de/fileadmin/dena/Publikationen/PDFs/2022/STUDY_E-Kerosene_for_Commercial_Aviation.pdf`.

T. Brown and L. Reichenberg. Decreasing market value of variable renewables can be avoided by policy action. *Energy Economics*, 100:105354, 2021. doi: 10.1016/j.eneco.2021.105354.

T. Brown, J. Hörsch, and D. Schlachtberger. PyPSA: Python for Power System Analysis. *Journal of Open Research Software*, 6(1):4, 2018a. doi: 10.5334/jors.188.

T. Brown, D. Schlachtberger, A. Kies, S. Schramm, and M. Greiner. Synergies of sector coupling and transmission reinforcement in a cost-optimised, highly renewable European energy system. *Energy*, 160:720–739, 2018b. doi: 10.1016/j.energy.2018.06.222.

S. Brynolf, M. Taljegard, M. Grahn, and J. Hansson. Electrofuels for the transport sector: A review of production costs. *Renewable and Sustainable Energy Reviews*, 81:1887–1905, 2018. doi: 10.1016/j.rser.2017.05.288.

M. Buchhorn, B. Smets, L. Bertels, B. D. Roo, M. Lesiv, N.-E. Tsendbazar, M. Herold, and S. Fritz. Copernicus Global Land Service: Land Cover 100m: collection 3: epoch 2015: Globe, 2020. URL `https://zenodo.org/record/3939038`.

A. Buttler and H. Spliethoff. Current status of water electrolysis for energy storage, grid balancing and sector coupling via power-to-gas and power-to-liquids: A review. *Renewable and Sustainable Energy Reviews*, 82:2440–2454, 2018. doi: 10.1016/j.rser.2017.09.003.

K.-K. Cao, F. Cebulla, J. J. Gómez Vilchez, B. Mousavi, and S. Prehofer. Raising awareness in model-based energy scenario studies—a transparency checklist. *Energy, Sustainability and Society*, 6(1):28, 2016. doi: 10.1186/s13705-016-0090-z.

K.-K. Cao, J. Metzdorf, and S. Birbalta. Incorporating Power Transmission Bottlenecks into Aggregated Energy System Models. *Sustainability*, 10(6): 1916, 2018. doi: 10.3390/su10061916.

R. S. Capaz, E. M. De Medeiros, D. G. Falco, J. E. Seabra, P. Osseweijer, and J. A. Posada. Environmental trade-offs of renewable jet fuels in Brazil: Beyond the carbon footprint. *Science of The Total Environment*, 714:136696, 2020. doi: 10.1016/j.scitotenv.2020.136696.

F. Carvalho, F. T. F. Silva, A. Szklo, and J. Portugal-Pereira. Potential for biojet production from different biomass feedstocks and consolidated technological routes: a georeferencing and spatial analysis in Brazil. *Biofuels, Bioproducts and Biorefining*, 13(6):1454–1475, 2019. doi: 10.1002/bbb.2041.

W. R. Cervi, R. A. C. Lamparelli, J. E. A. Seabra, M. Junginger, S. Jong, and F. Hilst. Spatial modeling of techno-economic potential of biojet fuel production in Brazil. *GCB Bioenergy*, 12(2):136–157, 2020. doi: 10.1111/gcbb.12659.

W. R. Cervi, R. A. C. Lamparelli, B. C. Gallo, R. Oliveira Bordonal, J. E. A. Seabra, M. Junginger, and F. Hilst. Mapping the environmental and techno-economic potential of biojet fuel production from biomass residues in Brazil. *Biofuels, Bioproducts and Biorefining*, 15(1):282–304, 2021. doi: 10.1002/bbb.2161.

J. Chai, Z.-Y. Zhang, S.-Y. Wang, K. K. Lai, and J. Liu. Aviation fuel demand development in China. *Energy Economics*, 46:224–235, 2014. doi: 10.1016/j.eneco.2014.09.007.

M. Chang, J. Z. Thellufsen, B. Zakeri, B. Pickering, S. Pfenninger, H. Lund, and P. A. Østergaard. Trends in tools and approaches for modelling the energy transition. *Applied Energy*, 290:116731, 2021. doi: 10.1016/j.apenergy.2021.116731.

M. Child, C. Kemfert, D. Bogdanov, and C. Breyer. Flexible electricity generation, grid exchange and storage for the transition to a 100% renewable energy system in Europe. *Renewable Energy*, 139:80–101, 2019. doi: 10.1016/j.renene.2019.02.077.

B. Chèze, P. Gastineau, and J. Chevallier. Forecasting world and regional aviation jet fuel demands to the mid-term (2025). *Energy Policy*, 39(9):5147–5158, 2011. doi: 10.1016/j.enpol.2011.05.049.

A. J. Conejo, L. Baringo Morales, S. J. Kazempour, and A. S. Siddiqui. *Investment in Electricity Generation and Transmission*. Springer International Publishing, Cham, 2016. ISBN 978-3-319-29501-5.

E. B. Connelly, L. M. Colosi, A. F. Clarens, and J. H. Lambert. Risk Analysis of Biofuels Industry for Aviation with Scenario-Based Expert Elicitation. *Systems Engineering*, 18(2):178–191, 2015. doi: 10.1002/sys.21298.

L. Cortez, H. Cantarella, M. Moraes, L. Nogueira, U. Schuchardt, T. Franco, F. Nigro, A. Nassar, R. Leal, and R. Baldassin. Roadmap to a Sustainable

Aviation Biofuel: A Brazilian Case Study. In *Biofuels for Aviation*, pages 339–350. Elsevier, 2016. ISBN 978-0-12-804568-8. doi: 10.1016/B978-0-12-804568-8.00015-9.

P. A. Cremonez, M. Feroldi, C. d. J. de Oliveira, J. G. Teleken, H. J. Alves, and S. C. Sampaio. Environmental, economic and social impact of aviation biofuel production in Brazil. *New Biotechnology*, 32(2):263–271, 2015. doi: 10.1016/j.nbt.2015.01.001.

S. J. Davis, N. S. Lewis, M. Shaner, S. Aggarwal, D. Arent, I. L. Azevedo, S. M. Benson, T. Bradley, J. Brouwer, Y.-M. Chiang, C. T. M. Clack, A. Cohen, S. Doig, J. Edmonds, P. Fennell, C. B. Field, B. Hannegan, B.-M. Hodge, M. I. Hoffert, E. Ingersoll, P. Jaramillo, K. S. Lackner, K. J. Mach, M. Mastrandrea, J. Ogden, P. F. Peterson, D. L. Sanchez, D. Sperling, J. Stagner, J. E. Trancik, C.-J. Yang, and K. Caldeira. Net-zero emissions energy systems. *Science*, 360 (6396):eaas9793, 2018. doi: 10.1126/science.aas9793.

S. De Jong, K. Antonissen, R. Hoefnagels, L. Lonza, M. Wang, A. Faaij, and M. Junginger. Life-cycle analysis of greenhouse gas emissions from renewable jet fuel production. *Biotechnology for Biofuels*, 10(1):64, 2017. doi: 10.1186/s13068-017-0739-7.

L. M. de Souza, P. A. Mendes, and D. A. Aranda. Assessing the current scenario of the Brazilian biojet market. *Renewable and Sustainable Energy Reviews*, 98:426–438, 2018. doi: 10.1016/j.rser.2018.09.039.

DEA. Technology Data for Energy Storage, 2020a. URL `https://ens.dk/en/our-services/projections-and-models/technology-data/technology-data-energy-storage`.

DEA. Technology Data for Generation of Electricity and District Heating, 2020b. URL `https://ens.dk/en/our-services/projections-and-models/technology-data/technology-data-generation-electricity-and`.

DEA. Technology Data for Renewable Fuels, 2021. URL `https://ens.dk/en/our-services/projections-and-models/technology-data/technology-data-renewable-fuels`.

M. Decker, F. Schorn, R. C. Samsun, R. Peters, and D. Stolten. Off-grid power-to-fuel systems for a market launch scenario – A techno-economic assessment. *Applied Energy*, 250:1099–1109, 2019. doi: 10.1016/j.apenergy.2019.05.085.

Y. Deng. Open Brazilian Energy Data, 2023a. URL `https://gitlab.com/dlr-ve/esy/open-brazil-energy-data/open-brazilian-energy-data`. GitLab.

Y. Deng. PyPSA-Brazil, 2023b. URL `https://gitlab.com/dlr-ve/esy/open-brazil-energy-data/pypsa-brazil`.

Y. Deng, K.-K. Cao, and B. Wanke. Designing a Brazilian energy system model for studying energy planning at high spatial and temporal resolution. In *Volume 24: Sustainable Energy Solutions for a Post-COVID Recovery towards a Better Future: Part VII*, volume 24, page 6. Energy proceedings, 2021. ISBN 2004-2965. URL `https://doi.org/10.46855/energy-proceedings-9781`.

Y. Deng, K.-K. Cao, W. Hu, R. Stegen, v. K. von Krbek, R. Soria, P. R. R. Rochedo, and P. Jochem. Dataset: Harmonized and Open Energy Dataset for Modeling a Highly Renewable Brazilian Power System, 2022. URL `https://zenodo.org/record/7478165`.

C. M. Dennis, R. C. Walish, H. M. Pacini, T. A. Chisholm, and T. L. Acker. Improving hydrogeneration representation in a production cost model used for long-term transmission studies in the Western Interconnection. In *2011 IEEE/PES Power Systems Conference and Exposition*, pages 1–8, Phoenix, AZ, USA, 2011. IEEE. ISBN 978-1-61284-789-4. doi: 10.1109/PSCE.2011.5772586.

F. A. Diuana, C. Viviescas, and R. Schaeffer. An analysis of the impacts of wind power penetration in the power system of southern Brazil. *Energy*, 186:115869, 2019. doi: 10.1016/j.energy.2019.115869.

G. G. Dranka and P. Ferreira. Planning for a renewable future in the Brazilian power system. *Energy*, 164:496–511, 2018. doi: 10.1016/j.energy.2018.08.164.

S. Drünert, U. Neuling, T. Zitscher, and M. Kaltschmitt. Power-to-Liquid fuels for aviation – Processes, resources and supply potential under German conditions. *Applied Energy*, 277:115578, 2020. doi: 10.1016/j.apenergy.2020.115578.

N. Dudley. *Guidelines for applying protected area management categories including IUCN WCPA best practice guidance on recognising protected areas and assigning management categories and governance types*. IUCN, 2013. ISBN 978-2-8317-1636-7. URL `https://portals.iucn.org/library/node/30018`.

J. A. Duffie and W. A. Beckman. *Solar Engineering of Thermal Processes: Duffie/Solar Engineering 4e*. John Wiley & Sons, Inc., Hoboken, NJ, USA, 2013. ISBN 978-1-118-67160-3 978-0-470-87366-3.

J. Egerer, V. Grimm, K. Niazmand, and P. Runge. The economics of global green ammonia trade – "Shipping Australian wind and sunshine to Germany". *Applied Energy*, 334:120662, 2023. doi: 10.1016/j.apenergy.2023.120662.

ENTSO-E. Hydropower modelling – New database complementing PECD. Technical report, European Network of Transmission System Operators (ENTSO-E), 2019. URL `https://eepublicdownloads.entsoe.eu/clean-documents/sdc-documents/MAF/2019/Hydropower_Modelling_New_database_and_methodology.pdf`.

ENTSO-E. European Network of Transmission System Operators for Electricity, 2023. URL `https://transparency.entsoe.eu/dashboard/show`.

EPA. GHG Emission Factors Hub, 2022. URL `https://www.epa.gov/climateleadership/ghg-emission-factors-hub`.

EPE. Anuário estatístico de energia elétrica 2011, 2011. URL `https://www.epe.gov.br/sites-pt/publicacoes-dados-abertos/publicacoes/PublicacoesArquivos/publicacao-160/topico-168/Anu%C3%A1rio%20Estat%C3%ADstico%20de%20Energia%20El%C3%A9trica%202011.pdf`.

EPE. ESTUDOS PARA A EXPANSÃO DA TRANSMISSÃO: ANÁLISE TÉCNICO-ECONÔMICA E SOCIOAMBIENTAL DE ALTERNATIVAS:

RELATÓRIO R1. Govermental No EPE-DEE-RE-025/2020-rev0, Empresa de Pesquisa Energética (EPE), 2020a. URL https://www.epe.gov.br/sites-pt/publicacoes-dados-abertos/publicacoes/PublicacoesArquivos/publicacao-276/topico-525/EPE-DEE-RE-025-2020-rev0+SMA%20-%20Estudo%20para%20Controle%20de%20Tens%C3%A3o%20e%20Suprimento%20ao%20Extremo%20Sul%20da%20Bahia.pdf.

EPE. MDI_pde_2029: Code and input data for the investment decision model from Ten Year Expansion Plan – PDE, 2020b. URL https://github.com/equipesge/MDI_PDE_2029. original-date: 2019-11-29T13:25:36Z.

EPE. Plano Decenal de Expansão de Energia 2029. Technical report, Empresa de Pesquisa Energética (EPE), 2020c. URL https://www.epe.gov.br/sites-pt/publicacoes-dados-abertos/publicacoes/Documents/PDE%202029.pdf.

EPE. Sistema de Informações Geográficas do Setor Energético Brasileiro: Linhas de Transmissão, 2020d. URL https://gisepeprd2.epe.gov.br/WebMapEPE/.

EPE. Anuário Estatístico de Energia Elétrica 2021, 2021. URL https://www.epe.gov.br/pt/publicacoes-dados-abertos/publicacoes/anuario-estatistico-de-energia-eletrica.

EPE. Consumo de Energia Elétrica, 2022a. URL https://www.epe.gov.br/pt/areas-de-atuacao/energia-eletrica/consumo-de-energia-el%C3%A9trica.

EPE. Oferta de Energia Elétrica – PNE2050. Technical report, Empresa de Pesquisa Energética (EPE), 2022b. URL https://www.epe.gov.br/sites-pt/publicacoes-dados-abertos/publicacoes/PublicacoesArquivos/publicacao-227/topico-563/NT_PR_003.22_Oferta.pdf.

EPE and MME. Plano Nacional de Energia 2050. Technical report, Ministério de Minas e Energia (MME), Empresa de Pesquisa Energética (EPE), Brasília, Brazil, 2020. URL https://www.epe.gov.br/pt/publicacoes-dados-abertos/publicacoes/Plano-Nacional-de-Energia-2050.

ESMAP. Global photovoltaic power potential by country. Technical report, The Energy Sector Management Assistance Program (ESMAP), Washington, DC: World Bank, 2020. URL http://documents.worldbank.org/curated/en/466331592817725242/Global-Photovoltaic-Power-Potential-by-Country.

P. C. V. Esmeraldo. Technical benefits of HVDC lines and experience of technical benefits of HVDC lines and experience of HVDC projects: Brazil, China, and perspectives in Latin America, 2020. URL https://energia.gob.cl/sites/default/files/mini-sitio/07_stategrid_paulo_esmeraldo.pdf.

EU. Directive 2003/87/EC of the European Parliament and of the Council of 13 October 2003 establishing a scheme for greenhouse gas emission allowance trading within the Community and amending Council Directive 96/61/EC. Technical Report 32003L0087, Official Journal of the European Union, 2003. URL http://data.europa.eu/eli/dir/2003/87/oj/eng.

European Central Bank. Euro reference exchange rate: US dollar (USD), 2022a. URL https://www.ecb.europa.eu/stats/policy_and_exchange_rates/euro_reference_exchange_rates/html/eurofxref-graph-usd.en.html.

European Central Bank. Euro reference exchange rate: Brazilian real (BRL), 2022b. URL https://www.ecb.europa.eu/stats/policy_and_exchange_rates/euro_reference_exchange_rates/html/eurofxref-graph-brl.en.html.

European Central Bank. Euro reference exchange rate: Pound sterling (GBP), 2023. URL https://www.ecb.europa.eu/stats/policy_and_exchange_rates/euro_reference_exchange_rates/html/eurofxref-graph-gbp.en.html.

European Commission. Updated analysis of the non-CO_2 climate impacts of aviation and potential policy measures pursuant to EU Emissions Trading System Directive Article 30(4). Technical report, European Commission, 2020. URL https://eur-lex.europa.eu/legal-content/EN/TXT/PDF/?uri=CELEX:52020DC0747.

European Commission. Regulation of the European Parliament and of the Council: on ensuring a level playing field for sustainable air transport: SEC(2021) 561 final - SWD(2021) 633 final - SWD(2021) 634 final, 2021. URL https://ec.europa.eu/info/sites/default/files/refueleu_aviation_-_sustainable_aviation_fuels.pdf.

M. Fasihi and C. Breyer. Baseload electricity and hydrogen supply based on hybrid PV-wind power plants. *Journal of Cleaner Production*, 243:118466, 2020. doi: 10.1016/j.jclepro.2019.118466.

M. Fasihi, D. Bogdanov, and C. Breyer. Long-Term Hydrocarbon Trade Options for the Maghreb Region and Europe—Renewable Energy Based Synthetic Fuels for a Net Zero Emissions World. *Sustainability*, 9(2):306, 2017. doi: 10.3390/su9020306.

Federal Government of Brazil. LEI Nº 9.478 DE 06 DE AGOSTO DE 1997: Dispõe sobre a política energética nacional, as atividades relativas ao monopólio do petróleo, institui o Conselho Nacional de Política Energética e a Agência Nacional do Petróleo e dá outras providências, 1997. URL http://www.planalto.gov.br/ccivil_03/leis/l9478.htm?origin=instituicao.

Federal Government of Brazil. LEI Nº 12.490, DE 16 DE SETEMBRO DE 2011, 2011. URL http://www.planalto.gov.br/ccivil_03/_Ato2011-2014/2011/Lei/L12490.htm?origin=instituicao.

Federal Government of Brazil. Decreto Nº 8777: Institui a Política de Dados Abertos do Poder Executivo federal, 2016. URL http://www.planalto.gov.br/CCIVIL_03/_Ato2015-2018/2016/Decreto/D8777.htm.

Federal Government of Brazil. LEI Nº 13.576, DE 26 DE DEZEMBRO DE 2017: Dispõe sobre a Política Nacional de Biocombustíveis (RenovaBio) e dá outras providências, 2017. URL http://www.planalto.gov.br/ccivil_03/_ato2015-2018/2017/lei/L13576.htm?origin=instituicao.

Federal Government of Brazil. Decreto Nº 9903: Altera o Decreto nº 8.777, de 11 de maio de 2016, que institui a Política de Dados Abertos do Poder Executivo federal, para dispor sobre a gestão e os direitos de uso de dados abertos., 2019. URL https://www.planalto.gov.br/ccivil_03/_Ato2019-2022/2019/Decreto/D9903.htm.

Federal Government of Brazil. Portal de Dados Abertos, 2023. URL https://dados.gov.br/home.

Federal Republic of Germany. PtL-Roadmap: Sustainable aviation fuel from renewable energy sources for aviation in Germany, 2021. URL https://bmdv.bund.de/SharedDocs/DE/Anlage/G/ptl-roadmap-englisch.pdf?__blob=publicationFile.

T. Fichter, R. Soria, A. Szklo, R. Schaeffer, and A. F. Lucena. Assessing the potential role of concentrated solar power (CSP) for the northeast power system of Brazil using a detailed power system model. *Energy*, 121:695–715, 2017. doi: 10.1016/j.energy.2017.01.012.

D. Z. Fitiwi, M. Lynch, and V. Bertsch. Power system impacts of community acceptance policies for renewable energy deployment under storage cost uncertainty. *Renewable Energy*, 156:893–912, 2020. doi: 10.1016/j.renene.2020.03.110.

U. J. Frey. Multiple method modelling reveals lack of robustness in natural resource management research. *Journal of Environmental Management*, 281:111812, 2021. doi: 10.1016/j.jenvman.2020.111812.

Fuel Tank Shop. 10000 Litre Bunded Steel Oil Tank, 2023. URL https://www.fueltankshop.co.uk/10000-litre-bunded-steel-oil-tank/p4156.

P. Gabrielli, M. Gazzani, and M. Mazzotti. The Role of Carbon Capture and Utilization, Carbon Capture and Storage, and Biomass to Enable a Net-Zero-CO_2 Emissions Chemical Industry. *Industrial & Engineering Chemistry Research*, 59(15):7033–7045, 2020. doi: 10.1021/acs.iecr.9b06579. Publisher: American Chemical Society.

H. Gils, S. Simon, and R. Soria. 100% Renewable Energy Supply for Brazil—The Role of Sector Coupling and Regional Development. *Energies*, 10(11):1859, 2017. doi: 10.3390/en10111859.

T. Gleeson, K. M. Befus, S. Jasechko, E. Luijendijk, and M. B. Cardenas. The global volume and distribution of modern groundwater. *Nature Geoscience*, 9 (2):161–167, 2016. doi: 10.1038/ngeo2590.

A. Gonzalez-Garay, C. Heuberger-Austin, X. Fu, M. Klokkenburg, D. Zhang, A. Van Der Made, and N. Shah. Unravelling the potential of sustainable aviation fuels to decarbonise the aviation sector. *Energy & Environmental Science*, 15(8):3291–3309, 2022. doi: 10.1039/D1EE03437E.

F. Gotzens, H. Heinrichs, J. Hörsch, and F. Hofmann. Performing energy modelling exercises in a transparent way – The issue of data quality in power plant databases. *Energy Strategy Reviews*, 23:1–12, 2019. doi: 10.1016/j.esr.2018.11.004.

J. Graham, B. Jonsson, and R. S. Moni. The Galabi 2000 MW interconnection back-to-back HVDC to connect weak AC systems. *Citeseer*, 2002. URL `https://library.e.abb.com/public/0d50a8fce76db2c9c1256fda003b4d43/THE%20GARABI%202000%20MW%20INTERCONNECTION.pdf`. ABB Utilities AB, SE-771 80 Ludvika, Sweden.

J. Graham, T. Holmgren, P. Fischer, and N. Shore. The Rio Madeira HVDC System – Design aspects of Bipole 1 and the connector to Acre-Rondônia. In *DC systems and power electronics*, session materials, page 10. CIGRE, 2012. URL `https://library.e.abb.com/public/7b09a3fdfbc8f540c1257a8600290bf2/The%20Rio%20Madeira%20HVDC%20System%20John%20Graham.pdf`.

Gurobi Optimization. Gurobi Optimizer Reference Manual: Version 9.1, 2021. URL `https://www.gurobi.com/wp-content/plugins/hd_documentations/documentation/9.1/refman.pdf`.

S. Hagspiel, C. Jägemann, D. Lindenberger, T. Brown, S. Cherevatskiy, and E. Tröster. Cost-optimal power system extension under flow-based market coupling. *Energy*, 66:654–666, 2014. doi: 10.1016/j.energy.2014.01.025.

J. Hampp, M. Düren, and T. Brown. Import options for chemical energy carriers from renewable sources to Germany. *PLOS ONE*, 18(2):e0262340, 2023. doi: 10.1371/journal.pone.0281380.

C. Hank, A. Sternberga, N. Köppel, M. Holst, T. Smolinka, A. Schaadt, C. Hebling, and H.-M. Henning. Energy efficiency and economic assessment of imported energy carriers based on renewable electricity. *Sustainable Energy & Fuels*, 1 (3):458–466, 2017. doi: 10.1039/C7SE00062F.

K. Hansen. Decision-making based on energy costs: Comparing levelized cost of energy and energy system costs. *Energy Strategy Reviews*, 24:68–82, 2019. doi: 10.1016/j.esr.2019.02.003.

F. Harvey. Airlines agree to curb their greenhouse gas emissions by 2020, 2013. URL `https://www.theguardian.com/environment/2013/jun/04/airlines-agree-to-curb-greenhouse-gas-emissions`.

S. Herreras Martínez, A. Koberle, P. Rochedo, R. Schaeffer, A. Lucena, A. Szklo, S. Ashina, and D. P. van Vuuren. Possible energy futures for Brazil and Latin America in conservative and stringent mitigation pathways up to 2050. *Technological Forecasting and Social Change*, 98:186–210, 2015. doi: 10.1016/j.techfore.2015.05.006.

H. Hersbach, B. Bell, P. Berrisford, S. Hirahara, A. Horányi, J. Muñoz-Sabater, J. Nicolas, C. Peubey, R. Radu, D. Schepers, A. Simmons, C. Soci, S. Abdalla, X. Abellan, G. Balsamo, P. Bechtold, G. Biavati, J. Bidlot, M. Bonavita, G. Chiara, P. Dahlgren, D. Dee, M. Diamantakis, R. Dragani, J. Flemming, R. Forbes, M. Fuentes, A. Geer, L. Haimberger, S. Healy, R. J. Hogan, E. Hólm, M. Janisková, S. Keeley, P. Laloyaux, P. Lopez, C. Lupu, G. Radnoti, P. Rosnay, I. Rozum, F. Vamborg, S. Villaume, and J. Thépaut. The ERA5 global reanalysis. *Quarterly Journal of the Royal Meteorological Society*, 146(730): 1999–2049, 2020. doi: 10.1002/qj.3803.

P.-M. Heuser, D. S. Ryberg, T. Grube, M. Robinius, and D. Stolten. Techno-economic analysis of a potential energy trading link between Patagonia and

Japan based on CO_2 free hydrogen. *International Journal of Hydrogen Energy*, 44(25):12733–12747, 2019. doi: 10.1016/j.ijhydene.2018.12.156.

J. Holladay, Z. Abdullah, and J. Heyne. Sustainable Aviation Fuel: Review of Technical Pathways. Technical report, U.S Department of Energy, Bioenergy Technologies Office, Washington, DC, 2020. URL https://www.energy.gov/eere/bioenergy/downloads/sustainable-aviation-fuel-review-technical-pathways-report.

W. F. Holmgren, C. W. Hansen, and M. A. Mikofski. pvlib python: a python package for modeling solar energy systems. *Journal of Open Source Software*, 3(29):884, 2018. doi: 10.21105/joss.00884.

J. Hörsch, F. Hofmann, D. Schlachtberger, and T. Brown. PyPSA-Eur: An Open Optimisation Model of the European Transmission System. *Energy Strategy Reviews*, 22:207–215, 2018a. doi: 10.1016/j.esr.2018.08.012.

J. Hörsch, H. Ronellenfitsch, D. Witthaut, and T. Brown. Linear optimal power flow using cycle flows. *Electric Power Systems Research*, 158:126–135, 2018b. doi: 10.1016/j.epsr.2017.12.034.

IATA. Annual Review 2018. Technical report, International Air Transport Association (IATA), 2018. URL https://www.iata.org/contentassets/c81222d96c9a4e0bb4ff6ced0126f0bb/iata-annual-review-2018.pdf.

IATA. Net-Zero Carbon Emissions by 2050, 2021. URL https://www.iata.org/en/pressroom/pressroom-archive/2021-releases/2021-10-04-03/.

IBGE. Áreas Territoriais, 2018a. URL https://www.ibge.gov.br/geociencias/organizacao-do-territorio/estrutura-territorial/15761-areas-dos-municipios.html?edicao=24050&t=acesso-ao-produto. Territorial Areas.

IBGE. Estimativas da população residente para os municípios e para as unidades da federação | IBGE, 2018b. URL https://www.ibge.gov.br/estatist icas/sociais/populacao/9103-estimativas-de-populacao.html?=&t=downloads.

IBGE. Produto Interno Bruto dos Municípios, 2018c. URL https://www.ibge.gov.br/estatisticas/economicas/contas-nacionais/9088-produto-interno-bruto-dos-municipios.html?edicao=29720&t=downloads. Gross Domestic Product of Municipalities.

IBGE. Malha Municipal: Municipio_2021, UFs, 2021. URL https://www.ibge.gov.br/geociencias/organizacao-do-territorio/malhas-territoriais/15774-malhas.html?=&t=downloads.

ICAO. Manual on Air Traffic Forecasting (Doc 8991), 2006. URL https://store.icao.int/en/manual-on-air-traffic-forecasting-doc-8991.

ICAO. Enviromental Protection: Volumn IV, Carbon Offsetting and Reduction Scheme for International Aviation (CORSIA), 2018a. URL https://elibrary.icao.int/home/product-details/229739?_gl=1*1fj9rif*_ga*MTIyNzEzMDA5Ny4xNjc2ODg4OTky*_ga_992N3YDLBQ*MTY3NjkzMTE0Ny4yLjEuMTY3NjkzMTE4NC4wLjAuMA.

ICAO. Sustainable Aviation Fuels Guide. Technical report, International Civil Aviation Organization (ICAO), 2018b. URL https://www.icao.int/environmental-protection/Documents/Sustainable%20Aviation%20Fuels%20Guide_100519.pdf.

ICAO. Aviation and the Environment: Outlook. Technical report, ICAO, 2019a. URL https://www.icao.int/environmental-protection/Documents/EnvironmentalReports/2019/ENVReport2019_pg24-38.pdf.

ICAO. Guidance on the Development of States' Action Plan on CO_2 Emissions Reduction Activities (Doc 9988), 2019b. URL https://store.icao.int/en/guidance-on-the-development-of-states-action-plan-on-co2-emissions-reduction-activities-doc-9988. 3rd edition.

ICAO. Resolution A40-18: Consolidated statement of continuing ICAO policies and practices related to environmental protection - Climate change. Technical report, International Civil Aviation Organization (ICAO), 2019c. URL https://www.icao.int/environmental-protection/Documents/Assembly/Resolution_A40-18_Climate_Change.pdf.

ICAO. CORSIA Default Life Cycle Emissions Values for CORSIA Eligible Fuels. Technical report, ICAO, 2021a. URL https://www.icao.int/environmental-protection/CORSIA/Documents/ICAO%20document%2006%20-%20Default%20Life%20Cycle%20Emissions%20-%20March%202021.pdf.

ICAO. CORSIA Sustainability Criteria for CORSIA Eligible Fuels. Technical report, ICAO, 2021b. URL https://www.icao.int/environmental-protection/CORSIA/Documents/ICAO%20document%2005%20-%20Sustainability%20Criteria%20-%20November%202021.pdf.

ICAO. CORSIA Methodology for Calculating Actual Life Cycle Emissions Values. Technical report, ICAO, 2022a. URL https://www.icao.int/environmental-protection/CORSIA/Documents/CORSIA_Eligible_Fuels/ICAO%20document%2007%20-%20Methodology%20for%20Actual%20Life%20Cycle%20Emissions%20-%20June%202022.pdf.

ICAO. Innovation for a green transition: 2022 Environmental Report. Technical report, International Civil Aviation Organization (ICAO), 2022b. URL https://www.icao.int/environmental-protection/Documents/EnvironmentalReports/2022/ICAO%20ENV%20Report%202022%20F4.pdf#search=Aviation%20Green%20Transition%3A%20Chartering%20a%20path%20to%20sustainable%20flying%20future.

IEA. *CO_2 Emissions from Fuel Combustion 2019*. OECD, 2019. ISBN 978-92-64-91310-3 978-92-64-32021-5. doi: 10.1787/2a701673-en.

IEA. World Energy Outlook 2021. License: CC BY 4.0, International Energy Agency (IEA), IEA, Paris, 2021a. URL https://www.iea.org/reports/world-energy-outlook-2021.

IEA. World Energy Model Documentation, 2021b. URL https://iea.blob.core.windows.net/assets/932ea201-0972-4231-8d81-356300e9fc43/WEM_Documentation_WEO2021.pdf.

S. A. Ikonnikova, B. R. Scanlon, and S. A. Berdysheva. A global energy system perspective on hydrogen Trade: A framework for the market color and the size analysis. *Applied Energy*, 330:120267, 2023. doi: 10.1016/j.apenergy.2022.120267.

IPCC. *Global Warming of 1.5°C: IPCC Special Report on Impacts of Global Warming of 1.5°C above Pre-industrial Levels in Context of Strengthening Response to Climate Change, Sustainable Development, and Efforts to Eradicate Poverty*. Cambridge University Press, 1 edition, 2022a. ISBN 978-1-00-915794-0 978-1-00-915795-7. doi: 10.1017/9781009157940.

IPCC. Mitigation Pathways Compatible with 1.5°C in the Context of Sustainable Development. In *Global Warming of 1.5°C. An IPCC Special Report on the impacts of global warming of 1.5°C above pre-industrial levels and related global greenhouse gas emission pathways, in the context of strengthening the global response to the threat of climate change, sustainable development, and efforts to eradicate poverty*, page 82. Cambridge University Press, 1 edition, 2022b. ISBN 978-1-00-915794-0 978-1-00-915795-7. doi: 10.1017/9781009157940.

IRENA. Renewable power generation costs in 2021, 2022. URL https://mc-cd8320d4-36a1-40ac-83cc-3389-cdn-endpoint.azureedge.net/-/media/Files/IRENA/Agency/Publication/2022/Jul/IRENA_Power_Generation_Costs_2021.pdf?rev=0d045caf72cd4ecd8f660b69c204fa81.

ISO. ISO 3166 - Country Codes, 2022. URL https://www.iso.org/iso-3166-country-codes.html.

T. V. Jensen and P. Pinson. RE-Europe, a large-scale dataset for modeling a highly renewable European electricity system. *Scientific Data*, 4(1):170175, 2017. doi: 10.1038/sdata.2017.175.

T. Junne, M. Xiao, L. Xu, Z. Wang, P. Jochem, and T. Pregger. How to assess the quality and transparency of energy scenarios: Results of a case study. *Energy Strategy Reviews*, 26:100380, 2019. doi: 10.1016/j.esr.2019.100380.

M. Kaltschmitt and U. Neuling, editors. *Biokerosene: Status and Prospects*. Springer Berlin Heidelberg, Berlin, Heidelberg, 2018. ISBN 978-3-662-53063-4 978-3-662-53065-8. doi: 10.1007/978-3-662-53065-8.

Å. Killingtveit. Hydropower. In *Managing Global Warming*, pages 265–315. Elsevier, 2019. ISBN 978-0-12-814104-5. doi: 10.1016/B978-0-12-81410 4-5.00008-9.

B. C. Klein, M. F. Chagas, T. L. Junqueira, M. C. A. F. Rezende, T. d. F. Cardoso, O. Cavalett, and A. Bonomi. Techno-economic and environmental assessment of renewable jet fuel production in integrated Brazilian sugarcane biorefineries. *Applied Energy*, 209:290–305, 2018. doi: 10.1016/j.apenergy.2017.10.079.

L. Kriechbaum, G. Scheiber, and T. Kienberger. Grid-based multi-energy systems—modelling, assessment, open source modelling frameworks and challenges. *Energy, Sustainability and Society*, 8(1):35, 2018. doi: 10.1186/s137 05-018-0176-x.

D. H. König, M. Freiberg, R.-U. Dietrich, and A. Wörner. Techno-economic study of the storage of fluctuating renewable energy in liquid hydrocarbons. *Fuel*, 159:289–297, 2015. doi: 10.1016/j.fuel.2015.06.085.

Land and Water Development Division, FAO. Digital Soil Map of the World, 2020. URL `https://data.apps.fao.org/map/catalog/srv/eng/catalog.search#/metadata/446ed430-8383-11db-b9b2-000d939bc5d8`.

B. Lebrouhi, J. Djoupo, B. Lamrani, K. Benabdelaziz, and T. Kousksou. Global hydrogen development - A technological and geopolitical overview. *International Journal of Hydrogen Energy*, 47(11):7016–7048, 2022. doi: 10.1016/j.ijhydene.2021.12.076.

D. S. Lee, D. W. Fahey, P. M. Forster, P. J. Newton, R. C. Wit, L. L. Lim, B. Owen, and R. Sausen. Aviation and global climate change in the 21st century. *Atmospheric Environment*, 43(22-23):3520–3537, 2009. doi: 10.1016/j.atmosenv.2009.04.024.

D. S. Lee, D. W. Fahey, A. Skowron, M. R. Allen, U. Burkhardt, Q. Chen, S. J. Doherty, S. Freeman, P. M. Forster, J. Fuglestvedt, A. Gettelman, R. R. De León, L. L. Lim, M. T. Lund, R. J. Millar, B. Owen, J. E. Penner, G. Pitari, M. J. Prather, R. Sausen, and L. J. Wilcox. The contribution of global aviation to anthropogenic climate forcing for 2000 to 2018. *Atmospheric Environment*, 244:117834, 2021. doi: 10.1016/j.atmosenv.2020.117834.

B. Lehner and P. Döll. Development and validation of a global database of lakes, reservoirs and wetlands. *Journal of Hydrology*, 296(1-4):1–22, 2004. doi: 10.1016/j.jhydrol.2004.03.028.

B. Lehner, C. R. Liermann, C. Revenga, C. Vörösmarty, B. Fekete, P. Crouzet, P. Döll, M. Endejan, K. Frenken, J. Magome, C. Nilsson, J. C. Robertson, R. Rödel, N. Sindorf, and D. Wisser. High-resolution mapping of the world's reservoirs and dams for sustainable river-flow management. *Frontiers in Ecology and the Environment*, 9(9):494–502, 2011. doi: 10.1890/100125.

M. S. Lester, R. Bramstoft, and M. Münster. Analysis on Electrofuels in Future Energy Systems: A 2050 Case Study. *Energy*, 199:117408, 2020. doi: 10.1016/j.energy.2020.117408.

M. Lima, L. Mendes, G. Mothé, F. Linhares, M. de Castro, M. da Silva, and M. Sthel. Renewable energy in reducing greenhouse gas emissions: Reaching the goals of the Paris agreement in Brazil. *Environmental Development*, 33:100504, 2020. doi: 10.1016/j.envdev.2020.100504.

H. Liu, G. B. Andresen, T. Brown, and M. Greiner. A high-resolution hydro power time-series model for energy systems analysis: Validated with Chinese hydro reservoirs. *MethodsX*, 6:1370–1378, 2019. doi: 10.1016/j.mex.2019.05.024.

P. Lobo, D. E. Hagen, and P. D. Whitefield. Comparison of PM Emissions from a Commercial Jet Engine Burning Conventional, Biomass, and Fischer–Tropsch Fuels. *Environmental Science & Technology*, 45(24):10744–10749, 2011. doi: 10.1021/es201902e.

B. Lux, J. Gegenheimer, K. Franke, F. Sensfuß, and B. Pfluger. Supply curves of electricity-based gaseous fuels in the MENA region. *Computers & Industrial Engineering*, 162:107647, 2021. doi: 10.1016/j.cie.2021.107647.

N. MacDowell, N. Florin, A. Buchard, J. Hallett, A. Galindo, G. Jackson, C. S. Adjiman, C. K. Williams, N. Shah, and P. Fennell. An overview of CO_2 capture technologies. *Energy & Environmental Science*, 3(11):1645, 2010. doi: 10.1039/c004106h.

M. Masiol and R. M. Harrison. Aircraft engine exhaust emissions and other airport-related contributions to ambient air pollution: A review. *Atmospheric Environment*, 95:409–455, 2014. doi: 10.1016/j.atmosenv.2014.05.070.

C. Matke, W. Medjroubi, and D. Kleinhans. SciGRID—An Open Source Reference Model for the European Transmission Network, 2016. URL `http://www.scigrid.de/`.

N. Mattsson, V. Verendel, F. Hedenus, and L. Reichenberg. An autopilot for energy models – Automatic generation of renewable supply curves, hourly capacity factors and hourly synthetic electricity demand for arbitrary world regions. *Energy Strategy Reviews*, 33:100606, 2021. doi: 10.1016/j.esr.2020.100606.

S. Maurice. *Surface Production Operations: Volume 5: Pressure Vessels, Heat Exchangers, and Aboveground Storage Tanks*. Gulf Professional Publishing, 1st edition edition, 2021. ISBN 978-0-12-803744-7.

R. Mawhood, E. Gazis, S. de Jong, R. Hoefnagels, and R. Slade. Production pathways for renewable jet fuel: a review of commercialization status and future prospects: Renewable jet fuel technologies: commercialisation status and future prospects. *Biofuels, Bioproducts and Biorefining*, 10(4):462–484, 2016. doi: 10.1002/bbb.1644.

M. Mazraati and O. M. Alyousif. Aviation fuel demand modelling in OECD and developing countries: impacts of fuel efficiency. *OPEC Energy Review*, 33(1): 23–46, 2009. doi: 10.1111/j.1753-0237.2009.00161.x.

M. Mazraati and Y. O. Faquih. Modelling aviation fuel demand: the case of the United States and China. *OPEC Energy Review*, 32(4):323–342, 2008. doi: 10.1111/j.1753-0237.2009.00156.x.

W. Medjroubi, U. P. Müller, M. Scharf, C. Matke, and D. Kleinhans. Open Data in Power Grid Modelling: New Approaches Towards Transparent Grid Models. *Energy Reports*, 3:14–21, 2017. doi: 10.1016/j.egyr.2016.12.001.

M. Melikoglu. Modelling and forecasting the demand for jet fuel and bio-based jet fuel in Turkey till 2023. *Sustainable Energy Technologies and Assessments*, 19:17–23, 2017. doi: 10.1016/j.seta.2016.11.005.

M. Micheli, D. Moore, V. Bach, and M. Finkbeiner. Life-Cycle Assessment of Power-to-Liquid Kerosene Produced from Renewable Electricity and CO_2 from Direct Air Capture in Germany. *Sustainability*, 14(17):10658, 2022. doi: 10.3390/su141710658.

Ministry of Infrastructure. Brazil's Action Plan on CO_2 Emissions Reduction from Aviation: Base Year 2018. Govermental, Ministry of Infrastructure, 2019. URL `https://www.gov.br/anac/pt-br/assuntos/meio-ambiente/arquivos/BrazilsActionPlanonCO2EmissionsReductionfromAviation3rdEditionBaseYear2018.pdf`.

R. H. Moore, K. L. Thornhill, B. Weinzierl, D. Sauer, E. D'Ascoli, J. Kim, M. Lichtenstern, M. Scheibe, B. Beaton, A. J. Beyersdorf, J. Barrick, D. Bulzan, C. A. Corr, E. Crosbie, T. Jurkat, R. Martin, D. Riddick, M. Shook, G. Slover, C. Voigt, R. White, E. Winstead, R. Yasky, L. D. Ziemba, A. Brown, H. Schlager, and B. E. Anderson. Biofuel blending reduces particle emissions from aircraft engines at cruise conditions. *Nature*, 543(7645):411–415, 2017. doi: 10.1038/nature21420.

K. Moriarty and A. Kvien. U.S. Airport Infrastructure and Sustainable Aviation Fuel. Technical Report NREL/TP–5400-78368, 1768316, MainId:32285, Federal Aviation Administration (FAA), 2021. URL `https://www.osti.gov/servlets/purl/1768316/`.

P. T. Moseley and J. Garche. *Electrochemical Energy Storage for Renewable Sources and Grid Balancing*. Elsevier, 2015. ISBN 978-0-444-62616-5.

E. Müller-Casseres, F. Carvalho, T. Nogueira, C. Fonte, M. Império, M. Poggio, H. K. Wei, J. Portugal-Pereira, P. R. Rochedo, A. Szklo, and R. Schaeffer. Production of alternative marine fuels in Brazil: An integrated assessment perspective. *Energy*, 219:119444, 2021. doi: 10.1016/j.energy.2020.119444.

F. Neumann, E. Zeyen, M. Victoria, and T. Brown. Benefits of a Hydrogen Network in Europe, 2022. URL http://arxiv.org/abs/2207.05816.

D. B. Newell and E. Tiesinga. *The international system of units (SI): 2008 edition*. NIST SP 330, 2008 edition. National Institute of Standards and Technology, Gaithersburg, MD, 2019. doi: 10.6028/NIST.SP.330-2019. URL https://doi.org/10.6028/NIST.SP.330-2019.

L. P. P. Nogueira, A. Frossard Pereira de Lucena, R. Rathmann, P. Rua Rodriguez Rochedo, A. Szklo, and R. Schaeffer. Will thermal power plants with CCS play a role in Brazil's future electric power generation? *International Journal of Greenhouse Gas Control*, 24:115–123, 2014. doi: 10.1016/j.ijggc.2014.03.002.

D. Oeding and B. R. Oswald. *Elektrische Kraftwerke und Netze*. Springer Berlin Heidelberg, Berlin, Heidelberg, 2011. ISBN 978-3-642-19245-6 978-3-642-19246-3.

ONS. Boletim Mensal de Geração Solar Fotovoltaica. Technical report, Operador Nacional do Sistema Elétrico (ONS), 2021a. URL https://www.ons.org.br/AcervoDigitalDocumentosEPublicacoes/Boletim%20Mensal%20de%20Gera%C3%A7%C3%A3o%20Solar%202020-04.pdf.

ONS. Histórico da Operação: Geração de Energia, 2021b. URL http://www.ons.org.br:80/Paginas/resultados-da-operacao/historico-da-operacao/geracao_energia.aspx.

ONS. Histórico da Operação: Energia Natural Afluente por Subsistema, 2021c. URL http://www.ons.org.br:80/Paginas/resultados-da-operaca o/historico-da-operacao/energia_afluente_subsistema.aspx. year: 2000-2020.

ONS. Histórico da Operação: Curva de Carga Horária, 2021d. URL http://www.ons.org.br:80/Paginas/resultados-da-operacao/historico-da-operacao/curva_carga_horaria.aspx.

ONS. Histórico da Operação: Intercâmbios de Energia, 2021e. URL http://www.ons.org.br:80/Paginas/resultados-da-operacao/historico-da-operacao/intercambios_energia.aspx.

ONS. Mapa do Sistema de Transmissao: Horizonte 2024, 2021f. URL http://www.ons.org.br:80/paginas/sobre-o-sin/mapas.

ONS. Reserva Girante na Demanda Máxima do SIN, 2021g. URL https://sdro.ons.org.br/SDRO/DIARIO/2021_06_28/HTML/13_ReservaGiranteDemandaMaxima.html.

ONS. Capacidade Instalada de Geração, 2022a. URL https://dados.ons.org.br/dataset/capacidade-geracao.

ONS. DADOS DA CAPACIDADE INSTALADA DE GERAÇÃO, 2022b. URL https://ons-dl-prod-opendata.s3.amazonaws.com/dataset/capacidade-geracao/DicionarioDados_Capacidade_Instalada_Geracao.pdf.

ONS. EAR Diário por Subsistema: 2019, 2022c. URL https://dados.ons.org.br/dataset/ear-diario-por-subsistema.

ONS. Energia Agora: Reservatórios, 2022d. URL http://www.ons.org.br:80/paginas/energia-agora/reservatorios.

ONS. ONS Adota Conceito de Carga Global na Programação Diária e na Operação, 2022e. URL http://www.ons.org.br:80/Paginas/Noticias/20210303-ons-implementa-carga-global-na-programacao-e-operacao.aspx.

ONS, EPE, and CCEE. AVALIAÇÃO E COMPATIBILIZAÇÃO DAS INFORMAÇÕES DE GERAÇÃO, CARGA E CONSUMO DE ENERGIA ELÉTRICA NO SIN, 2016. URL https://www.epe.gov.br/sites-pt/publicacoes-dados-abertos/publicacoes/PublicacoesArquivos/publicacao-251/topico-315/NT_Carga_ONS-EPE-CCEE%20_07-12-2016[1].pdf. Rio de Janeiro.

OpenStreetMap conbributors. OpenStreetMap, 2023. URL https://www.openstreetmap.org/.

M. Parzen, H. Abdel-Khalek, E. Fedotova, M. Mahmood, M. M. Frysztacki, J. Hampp, L. Franken, L. Schumm, F. Neumann, D. Poli, A. Kiprakis, and D. Fioriti. PyPSA-Earth. A new global open energy system optimization model demonstrated in Africa. *Applied Energy*, 341:121096, 2023. doi: 10.1016/j.apenergy.2023.121096.

J.-F. Pekel, A. Cottam, N. Gorelick, and A. S. Belward. High-resolution mapping of global surface water and its long-term changes. *Nature*, 540(7633):418–422, 2016. doi: 10.1038/nature20584.

J. E. Penner, D. H. Lister, D. J. Griggs, D. J. Dokken, and M. McFarland. Aviation and the Global Atmosphere. Technical report, Intergovernmental Panel on Climate Change (IPCC), 1999. URL https://www.ipcc.ch/site/assets/uploads/2018/03/av-en-1.pdf.

J. Perner and D. Bothe. International aspects of a Power-to-X Roadmap. frontier economics, World Energy Council, 2018. URL https://www.efuel-alliance.eu/fileadmin/Downloads/20181018_WEC_Germany_PTXroadmap_Full-study-englisch.pdf.

M. S. Peters, K. D. Timmerhaus, and R. E. West. *Plant design and economics for chemical engineers*. McGraw-Hill chemical engineering series. McGraw-Hill, New York, 5th ed edition, 2003. ISBN 978-0-07-239266-1.

M. Pfennig, D. Böttger, B. Häckner, D. Geiger, C. Zink, A. Bisevic, and L. Jansen. Global GIS-based potential analysis and cost assessment of Power-to-X fuels in 2050, 2022.

S. Pfenninger and I. Staffell. Long-term patterns of European PV output using 30 years of validated hourly reanalysis and satellite data. *Energy*, 114:1251–1265, 2016. doi: 10.1016/j.energy.2016.08.060.

S. Pfenninger, A. Hawkes, and J. Keirstead. Energy systems modeling for twenty-first century energy challenges. *Renewable and Sustainable Energy Reviews*, 33:74–86, 2014. doi: 10.1016/j.rser.2014.02.003.

S. Pfenninger, J. DeCarolis, L. Hirth, S. Quoilin, and I. Staffell. The importance of open data and software: Is energy research lagging behind? *Energy Policy*, 101:211–215, 2017. doi: 10.1016/j.enpol.2016.11.046.

S. Pfenninger, L. Hirth, I. Schlecht, E. Schmid, F. Wiese, T. Brown, C. Davis, M. Gidden, H. Heinrichs, C. Heuberger, S. Hilpert, U. Krien, C. Matke, A. Nebel, R. Morrison, B. Müller, G. Pleßmann, M. Reeg, J. C. Richstein, A. Shivakumar, I. Staffell, T. Tröndle, and C. Wingenbach. Opening the black box of energy modelling: Strategies and lessons learned. *Energy Strategy Reviews*, 19:63–71, 2018. doi: 10.1016/j.esr.2017.12.002.

K. Poncelet, E. Delarue, D. Six, J. Duerinck, and W. D'haeseleer. Impact of the level of temporal and operational detail in energy-system planning models. *Applied Energy*, 162:631–643, 2016. doi: 10.1016/j.apenergy.2015.10.100.

J. Portugal-Pereira, R. Soria, R. Rathmann, R. Schaeffer, and A. Szklo. Agricultural and agro-industrial residues-to-energy: Techno-economic and environmental assessment in Brazil. *Biomass and Bioenergy*, 81:521–533, 2015. doi: 10.1016/j.biombioe.2015.08.010.

M. G. Prina, G. Manzolini, D. Moser, B. Nastasi, and W. Sparber. Classification and challenges of bottom-up energy system models - A review. *Renewable and Sustainable Energy Reviews*, 129:109917, 2020. doi: 10.1016/j.rser.2020.10 9917.

M. Prussi, U. Lee, M. Wang, R. Malina, H. Valin, F. Taheripour, C. Velarde, M. D. Staples, L. Lonza, and J. I. Hileman. CORSIA: The first internationally adopted approach to calculate life-cycle GHG emissions for aviation fuels. *Renewable* *and Sustainable Energy Reviews*, 150:111398, 2021. doi: 10.1016/j.rser.2021.111398.

PyPSA developers. PyPSA: Python for Power System Analysis: V0.22.0, 2023. URL `https://zenodo.org/record/3946412`.

K. Riahi, C. Bertram, D. Huppmann, J. Rogelj, V. Bosetti, A.-M. Cabardos, A. Deppermann, L. Drouet, S. Frank, O. Fricko, S. Fujimori, M. Harmsen, T. Hasegawa, V. Krey, G. Luderer, L. Paroussos, R. Schaeffer, M. Weitzel, B. van der Zwaan, Z. Vrontisi, F. D. Longa, J. Després, F. Fosse, K. Fragkiadakis, M. Gusti, F. Humpenöder, K. Keramidas, P. Kishimoto, E. Kriegler, M. Meinshausen, L. P. Nogueira, K. Oshiro, A. Popp, P. R. R. Rochedo, G. Ünlü, B. van Ruijven, J. Takakura, M. Tavoni, D. van Vuuren, and B. Zakeri. Cost and attainability of meeting stringent climate targets without overshoot. *Nature Climate Change*, 11(12):1063–1069, 2021. doi: 10.1038/s41558-021-01215-2.

I. Ridjan, B. V. Mathiesen, and D. Connolly. Synthetic fuel production costs by means of solid oxide electrolysis cells. *Energy*, 76:104–113, 2014. doi: 10.1016/j.energy.2014.04.002.

H.-K. Ringkjøb, P. M. Haugan, and I. M. Solbrekke. A review of modelling tools for energy and electricity systems with large shares of variable renewables. *Renewable and Sustainable Energy Reviews*, 96:440–459, 2018. doi: 10.1016/j.rser.2018.08.002.

P. R. R. Rochedo, B. Soares-Filho, R. Schaeffer, E. Viola, A. Szklo, A. F. P. Lucena, A. Koberle, J. L. Davis, R. Rajão, and R. Rathmann. The threat of political bargaining to climate mitigation in Brazil. *Nature Climate Change*, 8(8):695–698, 2018. doi: 10.1038/s41558-018-0213-y.

E. Rodrigues, R. Pontes, J. Bandeira, and V. Aguiar. Analysis of the Incidence of Direct Lightning over a HVDC Transmission Line through EFD Model. *Energies*, 12(3):555, 2019. doi: 10.3390/en12030555.

T. H. Roos. The cost of production and storage of renewable hydrogen in South Africa and transport to Japan and EU up to 2050 under different scenarios.

International Journal of Hydrogen Energy, 46(72):35814–35830, 2021. doi: 10.1016/j.ijhydene.2021.08.193.

D. Schlachtberger, T. Brown, S. Schramm, and M. Greiner. The benefits of cooperation in a highly renewable European electricity network. *Energy*, 134: 469–481, 2017. doi: 10.1016/j.energy.2017.06.004.

P. Schmidt and W. Weindorf. Power-to-Liquids: Potentials and Perspectives. Technical report, Ludwig-Bölkow-Systemtechnik GmbH (LBST), 2016. URL `https://www.umweltbundesamt.de/sites/default/files/medien/377/publikationen/161005_uba_hintergrund_ptl_barrierrefrei.pdf`.

P. Schmidt, W. Zittel, W. Weindorf, T. Rakasha, and D. Goericke. Renewables in transport 2050 – Empowering a sustainable mobility future with zero emission fuels. In M. Bargende, H.-C. Reuss, and J. Wiedemann, editors, *16. Internationales Stuttgarter Symposium*, Proceedings, pages 185–199, Wiesbaden, 2016. Springer Fachmedien. doi: 10.1007/978-3-658-13255-2_15.

P. Schmidt, V. Batteiger, A. Roth, W. Weindorf, and T. Raksha. Power-to-Liquids as Renewable Fuel Option for Aviation: A Review. *Chemie Ingenieur Technik*, 90(1-2):127–140, 2018. doi: 10.1002/cite.201700129.

Y. Scholz. Renewable energy based electricity supply at low costs - Development of the REMix model and application for Europe, 2012. URL `http://dx.doi.org/10.18419/opus-2015`.

A. Schröder, F. Kunz, J. Meiss, and R. Mendelevitch. Current and prospective costs of electricity generation until 2050. Technical Report DIW Data Documentation No. 68, Deutsches Institut für Wirtschaftsforschung (DIW), Berlin, 2013. URL `https://www.econstor.eu/handle/10419/80348`.

A. W. Schäfer, A. D. Evans, T. G. Reynolds, and L. Dray. Costs of mitigating CO_2 emissions from passenger aircraft. *Nature Climate Change*, 6(4):412–417, 2016. doi: 10.1038/nclimate2865.

A. W. Schäfer, S. R. H. Barrett, K. Doyme, L. M. Dray, A. R. Gnadt, R. Self, A. O'Sullivan, A. P. Synodinos, and A. J. Torija. Technological, economic and environmental prospects of all-electric aircraft. *Nature Energy*, 4(2):160–166, 2018. doi: 10.1038/s41560-018-0294-x.

E. D. Sherwin. Electrofuel Synthesis from Variable Renewable Electricity: An Optimization-Based Techno-Economic Analysis. *Environmental Science & Technology*, 55(11):7583–7594, 2021. doi: 10.1021/acs.est.0c07955.

W. Short, D. Packey, and T. Holt. A manual for the economic evaluation of energy efficiency and renewable energy technologies. Technical Report NREL/TP–462-5173, 35391, National Renewable Energy Lab (NREL), 1995. URL `http://www.osti.gov/servlets/purl/35391-NqycFd/webviewable/`.

J. Silva, C. Ribeiro, and R. Guedes. Roughness length classification of Corine Land Cover classes. In *Proceedings of the European Wind Energy Conference*, volume 710, page 110, Milan,Italy, 2007.

J. L. d. S. Soito and M. A. V. Freitas. Amazon and the expansion of hydropower in Brazil: Vulnerability, impacts and possibilities for adaptation to global climate change. *Renewable and Sustainable Energy Reviews*, 15(6):3165–3177, 2011. doi: 10.1016/j.rser.2011.04.006.

Solargis. Global Solar Atlas 2.0: A free web-based application developed and operated by the company Solargis s.r.o. on behalf of the World Bank Group, utilizing Solargis data, with funding provided by the Energy Sector Management Assistance Program (ESMAP), 2019. URL `https://globalsolaratlas.info/map`.

S. Song, H. Lin, P. Sherman, X. Yang, C. P. Nielsen, X. Chen, and M. B. McElroy. Production of hydrogen from offshore wind in China and cost-competitive supply to Japan. *Nature Communications*, 12(1):6953, 2021. doi: 10.1038/s41467-021-27214-7.

R. Soria, A. F. Lucena, J. Tomaschek, T. Fichter, T. Haasz, A. Szklo, R. Schaeffer, P. Rochedo, U. Fahl, and J. Kern. Modelling concentrated solar power (CSP) in the Brazilian energy system: A soft-linked model coupling approach. *Energy*, 116:265–280, 2016. doi: 10.1016/j.energy.2016.09.080.

A. Soroudi. *Power System Optimization Modeling in GAMS*. Springer International Publishing, Cham, 2017. ISBN 978-3-319-62349-8 978-3-319-62350-4. doi: 10.1007/978-3-319-62350-4.

I. Staffell and S. Pfenninger. Using bias-corrected reanalysis to simulate current and future wind power output. *Energy*, 114:1224–1239, 2016. doi: 10.1016/j.energy.2016.08.068.

S. Sterl, D. Fadly, S. Liersch, H. Koch, and W. Thiery. Linking solar and wind power in eastern Africa with operation of the Grand Ethiopian Renaissance Dam. *Nature Energy*, 6(4):407–418, 2021. doi: 10.1038/s41560-021-00799-5.

D. Stetter. Enhancement of the REMix energy model - global renewable energy potentials optimized power plant siting and scenario validation, 2014. URL `http://dx.doi.org/10.18419/opus-6855`.

R. Stockli. Sea Surface Temperature, Salinity and Density, 2009. URL `https://svs.gsfc.nasa.gov/3652`.

B. Stoll, J. Andrade, S. Cohen, G. Brinkman, and C. Brancucci Martinez-Anido. Hydropower Modeling Challenges. Technical Report NREL/TP–5D00-68231, 1353003, National Renewable Energy Lab (NREL), 2017. URL `http://www.osti.gov/servlets/purl/1353003/`.

R. W. Stratton, P. J. Wolfe, and J. I. Hileman. Impact of Aviation Non-CO_2 Combustion Effects on the Environmental Feasibility of Alternative Jet Fuels. *Environmental Science & Technology*, 45(24):10736–10743, 2011. doi: 10.1021/es2017522.

F. Ueckerdt, C. Bauer, A. Dirnaichner, J. Everall, R. Sacchi, and G. Luderer. Potential and risks of hydrogen-based e-fuels in climate change mitigation. *Nature Climate Change*, 11(5):384–393, 2021. doi: 10.1038/s41558-021-01032-7.

UNFCCC. Federative Republic of Brazil: Paris Agreement: Nationally determined contribution (NDC). Technical report, United Nations Framework Convention on Climate Change (UNFCCC), Brasília, Brazil, 2022. URL https://unfccc.int/sites/default/files/NDC/2022-06/Updated%20-%20First%20NDC%20-%20%20FINAL%20-%20PDF.pdf.

R. Urraca, T. Huld, A. Gracia-Amillo, F. J. Martinez-de Pison, F. Kaspar, and A. Sanz-Garcia. Evaluation of global horizontal irradiance estimates from ERA5 and COSMO-REA6 reanalyses using ground and satellite-based data. *Solar Energy*, 164:339–354, 2018. doi: 10.1016/j.solener.2018.02.059.

H. L. van Soest, L. Aleluia Reis, L. B. Baptista, C. Bertram, J. Després, L. Drouet, M. den Elzen, P. Fragkos, O. Fricko, S. Fujimori, N. Grant, M. Harmsen, G. Iyer, K. Keramidas, A. C. Köberle, E. Kriegler, A. Malik, S. Mittal, K. Oshiro, K. Riahi, M. Roelfsema, B. van Ruijven, R. Schaeffer, D. Silva Herran, M. Tavoni, G. Unlu, T. Vandyck, and D. P. van Vuuren. Global roll-out of comprehensive policy measures may aid in bridging emissions gap. *Nature Communications*, 12(1):6419, 2021. doi: 10.1038/s41467-021-26595-z.

M. Victoria, K. Zhu, T. Brown, G. B. Andresen, and M. Greiner. The role of storage technologies throughout the decarbonisation of the sector-coupled European energy system. *Energy Conversion and Management*, 201:111977, 2019. doi: 10.1016/j.enconman.2019.111977.

E. Vyhmeister, G. J. Ruiz-Mercado, A. I. Torres, and J. A. Posada. Optimization of multi-pathway production chains and multi-criteria decision-making through sustainability evaluation: a biojet fuel production case study. *Clean Technologies and Environmental Policy*, 20(7):1697–1719, 2018. doi: 10.1007/s10098-018-1576-5.

F. Wang, R. Swinbourn, and C. Li. Shipping Australian sunshine: Liquid renewable green fuel export. *International Journal of Hydrogen Energy*, page S0360319922061870, 2023. doi: 10.1016/j.ijhydene.2022.12.326.

M. Wang, R. Dewil, K. Maniatis, J. Wheeldon, T. Tan, J. Baeyens, and Y. Fang. Biomass-derived aviation fuels: Challenges and perspective. *Progress in Energy and Combustion Science*, 74:31–49, 2019. doi: 10.1016/j.pecs.2019.04.004.

T. Wassermann, H. Muehlenbrock, P. Kenkel, and E. Zondervan. Supply chain optimization for electricity-based jet fuel: The case study Germany. *Applied Energy*, 307:117683, 2022. doi: 10.1016/j.apenergy.2021.117683.

T. Watanabe, K. Murata, S. Kamiya, and K. I. Ota. Cost Estimation of Transported Hydrogen, Produced by Overseas Wind Power Generations. In *Hydrogen Production Technologies - Part 2*, Essen, Germany, 2010. URL `https://core.ac.uk/reader/34995430`.

P. Wheeler and S. Bozhko. The More Electric Aircraft: Technology and challenges. *IEEE Electrification Magazine*, 2(4):6–12, 2014. doi: 10.1109/MELE.2014.2360720.

F. Wiese, I. Schlecht, W.-D. Bunke, C. Gerbaulet, L. Hirth, M. Jahn, F. Kunz, C. Lorenz, J. Mühlenpfordt, J. Reimann, and W.-P. Schill. Open Power System Data – Frictionless data for electricity system modelling. *Applied Energy*, 236: 401–409, 2019. doi: 10.1016/j.apenergy.2018.11.097.

C. L. Wilson and W. H. Matthews. *Inadvertent climate modification: Report of the study of man's impact on climate (SMIC)*. Cambridge, Mass. : MIT Press, 1971. ISBN 978-0-262-19101-2 978-0-262-69033-1.

World Bank. State and Trends of Carbon Pricing 2022. Technical report, World Bank, 2022. URL `http://hdl.handle.net/10986/37455`. Washington, DC: World Bank, License: CC BY 3.0 IGO.

S. H. L. Yim, G. L. Lee, I. H. Lee, F. Allroggen, A. Ashok, F. Caiazzo, S. D. Eastham, R. Malina, and S. R. H. Barrett. Global, regional and local health impacts of civil aviation emissions. *Environmental Research Letters*, 10(3): 034001, 2015. doi: 10.1088/1748-9326/10/3/034001.